UNIVERSITÀ DEGLI STUDI DI GENOVA

DISTAV - DIPARTIMENTO DI SCIENZE DELLA TERRA, DELL'AMBIENTE E DELLA VITA

BENEFICIAL EFFECTS OF NATURAL PRODUCTS ON IN-VITRO AND IN-VIVO MODELS

Author:

Farah Diab

Supervisor:

Prof. Laura Vergani

Coordinator of the PhD course: Prof. Marco scambelluri

This dissertation is submitted for the degree of

Doctor of Philosophy

In

SCIENCE AND TECHNOLOGY FOR THE ENVIRONMENT AND TERRITORY

Cycle XXXVI (2020-2023)

Declaration

I hereby declare that except where specific reference is made to the work of others, the contents of this dissertation are original and have not been submitted in whole for consideration for any other degree or qualification in this, or any other universities. This dissertation is my own work and contains nothing which is the outcome of work done in collaboration with others, except as specified in the text and Acknowledgements. This dissertation contains fewer than 65,000 words including bibliography, footnotes, tables and equations and has fewer than 150 figures.

January 2024

Acknowledgements

"God will elevate those of you who believe and those of you were given knowledge to high ranks" | Al-Mujadala 11 – Qur'an Kareem

In this section, I would like to share with you a part of my three-years journey, express my sincere gratitude to those who teach Farah firstly, and those who ease on Farah her bad days secondly.

Those who know Farah well, know how this PhD was really hard as a girl being apart of her family, trying her best to get merged into a totally different culture, and managing her life with all the ups and downs!

Firstly, I have to express my deep gratefulness to **Prof. Laura Vergani**; the one who taught me how to do research from A to Z, guided and supported me in every single step throughout my journey. Prof. Vergani didn't hesitate to give her time and efforts, to share her expertise, and to enrich my scientific knowledge. Prof. Vergani, I am greatly thankful to you!

Secondly, this PhD wouldn't have been possible without the guidance and help of DISTAV people. Credits to **Dr. Mohamad Khalil; "**the Godfather of research" as I used to call him, the one who believed in me since day 1, involved me in his work, and gave me the first push in my research journey. Thanks to **Dr. Nadia Serale** as she taught me most of the technical skills with patience and professionalism. Big thanks to my lab mates who helped me kindly in carrying out a lot of works especially during my mobility period. Last but not least, thanks to all the people in the department; researchers and technicians, who never hesitated to help me when I needed any support, in particular Dr. Teresa Balbi, who was always there for me.

Finally, I would like to show appreciation to my family as I want to dedicate special thanks to my dad, **Ali**, who has been my number one supporter in this journey and trusted me blindly. Thanks to my mom, **Fatima**, who paved my all-long path with prayers and tears. Thanks to my friends, my second family, for their support and encouragement.

Last but certainly most importantly, with all the love I can hold, I want to say thank you **Yahya,** my closest friend, my all-time partner, my support system, my favorite person. Thanks for all your unstoppable care, unconditional love, uncountable prepared meals! I cannot really express how thankful I am to you for being there for me, for being patient and kind in my moody days, for waiting me during late nights work… I am really out of words! Dear Yahya, Farah loves you endlessly!

Farah Diab

Abstract

Numerous plants, plant extracts, and plant-derived compounds are being explored for their beneficial effects against overweight, liver diseases, and aging. Obesity is associated with the increased prevalence of non-alcoholic fatty liver disease (NAFLD), becoming the most common liver disease in Western countries. Obesity and NAFLD are closely associated with many other metabolic alternations such as cardiovascular diseases and endothelial dysfunction. Aging is a multifactorial phenomenon characterized by degenerative processes closely connected to oxidative damage and chronic inflammation. Many herbs are widely employed as food and spices in the Mediterranean area, but also in folk medicine, and their use for the management of metabolic disorders is well documented. Thymbra spicata L., a member of the Lamiaceae family, is rich in phenolic compounds as carvacrol, and a popular remedy to prevent and/or counteract hyperlipidemia and oxidative stress. Hereby, the present PhD focused on studying the protective effects of carvacrol on in vitro cellular models of hepatic steatosis and endothelial dysfunction, investigating the effect of in vitro gastrointestinal digestion on the phenolic profile and biological activities of T. spicata, and demonstrating the effect of in vivo supplementation of polyphenol-enriched extracts from T. spicata on lifespan extension in Drosophila melanogaster. The outcome of this PhD shows that T. spicata could be promising bioactive products to develop natural therapeutic agents or dietary supplements to treat NAFLD, obesity-related metabolic disease, and aging.

Keywords:

List of Abbreviations

Abbreviation	Full Word
ABTS	2-2'-azino-bis (3-ethylbenzo-thiazoline-6-sulphonate) diammonium salt
A375	Melanoma Cancer Cell Line
BSA	Bovine Serum Albumin
BMI	Body Mass Index
CVD	Cardiovascular diseases
CVL	Carvacrol
DAPI	4′,6-diamidino-2-phenylindole
DCF-DA	2'-7'dichlorofluorescein
DMEM	Dulbecco's modified Eagle medium
DMSO	Dimethyl Sulfoxide
DPPH	1,1-diphenyl-2-picrylhydrazyl
EA	Eicosanoic Acid
FABS	Fatty Acid Binding Sites
FaO	Rat Hepatoma Cell Line
FDA	Food and Drug Administration
FFAs	Free Fatty Acids
FBS	Fetal Bovine Serum
FRAP	Ferric Reducing Antioxidant Power
GSH	Glutathione
HAS	Human Serum Albumin
HCT 116	Colorectal Cancer Cell Line
HCV	Human Endothelial Cell Line
HFD	High-fat Diet
HE	Human Endothelial Cell Line
HO	Heme oxygenase
LDs	Lipid Droplets

LDL	Low-density Lipoprotein
MDA	Malondialdehyde
MDA-MB 321	Breast Cancer Cell Line
MTT	3-(4,5-dimethylthiazol-2-yl)-2,5-diphenyltetrazol bromide
NAFLD	Non-alcoholic Fatty Liver Disease
NASH	Nonalcoholic steatohepatitis
NO	Nitric Oxide
NOx	Nitric Oxide
OA	Oleic Acid
PA	Palmitic Acid
PBS	Phosphate-buffered Saline
ROS	Reactive Oxygen Species
SA	Stearic Acid
SC	Steatotic Cells
SS	Simple Steatosis
TBA	Thiobarbituric Acid
TCC	Total Carbohydrate Contents
TFC	Total Flavonoid Content
TGs	Triglycerides
THAC	Total Hydroxycinnamic Acid
TPC	Total Phenol Content
TPrC	Total Protein Content
TrxR	Thioredoxin reductase
WHO	World Health Organization
qPCR	Quantitative real-time PCR

Contents

Contents

List of Figures

List of tables

Chapter 1   Introduction

Medicinal plants have a long history in traditional medicine for the management of diseases. Lamiaceae is the largest family of the Lamiales order, including more than 7000 species, mostly shrubs and herbs. Lamiaceae are typically cultivated as ornamental plants, but many of them are used as food and spices [1]. Many bioactive molecules have been isolated from Lamiaceae including alkaloids, phenolic acids, phenyl propanoids, flavonoids, terpenoids and other compounds such as hydrocarbons, sugars, lignans, and lignins. Plant parts (leaves, stems, or roots), extracts, and/or isolated compounds from Lamiaceae have been largely investigated for their pleiotropic biological effects, mainly antimicrobial, anti-inflammatory, antioxidant, and cytotoxic activities. A large body of studies has suggested the potential of the Lamiaceae in ameliorating metabolic disorders and aging-related dysfunctions.

1.1.   Lamiaceae: General aspects of the family

Lamiaceae is a plant family belonging to the Lamiales order, and it consists of 236 genera and 7200 species [2]. The family was known for a long time as Labiatae (nomen conservandum) or the mint family, but in the 1820 the name was changed to Lamiaceae. Lamiaceae includes the highest number of aromatic herbs, shrubs, and trees with quadrangular branches. The most important genera of this family are Salvia, Scutellaria, Stachys, Plectranthus, Hyptis, Teucrium, Vitex, Thymus, and Nepeta [3].

Lamiaceae inhabit different ecosystems and are widely cultivated [4], but it has been noticed that the major distribution of Lamiaceae species is in the Mediterranean area. Most of the species are aromatic plants and contain a mixture of bioactive compounds which led to their use in the cosmetic, pharmaceutical, and food industries, mainly under the form of essential oils [5]. Moreover, Lamiaceae species are promising potential sources of natural antioxidants, owing to their high polyphenol content. Natural antioxidants from various botanical sources

have been widely investigated as a potential alternative to synthetic antioxidants; for this reason, plants of Lamiaceae are regarded as a source of functional foods. We wish to emphasize this as the WHO suggests that plants with a long history of applications in folk medicine should be thoroughly evaluated for possible use in the treatment and prevention of diseases, and the Lamiaceae perfectly fall into this field.

1.2. Thymbra spicata L.

The genus Thymbra includes many thyme-like plants native to the Mediterranean region, mainly Lebanon, Turkey, and Greece [6]. *Thymbra spicata* L. (known in Lebanon as wild Za'atar shown in Figure 1.1) is traditionally used as a food and herbal tea, and in folk medicine as an antiseptic agent and to relieve headaches, toothaches, colds, asthma, and rheumatism, and this can be greatly attributed to its richness in phenolic compounds including phenolic acids (rosmarinic acid), phenolic monoterpenoids (carvacrol, thymol), and flavonoids (both glycosides and aglycones) [7].

The species *T. spicata* has gained much popularity as a remedy to combat hypercholesterolemia, oxidative stress, inflammation, and other health-promoting activities that are held accountable for potentially affecting the longevity of the individual. *In vivo* studies conducted on high-fat diet (HFD) fed mice showed that both ethanolic and aqueous extracts of *T. spicata* aerial parts possess anti-hypercholesterolaemic, antioxidant, and anti steatohepatitic potentials by reducing the plasmatic cholesterol, LDL, triglyceride levels and by increasing the plasmatic HDL and reduced glutathione (GSH) [8], [9]. A recent *in vitro* study proved that both the ethanolic and aqueous extracts of *T. spicata* aerial parts act as lipid lowering agents in a model of NAFLD by reducing the cytosolic lipid accumulation and the number of lipid droplets, the excess of intracellular free radicals and the consequent lipid peroxidation [10].
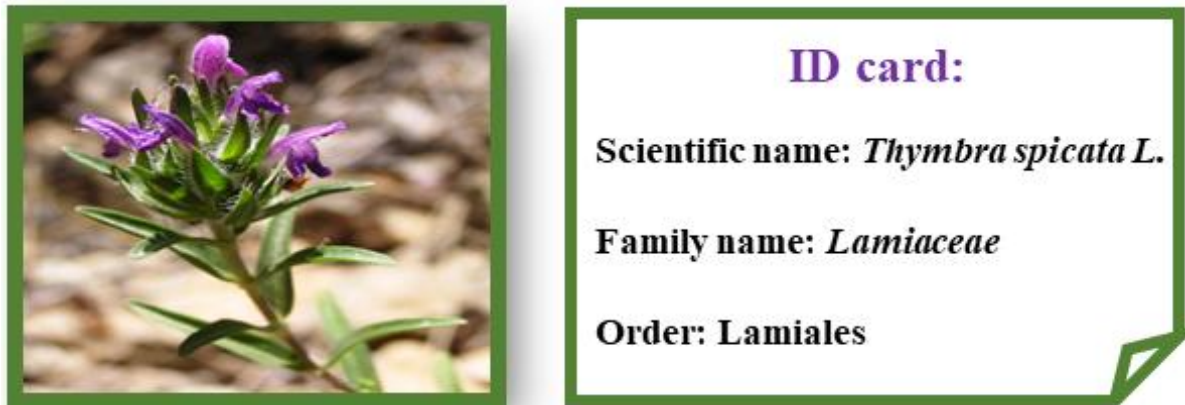
Figure 1.1 *Thymbra spicata* L. description.

1.3.   Metabolic disorders linked to excess energy intake

Excess energy intake correlates with the development of many metabolic disorders. Different energy-dense foods have different effects on metabolism. Well known are the effects of both a high-fat diet, and a high-fructose diet as well as their combination (high-fat/high-fructose diet). Obesity is an independent high-risk factor for metabolic diseases, such as type 2 diabetes and nonalcoholic fatty liver disease. The prevalence of nutritional imbalance-induced obesity is increasing worldwide due to a change in the constituents of our modern diet.

1.4.   Obesity

Excess energy intake is thought to be a major contributor to obesity, a condition characterized by the excessive accumulation of fat in the body. The World Health Organization (WHO) began sounding the alarm on global obesity in the 1990s and introduced the term "epidemic" in reference to obesity. Indeed, in 2016, more than 1.9 billion adults worldwide were overweight, and over 650 million out of these were obese, with the worldwide prevalence of obesity having nearly tripled between 1975 and 2016. In 2020, about 39 million children under the age of 5 were overweight or obese.

A reliable way to determine whether a person has too much body fat is to calculate the body mass index (BMI), which is a measure of body fat based on height and weight and is

defined as the body mass (in kilograms) divided by the square of the body height (in meters) and expressed in units of kg/m². BMI accounts for the fact that taller people have more tissue than shorter people, and so they tend to weigh more.

Obesity is a complex, chronic disease with several causes that lead to excessive body fat and poor health. Overweight and obesity are caused by many factors including behaviors like eating patterns, lack of sleep or physical activity, and some medicines, as well as genetics and family history. Unhealthy lifestyle habits, such as not getting enough physical activity and eating high-calorie, low-nutrient foods and beverages, can raise your risk of overweight and obesity. Lifestyle changes that can reduce weight include following a heart-healthy eating plan lower in calories and unhealthy saturated fats and increasing physical activity. The Food and Drug Administration (FDA) has also approved medicines and other treatments for weight loss. Surgery may also be a treatment option but is not available for everyone. However, due to the poor adherence to long-term weight loss diets there is significant interest in identifying therapeutic agents for the treatment of obesity. Currently, interest in plant-based food has grown in recent years due to their primary prevention potential. Indeed, more than 20,000 plant species are considered as putative reservoirs for new drugs [11]. A panel of pre and clinical studies showed the efficacy of different medicinal plants on several diseases like obesity, diabetes, and coronary diseases [12].

The global burden of obesity impacts across multiple organs and diseases (as described in Figure 1.2), and the main consequence is the metabolic syndrome, a clustering of disorders such as nonalcoholic fatty liver disease (NAFLD), diabetes mellitus, cardiovascular disease, stroke, cancers [13].

Mice fed with high energy food are used as a model system to understand the mechanisms of the impairment of metabolic homeostasis. However, *in vitro* cellular models

have also been considered reliable models as they mimic what is occurring in the liver during high fat feeding and/or obesity.

1.5.   Nonalcoholic fatty liver disease

Non-alcoholic fatty liver disease (NAFLD) is described by ectopic fat accumulation, mainly in the form of triglycerides (TGs), in hepatocytes of subjects who do not consume excess alcohol. Steatosis is histologically defined by the visible accumulation of macro- and/or microvascular lipid droplets (LDs) in cytosol of more than 5% in liver parenchyma [14].

NAFLD encompasses a large spectrum of liver abnormalities which range from the simple steatosis to nonalcoholic steatohepatitis (NASH), and may progress toward cirrhosis and hepatocellular carcinoma [15], [16]. In molecular terms, steatosis occurs when the rate of hepatic fatty acid uptake from plasma and/ or *de novo* fatty acid synthesis is greater than the rate of fatty acid oxidation and export, thus steatosis represents an imbalance in the complex network of metabolic events [17].

Recently, the "double-hit" hypothesis has been replaced by the "multiple-hit" hypothesis, offering a more comprehensive delineation of the pathogenesis of NAFLD [18]. Indeed, NAFLD is a multisystemic disease where hepatocytes, adipocytes, and endotheliocytes are involved causing an increase in the risk of several chronic diseases, which in turn worsen hepatic metabolism alterations. [18]. Indeed, NAFLD is a multisystemic disease where hepatocytes, adipocytes, and endotheliocytes are involved causing an increase in the risk of several chronic diseases, which in turn worsen hepatic metabolism alterations. Recently, the "double-hit" hypothesis has been replaced by the "multiple-hit" hypothesis, offering a more comprehensive delineation of the pathogenesis of NAFLD [18]. Indeed, NAFLD is a multisystemic disease where hepatocytes, adipocytes, and endotheliocytes are involved causing

an increase in the risk of several chronic diseases, which in turn worsen hepatic metabolism alterations.
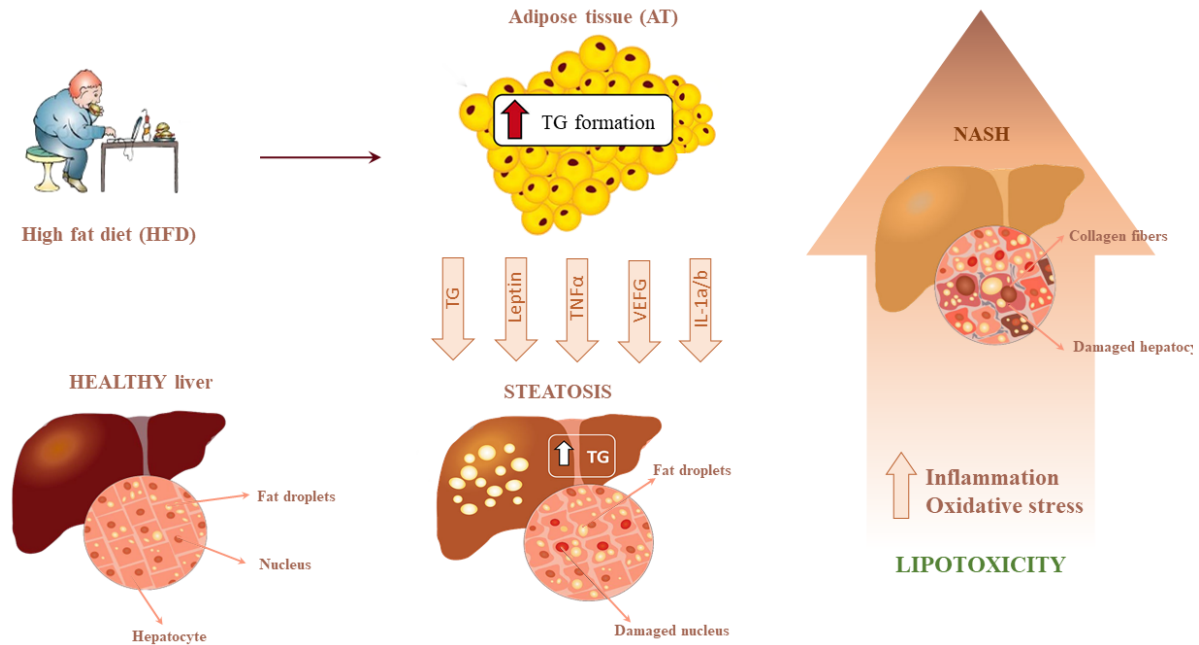
Figure 1.2 A representative scheme describing the effect of high fat diet (HFD) intake across multiple tissues and organs. Excess energy intake is stored in the adipose tissue (AT) in the form of triglycerides (TG). As AT acts as an endocrine organ, it secretes a panel of soluble factors including cytokines, which affect other organs. The multiple pathways of adipose-liver crosstalk contribute to the development and progression of liver diseases. Steatosis is characterized by the ectopic fat accumulation in fat droplets that might develop into nonalcoholic steatosis (NASH) by the action of lipotoxicity.

To date, no ideal pharmacological treatment is available for NAFLD [19]. Therefore, lifestyle modification, which includes a healthy diet and vigorous physical activity along with weight reduction, remains the first line treatment for NAFLD. However, due to the poor adherence to this type of treatment, especially for long-term weight loss diets, some of which may have harmful effects on the liver, there is significant interest in identifying therapeutic agents for the treatment and/or prevention of NAFLD progression. The potential adverse effects of conventional medical therapies led to identify novel complementary therapies that are both natural and safe products, such as herbal medicine and functional foods (e.g., fruits, vegetables), dry materials or their extracts [20].

1.6. Cardiovascular disease

Obesity is a chronic health condition that raises the risk for heart disease — the leading cause of death in the United States. Obesity-associated changes in cardiac function have been described as the "cardiomyopathy of obesity" as the cardiovascular complications primarily occur indirectly due to metabolic comorbidities of obesity [21].

During high-fat diet intake, the excessive uptake of FAs may overwhelm the hepatocyte capacity to store the TG leading to ectopic lipid deposition in key target-organs of cardiovascular control (heart, blood vessels, and kidneys) [22]. The development of atherogenic dyslipidemia, especially elevated plasma TG and remnant lipoprotein cholesterol levels, and small dense LDL particles that infiltrate the arterial wall promote the development of atherosclerotic plaques. Altered glucose metabolism and insulin resistance, hallmarks of NAFLD, can further exacerbate CVD risk [23]. Hyperlipidemia and hyperinsulinemia both stimulate FFAs transport into cardiomyocytes, where the excess of lipid accumulation causes cardiac dysfunction via several mechanisms, including the generation of ROS and the production of lipid metabolites such as diacylglycerols, ceramides, or acylcarnitines. At this stage, the heart tissue is exposed to high levels of fatty acids and carbohydrates, and lipids are deposited in vesicles in the myocardium (cardiac steatosis) [24].

Among treatment options, medicinal plants are frequently used, especially in developing countries. The cardio-protective properties of the various herbs are possibly due to their anti-oxidative, antihypercholesterolemic, anti-ischemic activities, and inhibition of platelet aggregation that reduce the risk of CVD.

1.7. In vitro cellular models of metabolic disorders

1.7.1. Cellular models for NAFLD

NAFLD represents the most common liver disease in Western countries. However, the regulatory pathways underlying the pathogenesis of this chronic disease are not fully understood. Accordingly, in an attempt to elucidate the mechanistic behind the progression of NAFLD, different *in vitro* models have been developed. A plethora of studies have shown that exposing hepatocytes to high concentrations of FAs *in vitro* can overload the cells with lipids mimicking *in vivo* the conditions of overweight/obesity.

For that reason, we set a simplified *in vitro* model using FaO hepatoma cell line, which express a broad array of liver-specific mRNAs maintaining hepatocyte-specific markers [25]. It is noteworthy that basal lipid content of FaO cells is much lower than that of primary hepatocytes, thus, steatogenic treatments resulted in a more rapid and pronounced triglyceride accumulation with respect to primary cultured hepatocytes. This model consists of lipid loading the hepatocytes by an oleate/palmitate mixture (2:1 molar ratio, final concentration 0.75 mmol/L) for 3hrs. Thereafter, steatotic cells were incubated for 24hrs with the tested extract or compound [26].

1.7.2. Cellular models for vascular disease

Endothelium is a semi-permeable barrier between the blood and the tissues, and acts as a metabolically active organ regulating vascular homeostasis. Endothelium dysfunction (ED) can occur in NAFLD [27], [28] as a consequence of Insulin Resistance (IR) which impairs various pathways leading to vascular endothelium damage and atherosclerosis [29], [30]. In fact, steatotic hepatocytes release several factors, FAs and TGs in primis, but also soluble mediators and membrane vesicles known as extracellular vesicles (EVs), into the blood that are then distributed in periphery [31].

In our idea, the cross-talk between the metabolically-dysfunctional steatotic liver and the vascular endothelium might unravel the pathogenetically-relevant mechanisms linking liver

and vascular system [32]. To do this, we developed an *in vitro* cellular model using HECV as an human endothelial cell-line isolated from the umbilical vein.

1.7.3. Aging

Aging is a natural physiological process triggered by different molecular pathways and biochemical events that are promoted by both environmental and genetic factors. Aging is characterized by a time-dependent decline of functional capabilities and impaired stress resistance, that damage biomolecules compromising cellular homeostasis. The factors involved in aging are commonly referred to as the "hallmarks of aging". Among them, oxidative stress and inflammation have been widely investigated. In 1956 Denham Harman [33] proposed "The Free Radical Theory of Aging" that has been updated in recent years to include the suggestion of a central role for reactive oxygen species (ROS) produced by mitochondria [34]. On the other hand, the term "inflammaging" has been created to indicate the significant contribution of low-grade, systemic inflammation to normal aging [35]. Besides, an impair in the body weight control seems to be strictly associated to a reduction in lifespan also through triggering the risk of many metabolic disorders [36].

The findings that the modification of environmental factors, such as diet, can increase lifespan, make natural dietary compounds extraordinary potential tools in the major healthcare challenge of delaying aging. Over the past 20 years, many studies have suggested that dietary polyphenols may exert beneficial effects as anti-aging compounds through the modulation of the hallmarks of aging, including inflammation, oxidative damage, and cell senescence [37]–[39].

Beneficial Effects of Carvacrol on In Vitro Models of Metabolically-Associated Liver
Steatosis and Endothelial Dysfunction: A Role for Fatty Acids in Interfering with Carvacrol
Binding to Serum Albumin

Chapter 2   Beneficial Effects of Carvacrol on In Vitro Models of Metabolically-Associated Liver Steatosis and Endothelial Dysfunction: A Role for Fatty Acids in Interfering with Carvacrol Binding to Serum Albumin

2.1. Introduction

Thyme-like plants are edible vegetables widely employed in the Mediterranean area as functional food and medicinal plants because of their antioxidant, antimicrobial, and cardioprotective properties [40], [41]. Carvacrol (2-methyl-5-(1-methylethyl)-phenol), a natural monoterpenic phenol (Table 2.1), is one of the main components of *Thymbra spicata* leaves representing around 60% of the volatile compounds, and around 25% of total polyphenols [10], [42]. Carvacrol is present in many other aromatic plants such as oregano *Origanum, Satureja* and *Thymus* species [43], [44]. Recently, we described the hepatoprotective potential of the ethanolic extract of *T. spicata* aerial parts enriched in carvacrol [10].

Nonalcoholic fatty liver disease (NAFLD) is the buildup of extra fat in liver parenchima (steatosis) that is not caused by alcohol [45]. In a percent of subjects, simple steatosis (SS) may progress to steatohepatitis (NASH) till to cirrhosis and hepatocellular carcinoma [46], [47]. With the worldwide spread of sedentary lifestyle and diet westernization, the prevalence of NAFLD has increased in many countries [48]. Moreover, NAFLD is strictly linked with high risk factor for atherosclerosis and cardiovascular disorders through the onset of endothelial dysfunction [49]. Nowadays, there are no definitive pharmacological therapies for NAFLD and lifestyle interventions can be the most effective approach [50]. Therefore, the use of medicinal plant extracts or functional food for metabolic disorders such as NAFLD is of growing interest [51], [52].

Beneficial Effects of Carvacrol on In Vitro Models of Metabolically-Associated Liver
Steatosis and Endothelial Dysfunction: A Role for Fatty Acids in Interfering with Carvacrol
Binding to Serum Albumin

The possible application of *T. spicata* extracts on human health strictly depends on the bioavailability of the bioactive constituents, which are mostly vehiculated through serum binding proteins. Albumin is the most abundant plasmatic protein acting in transport and deposition for many endogenous and exogenous molecules including fatty acids [53], amino acids, steroid hormones, metals, drugs and phytochemicals [54].Therefore, serum albumin plays important regulating the pharmacokinetics and distribution of many drugs in the body [55].
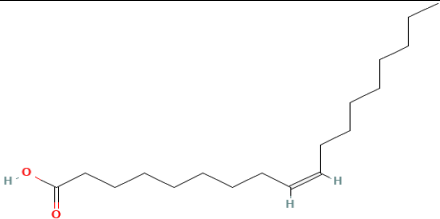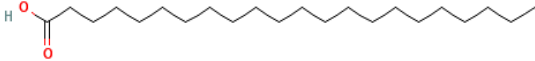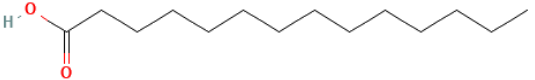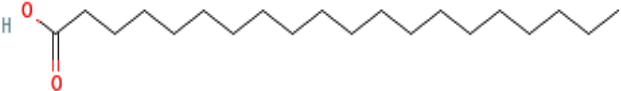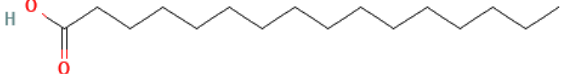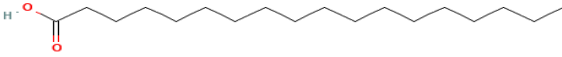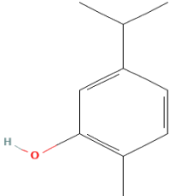
Because of its hydrophobicity, carvacrol as well as its isomer thymol and other monoterpene phenols, requires albumin to be transported to peripheral tissues [56], [57], and this binding is affected by other ligands, especially fatty acids (FAs). In physiological conditions, the human serum albumin (HSA) may bind approximately 0.1–2.0 moles of FAs per mole [58]. FA levels are significantly elevated in overweight/obese subjects compared to their healthy counterpart (the blood TGs increase from 0.82 to 2.38 mmol/L) [59], and also in NAFLD patients the serum FA levels increased from 2.4 mg/mL in overweight NAFLD patients to 2.7 mg/mL in obese NAFLD patients [60]. At high serum levels of FAs a molar ratio FA/HSA > 2 moles FAs per mole HSA has been hypothesized [58], [61]. In light of this, we hypothesized that excess circulating FAs might compete with carvacrol for binding HSA through `competitive-like' allosteric interaction thus decreasing its bioavailability and pharmacodynamics.

In order to evaluate the hepatoprotective and lipid lowering effects of carvacrol we used a well-established *in vitro* model for hepatic steatosis consisting in rat hepatoma FaO cells challenged with a mixture of oleate/palmitate [10], [62]. We used also human endothelial HECV cells exposed to hydrogen peroxide as an *in vitro* model of endothelium dysfunction, which is characteristic of metabolic syndrome [63], [64]. The binding rate of CVL to human serum albumin was assessed with the aim to verify if high concentration of long-chain fatty

Beneficial Effects of Carvacrol on In Vitro Models of Metabolically-Associated Liver
Steatosis and Endothelial Dysfunction: A Role for Fatty Acids in Interfering with Carvacrol
Binding to Serum Albumin

acids that typically are found *in vivo* in NAFLD patients might affect the HAS/carvacrol

binding.

Table 2.1 Structures of the different compounds. Chemical and 2D structure of carvacrol (CVL) and fatty acids employed in the study: Oleic acid (OA-C18), Docosanoic acid (DA-C22), Myristic acid (MA-C14),), Eicosanoic acid (EA-C20), Palmitic acid (PA-C16), and Stearic acid (SA-C18) [65].

Name	Chemical formula	Chemical structure
Oleic acid	$C_{18}H_{34}O_2$	
Docosanoic acid	$C_{22}H_{44}O_2$	
Myristic acid	$C_{14}H_{28}O_2$	
Eicosanoic acid	$C_{20}H_{40}O_2$	
Palmitic acid	$C_{16}H_{32}O_2$	
Stearic acid	$C_{18}H_{36}O_2$	
Carvacrol	$C_{10}H_{14}O$	

Beneficial Effects of Carvacrol on In Vitro Models of Metabolically-Associated Liver
Steatosis and Endothelial Dysfunction: A Role for Fatty Acids in Interfering with Carvacrol
Binding to Serum Albumin

2.2. Materials & Methods

2.2.1. Chemicals

All chemicals, unless otherwise indicated, were supplied by Sigma-Aldrich Corp. (Milan, Italy).

2.2.2. Cell culture and treatments

FaO cells (European Collection of Authenticated Cell Cultures-ECACC- Salisbury, Wiltshire, UK) are a rat hepatoma cell line maintaining hepatocyte-specific markers. Cells were grown in a humidified atmosphere with 5% CO2 at 37°C in Coon's modified Ham's F12 medium supplemented with L-Glutamine and 10% fetal bovine serum (FBS). For treatments, cells were grown until 80% confluence, and then incubated overnight in serum-free medium with 0.25% bovine serum albumin (BSA). HECV cells (Cell Bank and Culture-GMP-IST-Genoa, Italy) are a human endothelial cell line isolated from umbilical vein; they were grown at 37°C with 5% CO2 in Dulbecco's modified Eagle's medium High Glucose (D-MEM) supplemented with L-Glutamine and 10% FBS. To mimic *in vitro* the effect of a high fat diet, FaO cells were treated for 3 h with a mixture of oleate/palmitate at a final concentration of 0.75 mM (2:1 molar ratio). To induce oxidative stress, HECV cells were incubated for 1 h with H_2O_2 (100 μM). Thereafter, cells were incubated for 24h with increasing concentration of carvacrol (0, 1, 10 and 100 μM) [66]. For each experiment, treatment was performed in quadruplicates.

MTT assay was performed on FaO and HECV cells to exclude any cytotoxicity of the different treatments and of carvacrol. No significant changes were observed (data not shown).

2.2.3. Protein quantification

The protein content was determined by the Bradford assay using BSA as a standard [67].

2.2.4. Quantification of triglycerides

At indicate times, FaO cells were scraped, centrifuged and lysed and lipids were extracted in chloroform/methanol (2:1), then chloroform was evaporated [62]. Then, TG content was determined using the 'Triglycerides liquid' kit (Sentinel diagnostic, Milan, Italy). Spectrophotometric reading was performed with UV-VIS spectrophotometer. In parallel, TG content was determined in the culture medium. Values were normalized for the protein content. Data are expressed as percent TG content relative to controls.

2.2.5. Bodipy and DAPI staining

Cells grown on coverslips were rinsed with PBS and fixed with 4% paraformaldehyde for 20 min at room temperature. Neutral lipids were stained by incubation with 1 μg/mL BODIPY 493/503 (Molecular Probes, Life technologies, Monza, Italy) in PBS for 30 min [68]. After washing, nuclei were stained with 4′,6-diamidino-2-phenylindole DAPI, 5 μg/mL, (ProLong Gold medium with DAPI; Invitrogen), mounted and examined by using Olympus IX53 light microscope (Olympus, Milano, Italy), equipped with the standard epifluorescence filter set up. Representative images were captured with a CCD UC30 camera and a digital image acquisition software (CellSens Entry).

2.2.6. ROS quantification by DCF

The oxidation of the cell-permeant 2'-7' dichlorofluorescin diacetate (DCF-DA, Fluka, Germany) to 2'-7'dichlorofluorescein (DCF) allowed to quantify in situ the production of H_2O_2 and other ROS [69]. Stock solution of DCF-DA (10 mM in DMSO) was prepared and stored at -20°C in the dark. At the end of treatment, cells were scraped and gently spun down (600xg for 10 min at 4°C). After washing, cells were loaded with 10 mM DCF-DA in PBS for 30 min at 37°C in the dark. Then, cells were centrifuged, suspended in PBS and the fluorescence was measured fluorometrically (lex=495 nm; lem=525 nm). All measurements were performed in a LS50B fluorimeter (Perkin Elmer, USA) at 25°C using a water-thermostated cuvette holder.

2.2.7. Lipid peroxidation

Lipid peroxidation was determined spectrophotometrically through the thiobarbituric acid reactive substances (TBARS) assay which is based on the reaction of malondialdehyde (MDA; 1,1,3,3-tetramethoxypropane) with thiobarbituric acid (TBA) [70]. Briefly, 1 vol. of cell suspension was incubated for 45 min at 95°C with 2 vol. of TBA solution (0.375% TBA, 15% trichloroacetic acid, 0.25 N HCl). Then, 1 vol. of N-butanol was added and the organic phase was read at 532 nm in a UV-VIS spectrophotometer at 25°C using Peltier-thermostated cuvette holder. The MDA level was expressed as pmol MDA/mL/mg protein.

2.2.8. Nitrite/Nitrate (NOx) Levels

NO production was measured by spectrophotometric measurement of the end products, nitrites and nitrates, using the Griess reaction [71]. After treatments, nitrite accumulation (μmol NaNO2/mg sample protein) was calculated against a standard curve of sodium nitrite (NaNO2). All spectrophotometric analyses were carried out at 25°C recording absorbance at 540 nm.

2.2.9. Wound healing assay

The effect of H2O2 and CVL on HECV migration was evaluated using the wound healing assay [72]. The cells were seeded on 35×10 mm tissue culture dishes and incubated until confluence was reached, the cell monolayer was scraped with a p100 pipet tip making two crossing straight lines to create a "scratch". Then, five views on the cross were photographed by an inverted Olympus IX53 microscope (Olympus, Milan, Italy) and representative images were captured with a CCD UC30 camera and a digital image acquisition software (CellSens Entry). After scratching, cells were incubated with fresh medium containing 100 μM H_2O_2 for 1 hour, and then the medium was replaced with fresh medium in the absence or presence of CVL (0, 1, 10 and 100 μM). Set of images were acquired at 0, 6 and 24 h. To determine the migration of HECV, the images were analyzed using ImageJ free software (http://imagej.nih.gov/ij/). Percentage of the closed area was measured and compared with the

Beneficial Effects of Carvacrol on In Vitro Models of Metabolically-Associated Liver
Steatosis and Endothelial Dysfunction: A Role for Fatty Acids in Interfering with Carvacrol
Binding to Serum Albumin

value obtained before treatment. An increase of the percentage of closed area indicated the migration of cells. Data are means ± S.D. of at least three independent experiments.

2.2.10. Binding assays for CVL and HSA

Stock solutions of both high purity Carvacrol (>99%) (5 mg/mL), and of single long-chain fatty acids (5 mg/mL) were prepared in ethanol (96%). The following free fatty acids (FAs) were employed for the analyses: Myristic acid (MA-C14), Palmetic acid (PA-C16), Oleic acid (OA-C18), Stearic acid (SA-C18), Eicosanoic acid (EA-C20), Docosanoic acid (DA-C22). Stock solution of human serum albumin (HAS) (1 mg/mL, 15 µM) was prepared in 50 mM potassium phosphate buffer (pH 6.8) according to Mohammadi et al., 2009 with slight modifications [73].

2.2.11. UV-VIS absorption spectroscopy

Differential spectra allowed characterizing the binding of CVL to HSA in the presence and in absence of different FAs. Differential UV spectra were recorded in the range 240-350 nm using a Cary Varian1 spectrophotometer (Agilent, Milan, Italy) at room temperature (25°C). No differences were observed above 350 nm (data not reported). Briefly, tow double-compartment (A and B) quartz cuvettes containing 1 mL of 15 µM HSA and 150 µM of each single FAs were added thus obtaining 1:10 molar ratio HSA/FA. 1 mL of HSA in the presence and in absence of FFAs and phosphate buffer solutions were put in compartments A and B, respectively, of each cuvette and then the baseline was recorded.

In the first cuvette, the solutions in the two compartments were not mixed and carvacrol was added gradually (10µL each add) to compartment B and gently mixed inside the compartment. In sample cuvette (second cuvette), the contents of the two compartments were mixed together after each carvacrol addition and the UV spectra was recorded after each addition. The final concentration of CVL were 0, 0.16, 0.32, 0.48, 0.64, 0.80 and 0.96mM.

2.2.12. Fluorescence Spectroscopy

Beneficial Effects of Carvacrol on In Vitro Models of Metabolically-Associated Liver Steatosis and Endothelial Dysfunction: A Role for Fatty Acids in Interfering with Carvacrol Binding to Serum Albumin

---

Binding between CVL and HSA was measured by the quenching of the intrinsic fluorescence of HSA induced by the presence of CVL. The measurements were carried out using a Hitachi 4500 spectrofluorimeter (Hitachi, Tokyo, Japan). Fluorescence quenching of HSA (15 μM in 50 mM potassium phosphate buffer, pH 6.8) was measured in quartz cuvette by recording the emission upon addition of increasing concentrations of Carvacrol (0, 0.16, 0.32, 0.48, 0.64, 0.80 and 0.96 mM). For the quenching measurements, fluorescence spectra of 15 μM CVL-HSA binding were recorded in the absence or in the presence of 150 μM of each single FAs (1:10 molar ratio HSA/FA).

Emission spectra were recorded in a range 290 and 450 nm (λ_{em}) with λ_{ex}=285 nm [74]. The fluorescence data were corrected for inner filter effect using the following equation:

$$F_c = 1/F_{obs}\ e^{(A_{ex}/A_{em})/2} \qquad \textbf{\textit{Eq. 1}}$$

where Fc and Fobs are the corrected and observed fluorescence intensity while A_{ex} and A_{em} are the optical densities of the samples at the excitation and emission wavelengths.

Fluorescence quenching constants were calculated using the Stern-Volmer plot following the Equation [75].

$$F_0/F = 1+K_q\ \tau_0\ [carvacrol] = 1 + K_{sv}[carvacrol] \quad \textbf{\textit{Eq. 2}}$$

where F_0 indicates the fluorescence intensity before addition of the quencher, F is the total fluorescence intensity after addition of quencher to HSA, Kq is the bimolecular quenching rate constant τ_0 is the average lifetime of the fluorophore (Trp-214) alone and its value is around 10^{-8} s for most biomolecules. K_{sv} is the Stern-Volmer quenching constant, and [carvacrol] is the concentration of carvacrol (quencher).

The binding constant was calculated from the modified Stern-Volmer equation.

$$\frac{1}{(F0-F)} = \frac{1}{F0} + \frac{1}{(Kb\ F0)}\frac{1}{[carvacrol]} \qquad \textbf{\textit{Eq. 3}}$$

where Kb is the binding constant of Carvacrol to HSA in presence or in absence of different FAs, that can be calculated from the rate of intercept/slope values obtained from the plot 1/(F0-F) vs 1/[carvacrol]. Furthermore the number of bound carvacrol to HSA (n) where determined by plotting the double log graph of fluorescent data using the equation [76].

$$\log\frac{[F0-F]}{F} = \log K + n\log[carvacrol] \qquad \textbf{\textit{Eq. 4}}$$

2.2.13. Statistical analysis

Data are means ± S.D. of at least three independent experiments. Statistical analysis was performed using ANOVA with Tukey's post-test (GraphPad Software, Inc., San Diego, CA, USA).

2.3. Results

2.3.1. Carvacrol ameliorates steatosis and oxidative stress in hepatocytes

As expected, the exposure of FaO cells to oleate/palmitate mixture (0.75 mM) for 3 h induced a mild steatosis displayed as intracellular TG accumulation (+59% compared to control; $p \leq 0.01$) in steatotic cells (SC) (Figure 2.1A). When steatotic cells cell were treated for 24h with increasing concentrations of carvacrol (1, 10 and 100 μM) we observed a reduction in TG accumulation of -34% and -56% ($p \leq 0.01$), and -46% ($p \leq 0.05$), respectively, compared to SC. The lipid lowering effect of carvacrol was not dose-dependent, with the largest effect produced by the intermediate dose of 10 μM. As an attempt to counteract the excess lipid

accumulation, steatotic cells increased the TG secretion into the culture medium (+50% compared to control cells; p≤0.05), and incubation with carvacrol reduced the TG over secretion of about -50% (p≤0.05), -62% (p≤0.01) and -55% (p≤0.01) for CVL 1, 10 and 100 µM respectively, compared to steatotic cells (Figure 2.1B).

In parallel, cytosolic lipid droplets (LDs) were visualized in situ by fluorescent staining with BODIPY. The micrographs (Figure 2.1C) showed that the number and size of LD increased in SC cells (+224% of fluorescence intensity with respect to control; p≤0.0001), while carvacrol significantly reduced the fluorescence of about -110% and -86% (p≤0.0001) for 10 and 100 µM doses, respectively (Figure 2.1D). Also in this case we did not observe a dose dependence effect for carvacrol, and the largest effect was observed for the intermediate dose of 10 µM.

The protective effect of carvacrol against the fat-induced excess generation of ROS was tested fluorometrically using DCF probe (Figure 2.2A). Among the three tested concentrations, only the intermediate carvacrol concentration (10 µM) significantly counteracted the excess ROS generation (-38% compared to SC cells, $p \leq 0.01$). ROS production, visualized *in situ* by fluorescence microscopy of DCF-stained cells (Figure 2.2B) showed a higher and diffuse DCF fluorescence in SC cells compared to controls (+ 156%; $p \leq 0.0001$ of fluorescence intensity with respect to control), and DCF signal was reduced after treatment with carvacrol 10 and 100 µM with respect to control (-151% and -59% fluorescence intensity, respectively; $p \leq 0.0001$) (Figure 2.2C).

Beneficial Effects of Carvacrol on In Vitro Models of Metabolically-Associated Liver Steatosis and Endothelial Dysfunction: A Role for Fatty Acids in Interfering with Carvacrol Binding to Serum Albumin
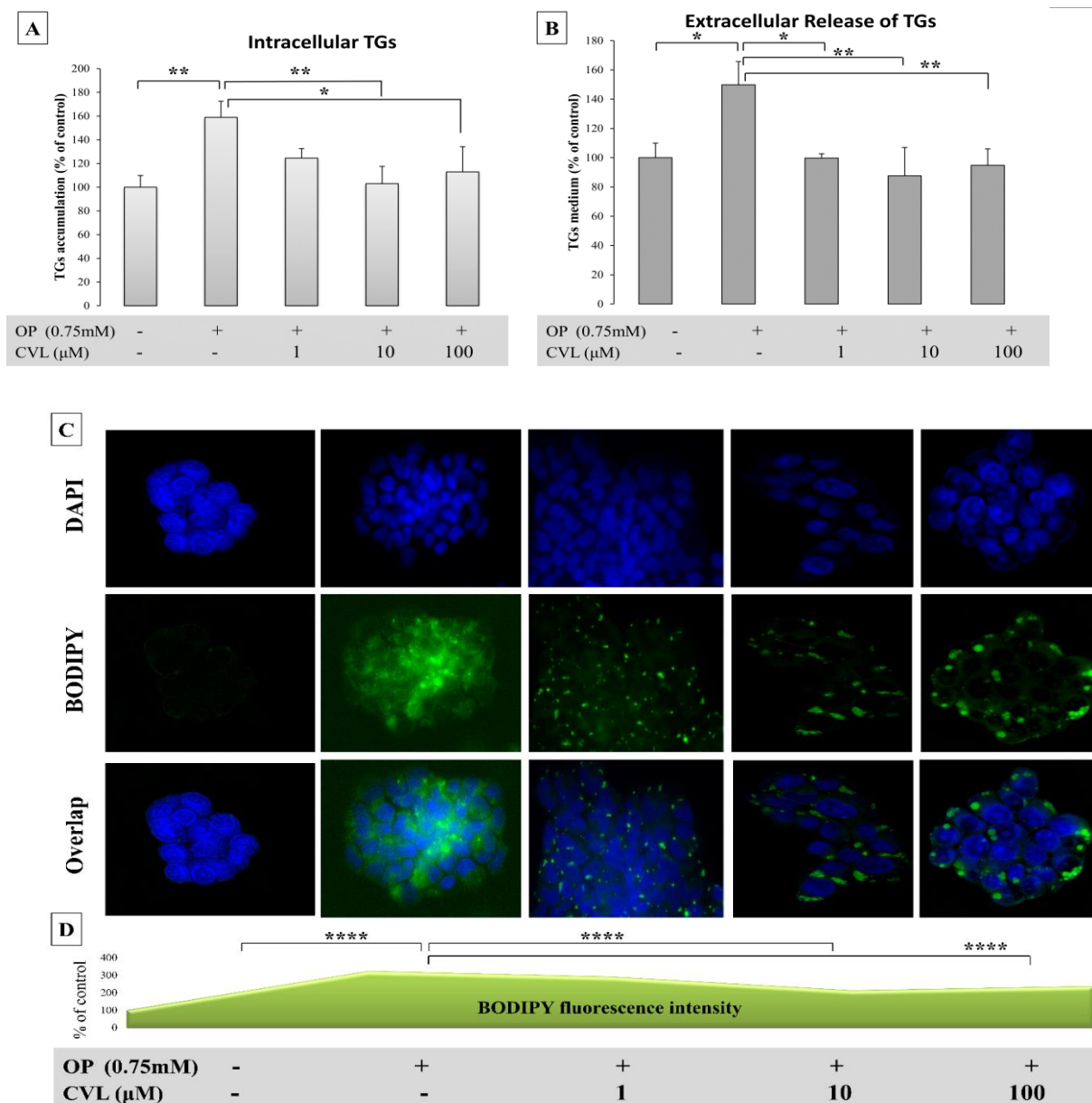
Figure 2.1 Effects of carvacrol on lipid accumulation in hepatic cells. In control and steatotic FaO cells (SC) treated with CVL (0, 1, 10 and 100 μM) for 24h we quantified: (A) intracellular TG content and (B) extracellular TG release into the medium by spectrophotometric assay; (C) neutral lipid accumulation by BODYPI staining and fluorescence microscopy. Images were acquired at Leica DMRB light microscope equipped with a Leica CCD camera DFC420C (Leica, Wetzlar, Germany), magnification 100x; Bar: 100μm. (D) Average fluorescence intensity of Lipid Droplets per cell calculated using ImageJ free software (http://imagej.nih.gov/ij/). Values are mean ± S.D from a least three independent experiments. Significant differences are denoted ,by symbols: *p≤0.05; **p≤0.01; ***p≤0.001; ****p≤0.0001.
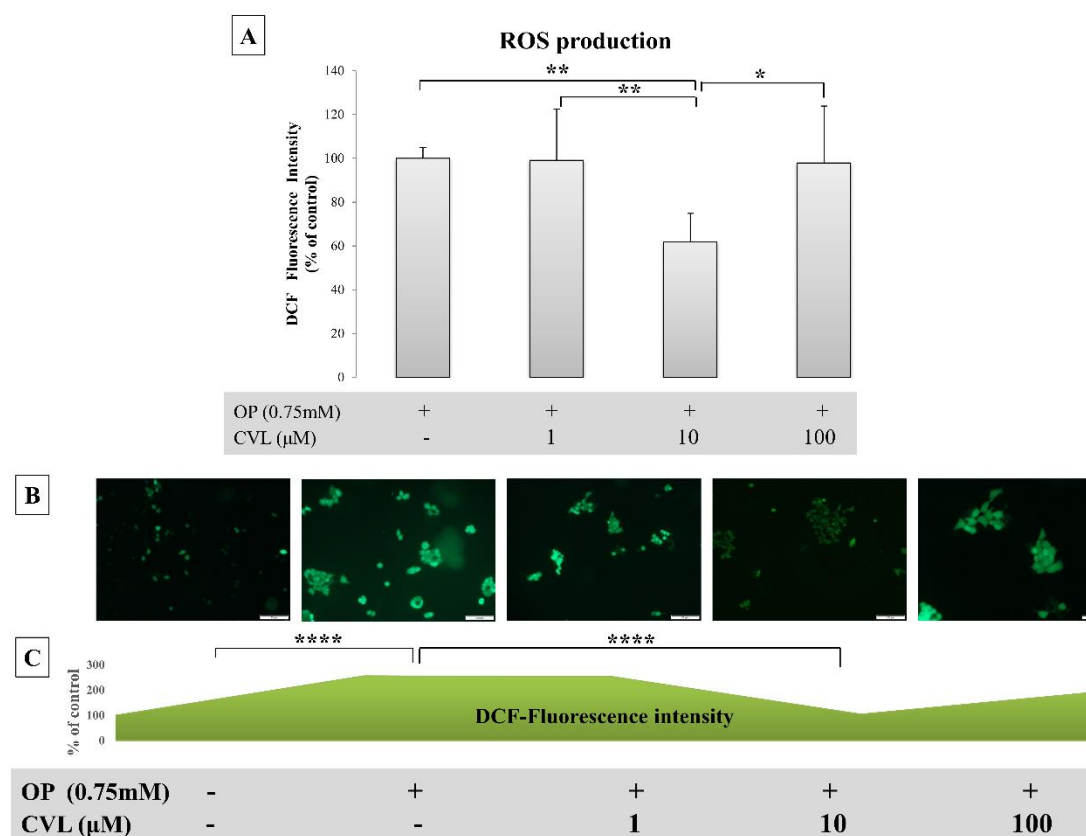
Figure 2.2 Effects of carvacrol on reactive oxygen species production in hepatic cells. The intracellular level of ROS, mainly hydrogen peroxide, were quantified (A) by spectrofluorimeter assay of DCF-stained FaO cells incubated in the absence (SC) or in the presence of CVL (1, 10 and 100 μ M). Values are mean ± S.D from a least three independent experiments. Significant differences are denoted by symbols: *p≤0.05; **p≤0.01; ****p≤0.0001 (B) the ROS level was visualized in situ by fluorescence microscopy. Images were acquired at Leica DMRB light microscope equipped with a Leica CCD camera DFC420C (Leica, Wetzlar, Germany), magnification 100x; Bar: 100 μ m. (C) Average fluorescence intensity of in situ ROS per cell were calculated using ImageJ free software (http://imagej.nih.gov/ij/). Values are mean ± S.D from a least three independent experiments.

2.3.2. Carvacrol protects the endothelial cells from the radical-dependent oxidative stress and dysfunction

Endothelial cells were exposed to 100 μM H_2O_2 for 1h to mimic an oxidative insult. The intracellular ROS production was quantified by fluorimetric analyses of DCF-stained

Beneficial Effects of Carvacrol on In Vitro Models of Metabolically-Associated Liver
Steatosis and Endothelial Dysfunction: A Role for Fatty Acids in Interfering with Carvacrol
Binding to Serum Albumin

HECV cells after treatments with carvacrol for 24 h (0, 1, 10 and 100 μM) (Figure 2.3A).

Exposure of endothelial cells to H_2O_2 resulted in a significant increase in DCF fluorescence

(+32%; p≤0.05), that was reduced by carvacrol leading to a significant decrease of -38%

(p≤0.05) and -68% (p≤0.0001) for 1 and 10 μM concentrations, respectively. A slight and not

significant decrease of DCF was observed upon carvacrol 100 μM treatment.
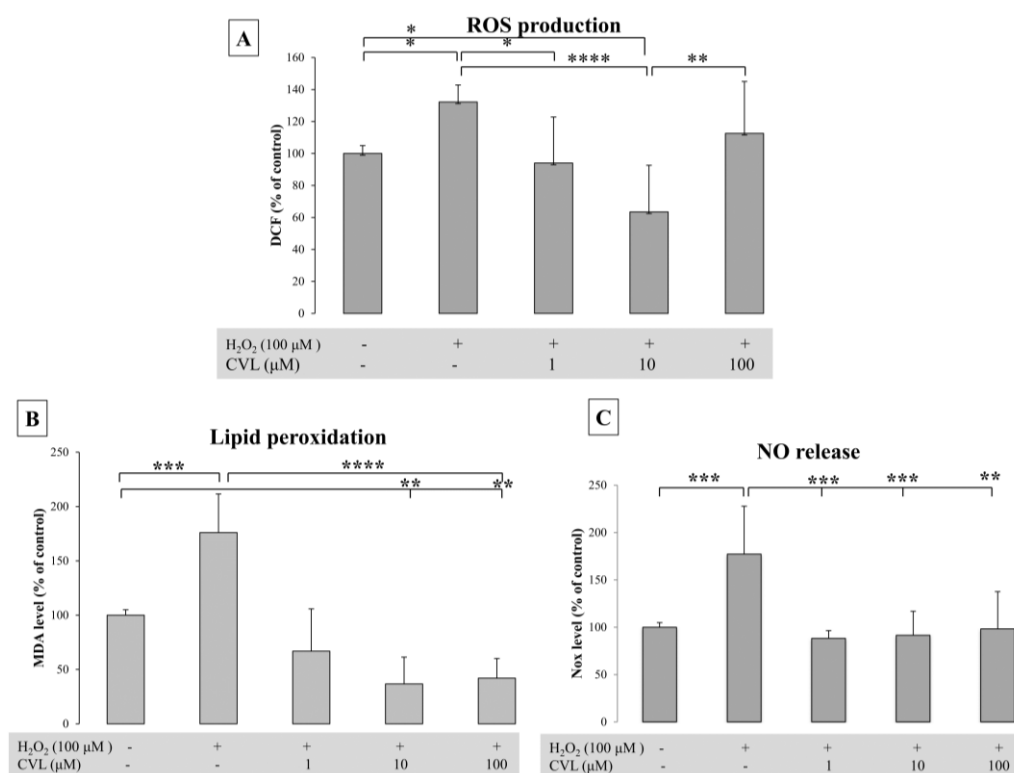
Figure 2.3 Effects of carvacrol on oxidative stress in endothelial cells. HECV cells exposed to H2O2 (100 μ

M) for 1h were then treated with CVL (1, 10 and 100 μ M) for 24h and analyzed. (A) ROS production was

quantified fluorometrically on DCF-stained cells as Fluorescence intensity arbitrary unit. (B) Intracellular

MDA level was quantified by TBARS assay as pmol MDA/mL x mg of sample protein; (C) Nitric oxide

production was quantified in the medium of HECV cells as μ mol NaNO2/mg sample protein by Griess

reaction. Values are expressed as % of control. Values are mean ± S.D from a least three independent

experiments. Significant differences are denoted by symbols: *p≤0.05; **p≤0.01; ***p≤0.001; ****p≤0.0001.

The down-stream effects of a ROS excess were assessed by quantifying the lipid-

peroxidation in terms of MDA production. In details, HECV cells exposed for 1h to 100 μM

H_2O_2, showed a marked increase in MDA level (+76%; $p \leq 0.001$) with respect to control (Figure 2.3B) However, treatment of H_2O_2-insulted HECV cells with increased concentrations of carvacrol (1, 10 and 100 μM) decreased significantly the MDA level about -109%, -139%, and -134% respectively; ($p \leq 0.0001$).

Wound size (% of control)

Hours	Ctrl	H_2O_2	CVL 1	CVL 10	CVL 100
0	100	100	100	100	100
6	84.30	87.91	84.97	87.08	89.73
24	51.24	67.22*	47.58#	54.71	64.33
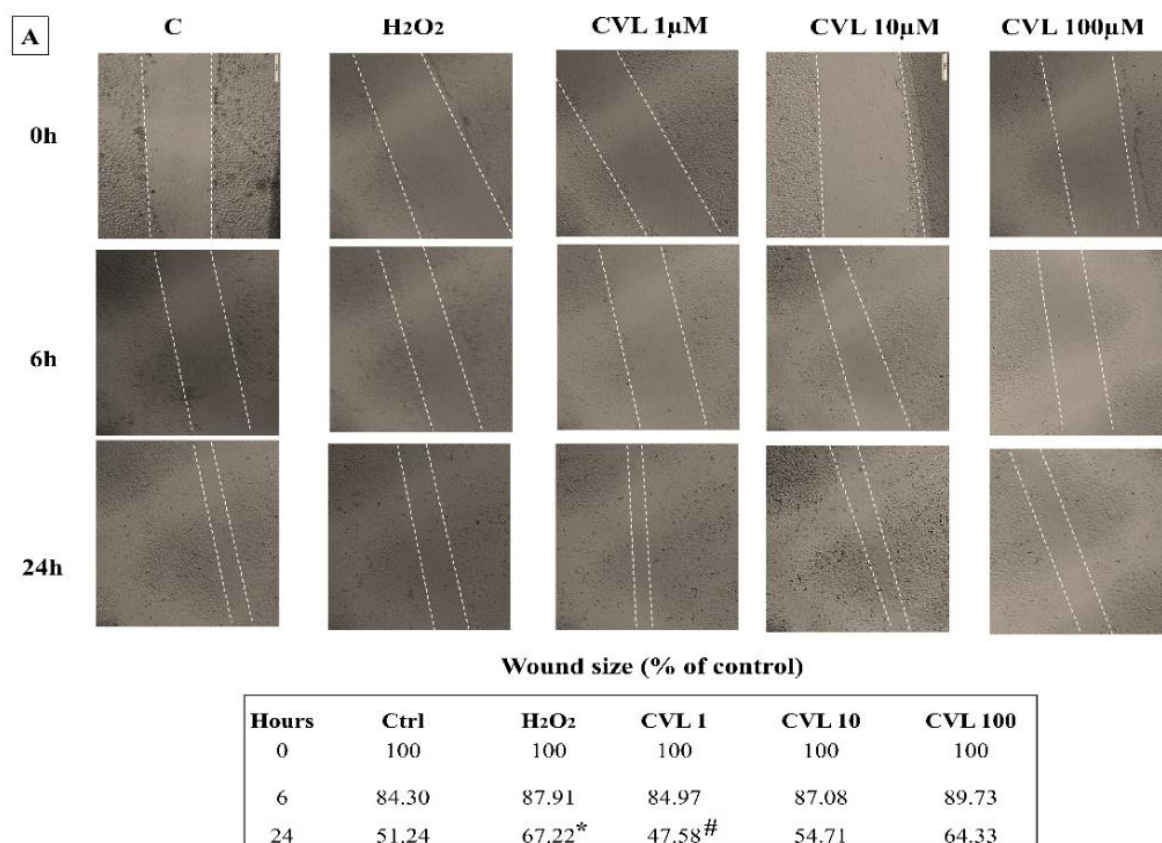
Figure 2.4 Effect of carvacrol on wound healing. HECV cells treated as described above were subjected to wound healing assay as described in Materials and Methods. (A) Images were acquired at 0, 6 and 24 h from the beginning of the assay using Leica DMRB light microscope equipped with a Leica CCD camera DFC420C (Leica, Wetzlar, Germany), magnification 4x; Bar: 100 μ m. T scratch assay representative images: the dotted lines define the areas lacking cells, the table reported the wound size as percentage of control at t0.

The effect of carvacrol on NO production; an important regulator in various types of inflammatory processes, was also assessed in HECV cells using Griess reagent. In H_2O_2-insulted cells, we observed a stimulation of NO release (+77% with respect of control, $p \leq 0.001$) (Figure 2.3C). Treatment with carvacrol decreased the NO release compared to H_2O_2-

Beneficial Effects of Carvacrol on In Vitro Models of Metabolically-Associated Liver
Steatosis and Endothelial Dysfunction: A Role for Fatty Acids in Interfering with Carvacrol
Binding to Serum Albumin

insulted cells of about -89% and -85% (for 1 and 10 μM, respectively; $p \leq 0.001$) and of -79%

(for 100 μM; $p \leq 0.01$).

B
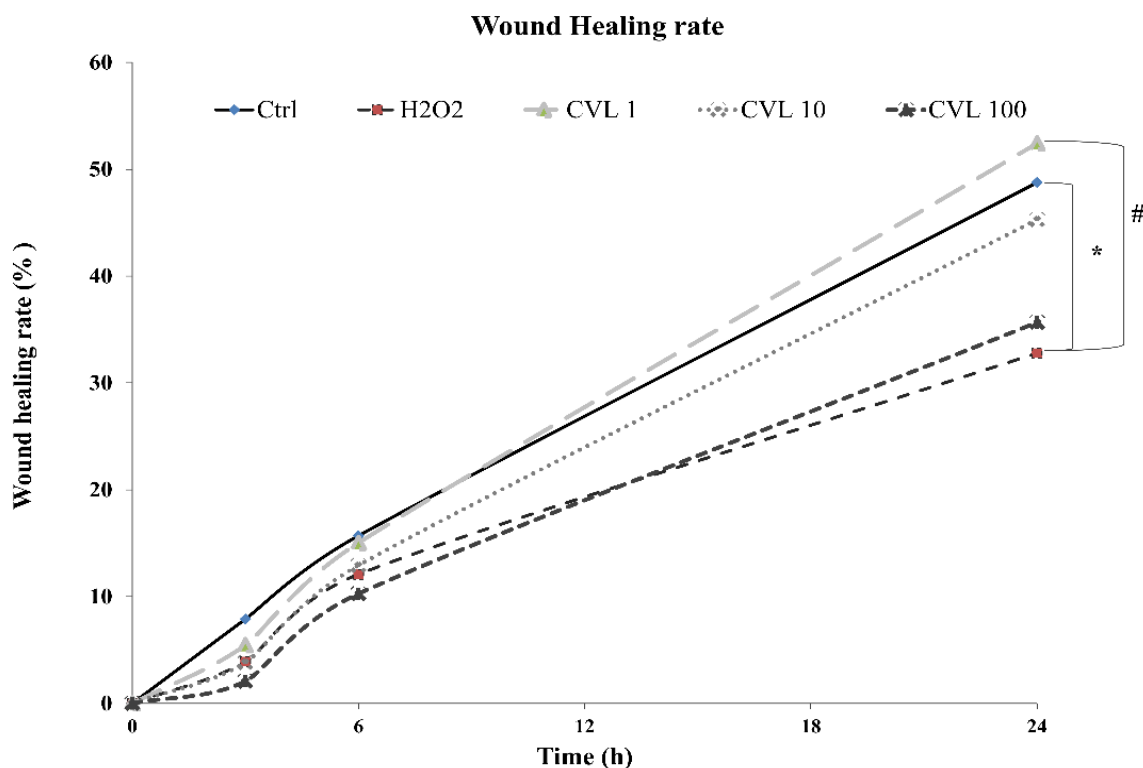
Figure 2.4 (B) Graphs representing the percentage of the closed area as compared to time=0. Values mean ±

S.D from at least three independent experiments. Significant differences are denoted by symbols: *$p \leq 0.05$.

The possible effect of carvacrol on cell proliferation and migration was tested by T-

scratch assay (Figure 2.4 A). Induction of moderate oxidative stress with H_2O_2 resulted in a

significant impair of the wound healing process at 24h (-16% of wound repair with respect to

control $p \leq 0.05$), while no significant differences in cell migration rates were noticed at 6h after

the scratch. Interestingly, only the lowest concentration of CVL (1μM) was able to accelerate

the wound healing resulting in a wound repair significantly higher to that of H_2O_2-insulted

cells (at t24, +18 % wound repair compared to H_2O_2-insulted HECV cells; $p \leq 0.05$) ((Figure

2.4 B).

Beneficial Effects of Carvacrol on In Vitro Models of Metabolically-Associated Liver
Steatosis and Endothelial Dysfunction: A Role for Fatty Acids in Interfering with Carvacrol
Binding to Serum Albumin
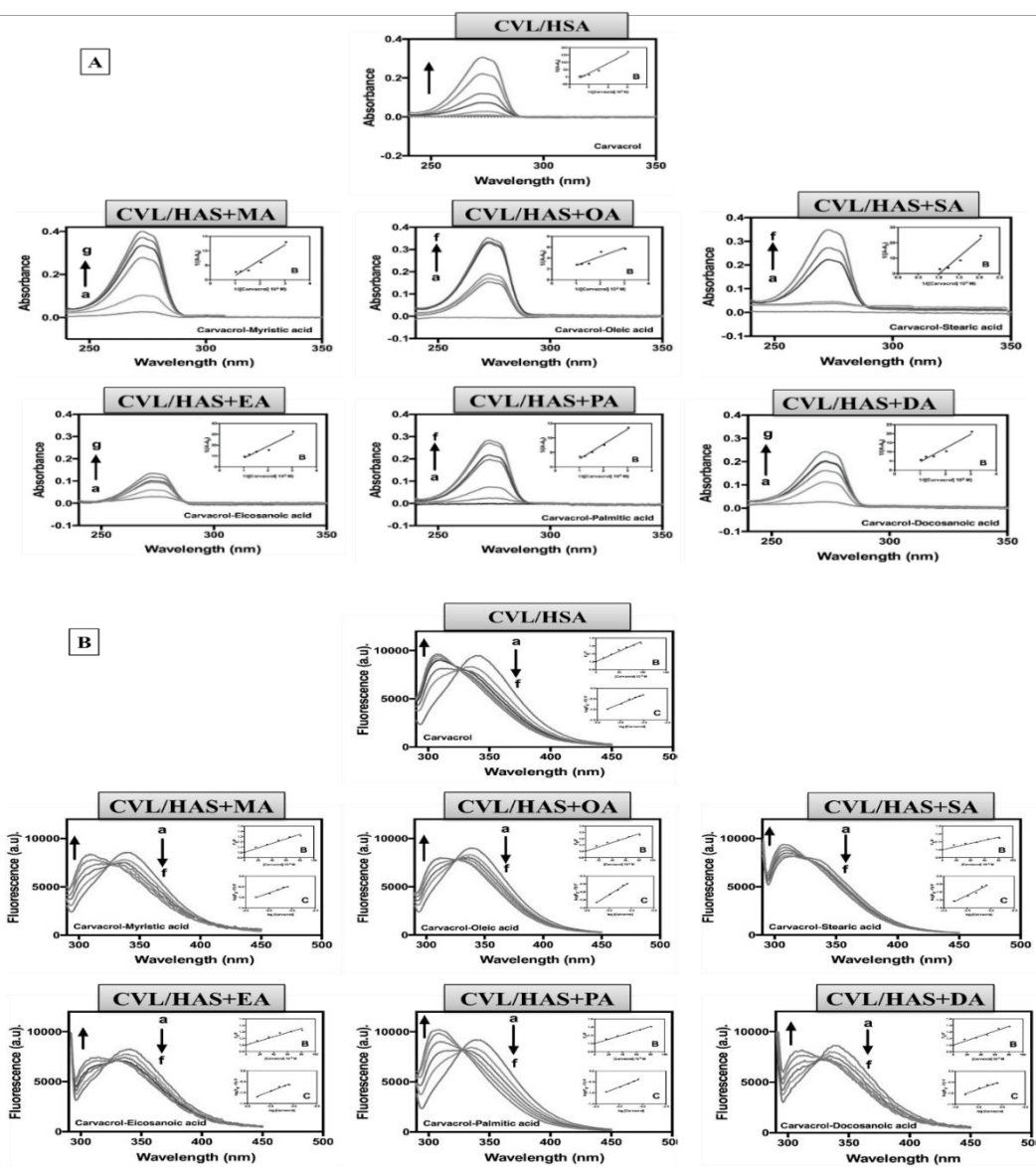
Figure 2.5 Carvacrol binding to human serum albumin in the absence and in the presence of FAs. Spectra for

CVL/HSA binding in absence or in presence of different FAs. Each successive curve was recorded after

accumulative addition of carvacrol (covering the range from 0 to 0.96 mM) to HSA solution (15 μM) in

absence or in presence of different fatty acids (150 μM of each FA; molar ratio HSA:FAs 1:10): Myristic acid

(MA-C14), Palmetic acid (PA-C16), Oleic acid (OA-C18), Stearic acid (SAC18), Eicosanoic acid (EA-C20),

Docosanoic acid (DA-C22). (A) Differential absorbance spectra were recorded in the range 240-350 nm using

a Cary Varian1 spectrophotometer. (B) Fluorescence spectra were recorded using a Hitachi 4500

spectrofluorimeter. All experiments were conducted in 50 mM potassium phosphate buffer (pH 6.8) at room

temperature (25° C). Direction of the arrows shows the increase of HSA-CVL concentration.

2.3.3. Exogenous FAs modulate Carvacrol−HSA binding

Carvacrol binds serum albumin for its transport in the blood, but also long-chain non-esterified fatty acids are vehiculated by albumin. In order to investigate if high levels of circulating FAs may interfere with the carvacrol binding to albumin we employed absorption and emission spectroscopy. For the analyses we employed the most common dietary long-chain fatty acids: Myristic acid (MA, C14:0), Palmitic acid (PA, C16:0), Oleic acid (OA, C18:1), Stearic acid (SA, C18:0), Eicosanoic acid (EA, C20:0) and Docosanoic acid (DA, C22:0) (Table 2.1). The analyses were performed using either low (15 μM) or high (150 μM) concentrations of each FA.

Differential absorption spectra of HSA in the presence of carvacrol at increasing concentrations (from 0 to 0.96 mM) were recorded in the absence or in the presence of distinct FAs. As shown in Figure 2.5A, the CVL/HSA complex leads to a maximum of absorbance at 272 nm. The increasing binding of CVL to albumin produced the increase of 272 nm peak in the differential absorption spectra. From the spectra we calculated the intrinsic binding constant (Ka) of carvacrol to HSA using equation 1 reported in Materials and Methods paragraph. When the Ka values were recorded in the presence of different FAs at high concentration (1:10 HSA/FA molar ratio), we obtained the Ka values listed in Table 2.2. A Ka value of $1.82 \ 10^3 \ M^{-1}$ was recorded for CVL/HSA in the absence of FAs, while the Ka values dramatically decreased in the presence of 150 μM of each FA: 0.403 (for DA), 0.286 (for EA), 0.765 (for MA), 0.636 (for OA), 0.519 (for PA) and 0.205 (for SA) $10^3 \ M^{-1}$. The largest interfering effects were produced by the saturated fatty acids EA and SA which reduced Ka of about 8, times comparing to CVL/HSA alone. On the other hand, a Ka reduction of about 3 times was observed for the other FAs.

The possible interfering effects of FAs on CVL/HSA binding were also investigated by emission spectroscopy int the above conditions. As shown in Figure 2.5B, after each addition of carvacrol, a gradual decrease in the fluorescence intensity and a blue shift (from 342nm to 312nm) with the appearance of isosbestic point at 326 nm, were observed in the emission spectra of HSA. When the binding constant (Kb) for CVL/HSA was calculated we found a Kb of 3.154 10^3 M^{-1}, which was approximately three times higher than that calculated in the presence of different FAs. The Kb values for CVL/HSA were reduced to 1.37, 1.108, 1.747, 1.95, 1.484, and 1.09 10^3 M^{-1} in the presence of 150 μM of DA, EA, MA, OA, PA and SA respectively (Table 2.2). Therefore, the fluorescence analyses confirmed the spectrophotometric measurements showing that the largest interfering effects were produced by the saturated fatty acids EA and SA which reduced Kb of about 3 times, while a lower effect was observed for the other FAs.

From all the results we can conclude that carvacrol has a rather low affinity for albumin (the binding constants Ka and Kb are rather low), and that this binding is further reduced   as by the presence of high concentrations of FAs in solution (1:10 HSA/FA molar ratio).

For a deeper understanding of the interfering effects of FAs on the CVL binding to serum albumin, we recorded the fluorescence quenching in the absence or in the presence of different FAs, as described in Materials and Methods section (Figure 2.5 B). The quenching constant Ksv for HSA/CVL was 540.9 10^3 M^{-1}, and it was reduced in the presence of FAs. In details, the Ksv decreased to 396.8, 315.6, 429.9, 345.5, 519.6 and 200.5 10^3 M^{-1} in the presence of DA, EA, MA, OA, PA and SA, respectively (Table 1). As well, quenching analyses confirmed that SA and EA showed the highest interfering potential against HAS/CVL binding. The number of binding sites (n) for CVL in the HSA molecule was calculated by Eq.3 and Eq.4 as

Beneficial Effects of Carvacrol on In Vitro Models of Metabolically-Associated Liver
Steatosis and Endothelial Dysfunction: A Role for Fatty Acids in Interfering with Carvacrol
Binding to Serum Albumin

described in Materials and Methods (Table1). The n value is about 1 (~ 0.7) both in the absence

or in the presence of FAs.

As control, we carried out the same experiments of CVL/HSA binding in the presence

of low concentrations of FAs (1:1 equimolar with HSA) corresponding to those observed in

humans in physiological conditions. We did not observe any relevant interfering effect of FAs

at low concentration on CVL/HSA binding (data not shown).

Table 2.2 For carvacrol (CVL) binding to human albumin (HSA) we listed the binding constants calculated by

absorption (Ka) and fluorescence spectroscopy (Kb), the fluorescence quenching constant (Ksv) and the

number of binding sites (n). All the values were calculated in the absence and in the presence of 150 μM of

each of the following long chain fatty acids: Myristic acid (MA-C14), Palmetic acid (PA-C16), Oleic acid (OA-

C18), Stearic acid (SA-C18), Eicosanoic acid (EA-C20), Docosanoic acid (DA-C22).

Sample	Ka $(10^3 \, M^{-1})$	Kb $(10^3 \, M^{-1})$	Ksv $(10^3 \, M^{-1})$	n
CVL+HSA	1.82	3.154	540.9 ($\pm$ 33.3)	0.70
CVL+HSA-DA	0.403	1.37	396.8 ($\pm$ 27.4)	0.73($\pm$0.08)
CVL+HSA-EA	0.286	1.108	315.6 ($\pm$ 17.0)	0.81($\pm$0.07)
CVL+HSA-MA	0.765	1.747	429.9 ($\pm$ 18.4)	0.76($\pm$0.05)
CVL+HSA-OA	0.636	1.95	345.5($\pm$ 16.9)	0.70($\pm$0.08)
CVL+HSA-PA	0.519	1.484	519.6 ($\pm$ 11.3)	0.82($\pm$0.06)
CVL+HSA-SA	0.205	1.09	200.5 ($\pm$ 12.5)	0.60($\pm$0.08)

2.4. DISCUSSION

In order to explore novel nutraceutical candidates, we tested the beneficial effect of

carvacrol in cellular models of metabolic disorders. Our results show that carvacrol ameliorated

lipid accumulation and oxidative stress in a model of hepatic steatosis and protected against

oxidative stress and dysfunction in a model of endothelial dysfunction. As further insight, we observed that the binding of carvacrol to serum albumin is reduced by the presence of high concentrations of long-chain fatty acids, which are known to be increased in patients with metabolic disorders.

A wide range of biological and pharmacological activities has been already descripted for carvacrol [77]. Many studies described the beneficial effects of this polyphenol in metabolic disorders linked to fatty liver. Kim et al., [78] reported the protective effect of carvacrol against hepatic steatosis in mice fed with high-fat. Moreover, many cellular and animal studies reported the hepatoprotective[79], [80] antihyperlipidemic [81], anti-inflammatory [82] and antioxidant [83] proprieties of carvacrol.

Simple hepatic steatosis, defined as an excess of fat stored in the hepatic parenchima, is the initial step of NAFLD, a condition that may progress to steatohepatitis, fibrosis, and ultimately cirrhosis [84]. Liver steatosis in humans is often associated with the metabolic syndrome and becomes predictive of increased cardiovascular risk. A definitive therapy for NAFLD is missing so far, although several drugs and nutraceuticals are being tested alone or in combination [47].

In order to test the beneficial effects of carvacrol we used rat hepatoma FaO cells exposed to a mixture of oleate/palmitate, which represent a reliable *in vitro* model for hepatic steatosis that has been widely employed in previous studies of our group [26], [85]. Data from intracellular TG quantification and LD microscopical analysis showed that all the carvacrol concentrations were effective on reducing the moderate steatosis. However, the intermediate concentration (10 μM) was the most effective leading to a fat reduction of about -50% compared to steatotic cells. Excess fat accumulation in hepatic cells is typically accompanied by increased oxidative stress [86]. We observed an increase in the intracellular ROS production

Beneficial Effects of Carvacrol on In Vitro Models of Metabolically-Associated Liver
Steatosis and Endothelial Dysfunction: A Role for Fatty Acids in Interfering with Carvacrol
Binding to Serum Albumin

in steatotic cells compared to controls and a reduction when steatotic cells were treated with carvacrol. Also in this case the intermediate carvacrol concentration (10 µM) was the most effective.

Endothelial damage is typically observed in metabolic syndrome as vascular endothelium is a major target of body oxidative stress which results from excess fat accumulation in the liver and adipose tissue [87]. ROS-induced endothelial dysfunction can increases vascular endothelial permeability and promotes leukocyte adhesion promoting early stage of atherosclerosis [88]. Endothelial cells exposed to hydrogen peroxide can mimic what happens *in vivo* in early atherosclerosis [89]. We showed that the H_2O_2-induced ROS generation and lipid peroxidation in HECV cells was counteracted by carvacrol treatment. Although all carvacrol concentrations reduced lipid peroxidation, the intermediate concentration (10 µM) was the most effective. Endothelium dysfunction is typically associated to changes in NO release, and we measured an increase in NO release upon exposure of HECV cells to oxidative insult such as H_2O_2, which was counteracted by carvacrol at all test concentrations. Chronic and non-healing wounds are associated with many disorder conditions and pathologies such as diabetes, obesity, and cardiovascular diseases [90]. Interestingly, our results showed that carvacrol was able to accelerate the wound repair after oxidative insults such as hydrogen peroxide. In HECV cells, carvacrol accelerated the cell migration that was impaired by H_2O_2. In particular, the lowest concentration of carvacrol (1 µM) was the most effective dose. This result suggests that carvacrol ameliorates the wound healing process in insulted endothelial cells, which represent a potential therapeutic agent against many disorders where oxidative stress and chronic wound are involved. Taken together, the data indicate a good potential of carvacrol as lipid lowering agent in steatotic hepatocytes and as antioxidant and anti-inflammatory agent in endothelial cells. We would emphasize as oxidative and

nitrosative stress pathways represent a link between the fatty liver and chronic inflammatory conditions that characterize metabolic syndrome such as endothelial dysfunction and atherosclerosis.
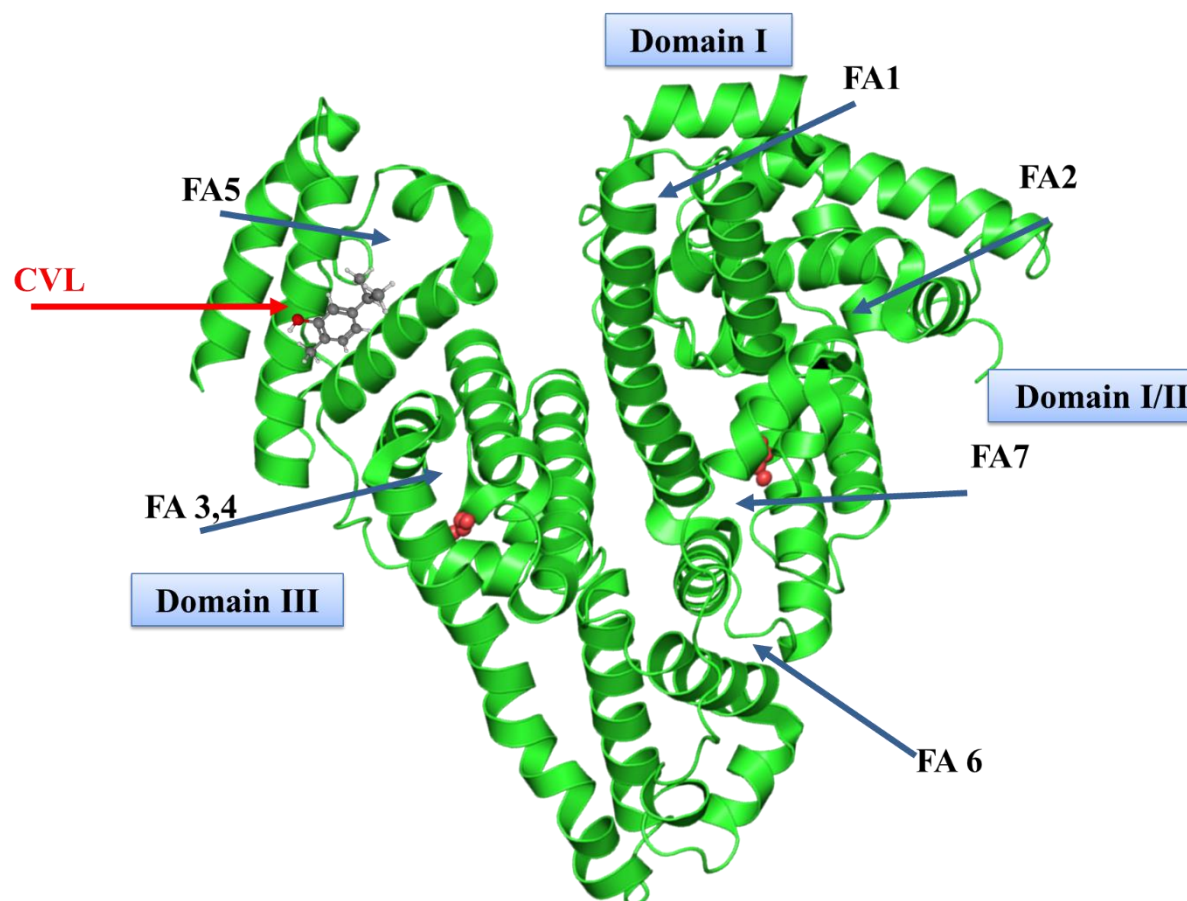
Figure 2.6 3D structure of human serum albumin and binding to carvacrol. The three dimensional (3D) structure of human serum albumin was downloaded from Protein Data Bank (PDB: https://www.rcsb.org/structure/4K2C). Localization of the three domains I, II and III and the seven major fatty acid binding sites (FABS 1-7) were shown. Carvacrol binding to the FABS 5 according to molecular docking study.

In searching for novel nutraceuticals with beneficial potential against fatty liver and metabolic disorders their transport in the blood must be tested as it largely influences bio-distribution, circulatory half-life and, consequently, pharmacokinetics of the compounds. Albumin is able to bind a wide variety of exogenous and endogenous substances and transport

them across the body. As carvacrol has a poor water solubility (1.25 mg/mL at 25 °C), it needs albumin for the transport in the blood [91]. Our experimental data by spectrophotometric and fluorimetric analyses found low binding constant values (Ka and Kb, respectively) for CVL/HSA binding of suggesting a rather low affinity of carvacrol for albumin. This low affinity may guarantee the efficient transport of carvacrol in the blood, but also its release in peripheral tissues.

Also long chain fatty acid are vehiculated by albumin which can bind up to seven FAs at the fatty acid binding sites (FABS) identified from 1 to 7. Each FABS shows a different affinity for FA binding (Figure 2.6). The subdomain IIIA is the preferential high affinity-binding site for FAs, while drugs prefer to bind the subdomains IIA and IB. However, the FA binding sites could overlap with the drug binding sites (Sudlow's sites I and II) [92], [93]; moreover, the binding of FAs could induce conformational changes in HSA resulting in the formation of new drug binding sites [94], [95]. Studies of molecular docking indicated that carvacrol preferentially binds to the FABS5 in the albumin 3D structure [96] (Figure 2.6). Our hypothesis was that the presence of high levels of fatty acids binding to HSA could influence the binding of CVL and interfere with its transport to the peripheral tissues. Both cooperative and competitive interactions between fatty acids and different classes of ligands have been reported in a number of studies on HAS [97], [98].

We tested the hypothesis that CVL/HSA binding might be altered by the simultaneous binding of FAs by spectrophotometric and fluorimetric measurements. At low concentrations (1:1 molar ratio with HSA) FAs did not significantly affect the carvacrol binding to HSA. We observed a decrease in the binding constants Ka and Kb, as well as in the fluorescence quenching constant Ksv, for CVL/HSA interaction in the presence of high levels of FAs. This may depend on the modification of HSA conformation due to FA binding which hinders the

insert of carvacrol molecule in the pocket of HSA. The larger effects were described for the saturated fatty acids EA (C20) and even more for SA (C18), which were able to reduce the binding constants (Ka and Kb) and the fluorescence quenching constant (Ksv) more than other FAs. In a previous paper, Rizzuti et al. [99] performed multiple molecular dynamics simulations and they found that SA binds with high affinity preferentially the FABS5 site, the same site of CVL. Therefore, our data suggest that CVL and SA may compete for the same binding site in HSA that could explain the lower binding force of CVL in HSA pre-complexed with high concentration of SA. In the same manner, we hypothesized that also EA can bind tightly to HSA at the FABS5 thus competing with CVL.

Therefore, we can conclude that, in the presence of high levels of circulating fatty acids, as it occurs in patients with metabolic disorders, the transport of carvacrol by albumin is less efficient and this has to be considered for defining the dose of carvacrol to be used as nutraceutical in patients with high fatty acid plasma levels such obese and NAFLD patients. However, further translational and clinical research needs to clarify tis important issue.

Chapter 3   Influence of Simulated In Vitro Gastrointestinal Digestion on the Phenolic Profile, Antioxidant, and Biological Activity of Thymbra spicata L. Extracts

3.1.   Introduction

Dietary phytochemicals are found abundantly in fruits, vegetables, grains, plant-based foods, and beverages [100]. Consumption of phytochemicals plays a main role in healthcare by preventing many chronic diseases including non-alcoholic fatty liver disease (NAFLD) [101], cardiovascular disease [102], neurodegenerative diseases [103], and some types of cancer [104]. For this reason, extracts from plants or plant parts have been largely tested to develop new functional foods for preventing/counteracting many chronic disorders [20]. Phenolic compounds (PCs) are the most abundant phytochemicals in many edible and medicinal plants, and they are the main responsible agents for the beneficial effects, especially the defense against oxidative stress [105]. PCs include numerous varieties of compounds classified into flavonoids and non-flavonoids: flavonoids include flavonols, flavones, flavan-3-ols, flavanones, and anthocyanins; non-flavonoid compounds include phenolic acids, volatile phenols, stilbenes, lignans, and coumarins [106].

Importantly, the bioavailability of several plant extracts as a source of PCs is likely affected by changes occurring during the gastrointestinal (GI) transit. Foods and nutraceuticals introduced by the oral route undergo digestive processes throughout GI compartments and cross physiological barriers that are able to influence their delivery [107]. Indeed, the main challenges for bioactive compounds are the rate and degree of absorption, as well as their solubility, stability, and permeability across the mucosal and intestinal barriers [108]. Moreover, metabolites can show completely different bioavailability compared to the parental phenolic compounds due to the physiological environment and cofactors [109], [110]. Experimental approaches using in vitro GI models can overcome difficulties associated with

human studies that are often poorly reproducible and comparable, expensive, time-consuming, and might generate ethical issues, depending on the study design and food being tested [111]. In fact, several digestion methods have been proposed in the literature review, often differing in the applied conditions. To give an example, the origin of the used enzymes (porcine, rabbit, or human); the environmental factors (pH, ionic strength, and digestion time); and other parameters such as the presence of phospholipids, digestive emulsifiers vs. their mixtures (e.g., pancreatin and bile salts), and the ratio of food bolus to digestive fluids, which alter enzyme activity, may considerably alter the results. While modifying some of these parameters with a possible and major impact on the matrix release or digestibility of some compounds, we were concerned with applying a standardized and practical simulated in vitro GI digestion method based on physiologically relevant conditions that can be applied for various endpoints and may be amended to accommodate further specific requirements mainly developing a more accurate in vitro human digestion model, taking into consideration the intestinal microbiota presence and conditions.

Lamiaceae is a family of mostly shrubs and herbs with a wide distribution worldwide, especially in the Mediterranean basin [1]. In this family, Thymbra spicata L., locally known as "Za'atar", is employed in the folk cookery (as salad or tea infusion), but also in traditional medicine, mainly for its antimicrobial and antiseptic properties [20]. Recent studies have revealed several beneficial properties of T. spicata L. leaves such as antioxidant, hypocholesterolemic, and anti-steatotic activities [10], as well as anti-inflammation [112], anti-proliferative, and pro-apoptotic [42] potential. The abundance of PCs in T. spicata L. leaves including phenolic acids (rosmarinic acid), phenolic monoterpenoids (carvacrol, thymol), and flavonoids (both glycosides and aglycones) stand behind the wide array of its pharmacological activities [7], [113]. The beneficial effects of T. spicata L. as herbal medicine or nutraceutical

preparation might be modified during the GI transit where the bioconversion is elicited by low gastric pH, digestive enzymes, and the microbiota [109].

In this context, our study aimed to assess if and how two different extracts from T. spicata L. aerial parts were modified after applying a simulated in vitro GI digestion method. The extracts before and after digestion were characterized for their composition in bioactive compounds and their antioxidant potential. The biological effects were assessed by cellular studies focusing on the antiproliferative capacity on different cancer cell lines.

3.2. Materials and Methods

3.2.1. Reagents and Enzymes

All reagents otherwise indicated, including enzymes, were purchased from Sigma-Aldrich Corp. (Milan, Italy). All reagents were of analytical purity.

3.2.2. Sources and Activities of Enzymes:

•   α-Amylase from human saliva (A0521-500 units/mg). α-Amylase catalyzes the hydrolysis of α-1,4 glycosidic linkage in oligosaccharides.

•   Pancreatin from porcine pancreas (P3292-100G). Pancreatin contains enzymatic components including trypsin, amylase and lipase, ribonuclease, and protease, produced by the exocrine cells of the porcine pancreas.

•   Pepsin from pig gastric mucosa (≈2500 units/mg protein). Pepsin is an aspartic endproteinase used for the unspecific hydrolysis of proteins and peptides in acidic media.

3.2.3. Plant Collection

Aerial parts of Thymbra spicata L. were collected from flowering plants growing in "Maarakeh", South Lebanon. Voucher specimen (L1.125/1) was authenticated by Prof. G.

Tohme (CNRS, Beirut, Lebanon) and was kept in the Herbarium of the Botanical Department-Lebanese University (Beirut, Lebanon). The in vitro gastrointestinal (GI) digestion of T. spicata aerial parts was performed according to protocol [114] with slight modifications in order to sequentially simulate the mouth, stomach, and small intestine digestion. The composition of buffers is reported in Table 3.1.

Table 3.1 Chemical composition of the buffer employed in the simulated digestion. SSF: salivary fluid; SGF: gastric fluid; SIF: intestinal fluid.

Volume (mL)						
Simulated Digestion Fluid	pH	KCl (0.5M)	KH2PO4 (0.5M)	NaHCO3 (1M)	NaCl (1.5M)	MgCl2(H2O)6 (0.15M)	Na2CO3 (0.5M)
SSF	7	15.1	3.7	6.8	-	0.5	0.06
SGF	3	6.9	0.9	12.5	11.8	0.4	0.5
SIF	7	6.6	0.8	42.5	9.6	1.1	-

3.2.4.   In Vitro Simulated Digestion

3.2.4.1.   Oral Digestion

To mimic the oral digestion, 25 g of T. spicata dried and powdered aerial parts were mixed with 25 mL SSF and 3 mL (stock 75 U/mL) α-salivary amylase (from human saliva), 0.2 mL CaCl2, and 5.8 mL distilled H2O and then incubated for 2 min at 37 °C on a magnetic stirrer.

3.2.4.2.   Gastric Digestion

To mimic the gastric digestion, 40 mL SGF, 7 mL pepsin (stock 25,000 U/mL), 0.03 mL CaCl2, and 3 mL distilled H2O were added to the oral outcome and the pH was lowered to

3.0 by HCl; the mixture was incubated for 2 h at 37 °C on a magnetic stirrer, and the pH was checked regularly.

3.2.4.3. Intestinal Digestion

To mimic the intestinal digestion, 50 mL of gastric outcome was mixed with 50 mL of SIF, 20 mL of pancreatin (stock 100 U/mL), 10 mL bile salt (stock 10 mM), 0.024 mL CaCl2, 6 mL distilled H2O, and 0.7 mL of 1 M HCl to neutralize the pH to 7.0.

3.2.4.4. Extract Preparation

The obtained mixture was incubated for 2 h at 37 °C on a magnetic stirrer. Then, the mixture was heated to 90 °C for 10 min to inactivate the enzymes used in the digestion process. At the end, the samples were centrifuged for 20 min at 7000 rpm. The pellet was incubated with ethanol (96%) at room temperature for 24 h with agitation. The solution was centrifuged for 20 min at 7000 rpm, obtaining a precipitate (TE) that was discharged, and the ethanol in the digested ethanolic extract (TE-dig) was removed using a rotavapor before the lyophilization of the residue. The supernatant obtained from the digestion process was divided into two parts. One part was lyophilized, obtaining the crude digested aqueous extract (TW-dig); the other one was dialyzed with membrane cut-off 3.5 kDa (Spectra/Por molecularporous membrane tubing, Thermo Fisher Scientific, Milan, Italy) against 250 mL of water for 24 h at 4 °C to separate the low molecular weight (mw) fraction (<3.5 kDa) and the high mw fraction (>3.5 kDa). The solutions inside the dialysis tube (>3.5 kDa) and out of the tube (<3.5 kDa) were lyophilized.

To prepare the undigested aqueous and ethanolic extracts (TW and TE, respectively), the same procedure was followed for extraction without the first part of enzymatic digestion. The detailed scheme of in vitro digestion and the obtained extracts and fractions is illustrated in Figure 3.1.
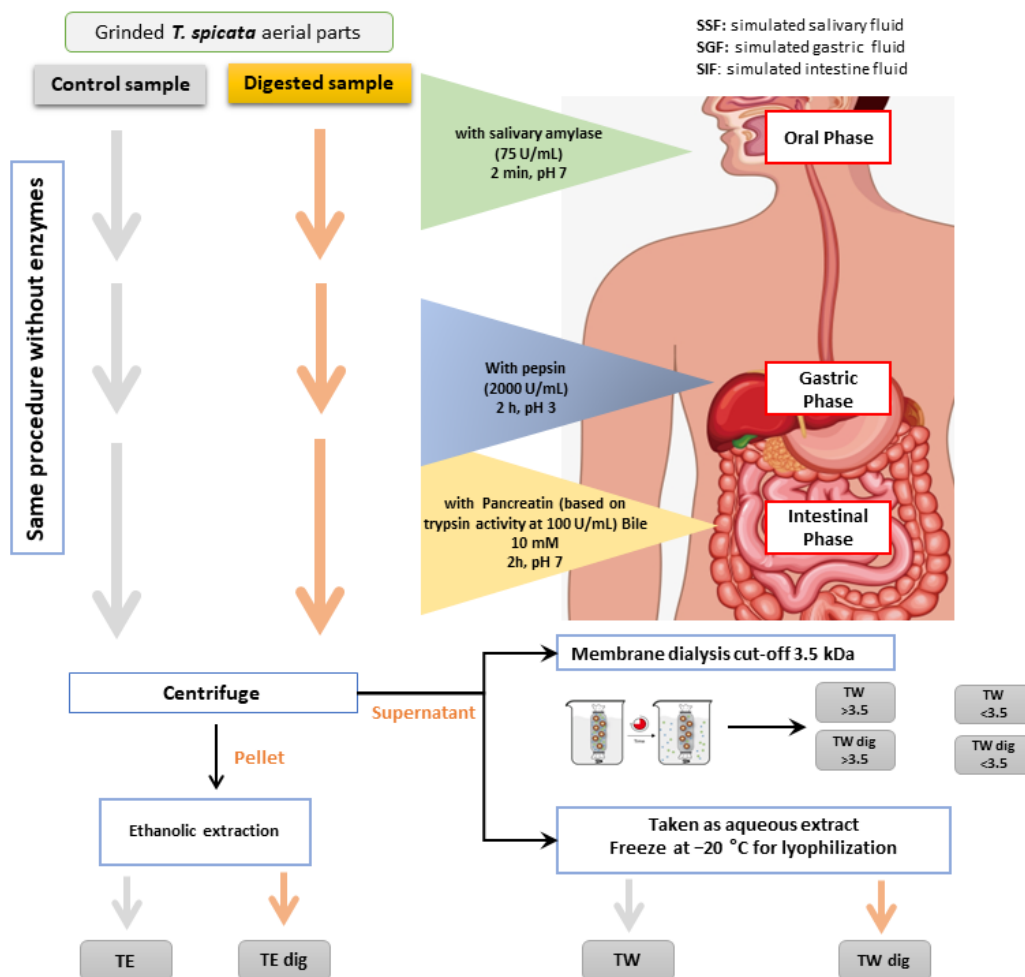
Figure 3.1 A schematic presentation describing the steps of the simulated digestion in the three phases: mouth, stomach, and intestine, in order to obtain the digested ethanolic (TE) and aqueous (TW) extracts. The same procedure was followed for preparation of crude extracts without the use of enzymatic digestion. The TW and TW dig were subjected to a membrane dialysis with a cut-off of 3.5 kDa to obtain low and high mw fractions.

3.2.4.5. Total Carbohydrate Content (TCC)

TCC was determined by the phenol-sulfuric acid colorimetric method [115]. Briefly, 0.5 mL of sample (1 mg/mL) was mixed with 0.5 mL 5% aqueous phenol and 2 mL of H2SO4 (96%). After incubation for 30 min at room temperature, the absorbance was read at 320 nm using a UV–VIS microplate reader (FLUOstar Optima, BMG Labtech, Ortenberg, Germany). The results were derived from a glucose calibration curve (0–200 µg/mL). Values are expressed as µg/mg extract.

3.2.5.   Total Protein Content (TPrC)

The protein content was determined by Bradford colorimetric method, using bovine serum albumin (BSA) as standard [67]. Briefly, 0.5 mL from each extract (1 mg/mL) was mixed with 0.5 mL of Bradford reagent; after 30 min incubation, the absorbance was measured at 595 nm using a UV–VIS microplate reader (FLUOstar Optima, BMG Labtech, Ortenberg, Germany). Data are expressed as $\mu g/g$.

3.2.6.   Total Phenol Quantification (TPC)

TPC was determined using the Folin–Ciocalteu method [116]. Briefly, 25μL aliquots of sample (1 mg/mL) were incubated with 125 μL of 10% (w/v) Folin–Ciocalteu reagent for 5 min; after adding 125 μL of Na_2CO_3 (10% w/v), the sample was incubated for 30 min in darkness at room temperature, and the absorbance was read at 320 nm using a UV–VIS microplate reader (FLUOstar Optima, BMG Labtech, Ortenberg, Germany). The results were derived from a gallic acid calibration curve (0–1000 ug/mL) prepared from a stock solution (1 mg/mL in ethanol). Values are expressed as mg of gallic acid equivalents (GAE) per gram of dried weight extract (mg of GAE/g extract).

3.2.7.   Total Flavonoid Quantification (TFC)

TFC was determined using the aluminium chloride colorimetric method [117]. Briefly, a 1 mL aliquot of sample (1 mg/mL) was mixed with 0.2 mL of 10% (w/v) methanolic $AlCl_3$ solution, 0.2 mL (1 M) potassium acetate, and 5.6 mL distilled H_2O. After incubation at room temperature in darkness for 30 min, the absorbance was read at 320 nm using a UV–VIS microplate reader. The results were derived from a calibration curve of quercetin (0–200 μg/mL) prepared from a stock solution (5 mg/mL in methanol). Values are expressed as mg of quercetin equivalent (QE) per gram of dried weight extract (mg of QE/g extract).

3.2.8.   Total Hydroxycinnamic Acid Content (THAC)

HCA was determined using the method by Custódio et al. [118]. Briefly, in a 96-well plate, 20 µL of sample (5 mg/mL) was mixed with 20 µL of 95% ethanol containing 0.1% HCl. After the addition of 160 µL of 2% HCl and 10 min incubation, the absorbance was read at 320 nm using a UV–VIS microplate reader. The results were derived from a calibration curve of rosmarinic acid (0–500 µg/mL) prepared from a stock solution (1 mg/mL in ethanol). Values are expressed as mg of rosmarinic acid equivalents (RAE) per gram of dried weight extract (mg of RAE/g extract).

3.2.9.   HPLC–MS Analysis

High-performance liquid chromatography coupled with tandem mass spectrometry (HPLC–MS/MS) was performed using an Agilent 1100 HPLC-MSD Ion Trap XCT system, equipped with an electrospray ion source (HPLC-ESI-MS) (Agilent Technologies, Santa Clara, CA, USA). Separation of extracts was performed on a Jupiter C18 column 1 × 150 mm with 3.5 µm particle size (Phenomenex, Torrance, CA, USA). As eluents, we used water (eluent A) and MeOH (eluent B), both added with 0.1% formic acid. The gradient employed was 15% eluent B for 5 min, linear to 100% eluent B in 35 min, and finally hold at 100% eluent B for another 5 min. The flow rate was set to 50 µL/min with a column temperature of 30 °C. The injection volume was 8 µL. Ions were detected in the positive and negative ion mode, in the m/z 100–800 range, and ion charged control with a target ion value of 100,000 and an accumulation time of 300 ms. A capillary voltage of 3300 V, nebulizer pressure of 20 psi, drying gas of 8 L/min, dry temperature of 325 °C, and 2 rolling averages (averages: 5) were the parameters set for the MS detection. MS/MS analysis was conducted using an amplitude optimized time by time for each compound. From the chromatograms, the percentage of PC for each extract was calculated based on the peak area.

3.2.10. Radical Scavenging Activity Assays

The radical scavenging activity was measured using the 1,1-diphenyl-2-picrylhydrazyl (DPPH) method [119]. In a 96-multiwell plate, 50 µL aliquot of sample (0–2 mg/mL) or of the standard Trolox (0–100 mg/mL) was added to 200 µL of DPPH solution (0.1 mM in methanol). After incubation in darkness for 30 min at 37 °C, the absorbance was measured at 490 nm using a UV–VIS microplate reader against DPPH solution as a blank. Values are expressed as half maximal inhibitory concentration IC50 (µg/mL) and Trolox equivalent (µg TE/mg dry extract).

The radical cation scavenging activity of each extract was measured using the 2-2′-azino-bis (3-ethylbenzo-thiazoline-6-sulphonate) diammonium salt (ABTS) method [120]. In a 96-multiwell plate, 50 µL aliquot of sample (0–2 mg/mL) was added to 200 µL of ABTS solution (5 mM). ATBS solution was prepared by oxidizing ABTS with MnO2 in distilled water for 30 min in the dark, and then the solution was filtered through filter paper. After 20 min incubation in darkness at room temperature, the absorbance was determined at 734 nm using a UV–VIS microplate reader against ABTS solution as a blank. Values are expressed as half maximal inhibitory concentration IC50 (µg/mL) and Trolox equivalent (µg TE/mg dry extract).

3.2.11. Ferric Reducing Antioxidant Power (FRAP) Assay

The reducing power was evaluated according to the ferric reducing antioxidant power (FRAP) assay [121]. In a 96-multiwell plate, 25 µL aliquot of sample (0–2 mg/mL) or of standard Trolox (0–100 µg/mL) was added to 175 µL of FRAP working solution containing 300 mmol/L acetate buffer (pH 3.6), 20 mmol/L ferric chloride, and 10 mmol/L TPTZ (2,4,6-tri (2-pyridyl)—S-triazine) made up in 40 mmol/L HCl. The three solutions were mixed at a 10:1:1 ratio (v:v:v). The mixture was incubated in darkness for 30 min at 37 °C and then the

absorbance was determined at 593 using a UV–VIS microplate reader against FRAP solution

as a blank. Values are expressed as Trolox equivalent (µg TE/mg dry extract).

3.2.12. Cell Culture

The human cancer cell lines MDA-MB-231 (breast adenocarcinoma), A375

(Melanoma), and HCT116 (colorectal carcinoma) were gently supplied from Prof. Bramucci

(Laboratory of Physiology, University of Camerino). The cancer cells were routinely

maintained in Dulbecco's modified Eagle's minimum essential medium (DMEM) or in RPMI-

1640 (Sigma-Aldrich, Beirut, Lebanon) supplemented with 10% heat-inactivated fetal bovine

serum (FBS), 2 mM glutamine, and 1% P/S at 37 °C in a humidified incubator containing 5%

CO_2.

3.2.13. Cell Proliferation Assay

The cytotoxicity of T. spicata extracts was assessed by the 3-(4,5-dimethylthiazol-2-

yl)-2,5-diphenyltetrazolium bromide (MTT) method [122]. Stock solution (50 mg/mL) of

extracts were prepared in dimethyl sulfoxide (DMSO) or in sterile distilled water. In addition,

the pure Carvacrol was used as positive control. Briefly, cells were seeded in a 96-well plate

(104 cells per well), and after 24 h, they were treated with increasing concentrations (0, 50,

100, and 200 µg/mL) of each extract for 24 h. At the end, 20 µL of MTT reagent (5.0 mg/mL)

was added, and the mixture was incubated for 3 h at 37 °C. After removing the unreacted MTT

dye, 100 µL DMSO was added to solubilize purple formazan crystals, and the absorbance was

recorded at 570 nm. The IC50 value (concentration that causes 50% growth inhibition) was

estimated as that leading to 50% absorbance decrease as compared to the control. Cell viability

was expressed in percentage with respect to the control.

3.2.14. Quantification of ROS Production

2′,7′-Dichlorodihydrofluorescein diacetate (H2DCF-DA; molecular probe) was employed to assess ROS generation [69]. Briefly, cells were seeded on a 96-well plate (105 cells/mL) and incubated overnight. After the treatments, cells were washed twice with PBS and then incubated with 10 μM of H2DCF-DA (in PBS) for 30 min at 37 °C. Then, ROS production level was measured fluorometrically using a microplate reader (lex = 495 nm; lem = 525 nm).

3.2.15. Quantification of Nitrite/Nitrate Levels

The nitric oxide NOx (nitrites and nitrates) level was measured by spectrophotometric measurement using the Griess reaction [71]. Briefly, 105 cells/mL were seeded on a 96-well plate and incubated overnight. After the treatments, NOx level in the medium was calculated using NaNO2 as a standard curve. Spectrophotometric analyses were performed at 546 nm using a microplate reader.

3.2.16. Statistical Analysis

All results were expressed as mean ± SD of at least three independent experiments. GraphPad Prism 8.0.1 software was used for statistical evaluation. Comparisons between different conditions were performed using ANOVA with Tukey's post-test. Difference between percentages was calculated by chi-squared test. The possible correlation between the measured parameters was tested by a two-tailed Pearson's correlation coefficient analysis. All statistical analysis were performed by GraphPad Software Prism 8.0.1, Inc. (San Diego, CA, USA).

3.3. Results

3.3.1. Characterization of T. spicata Extracts before and after Simulated Digestion

\
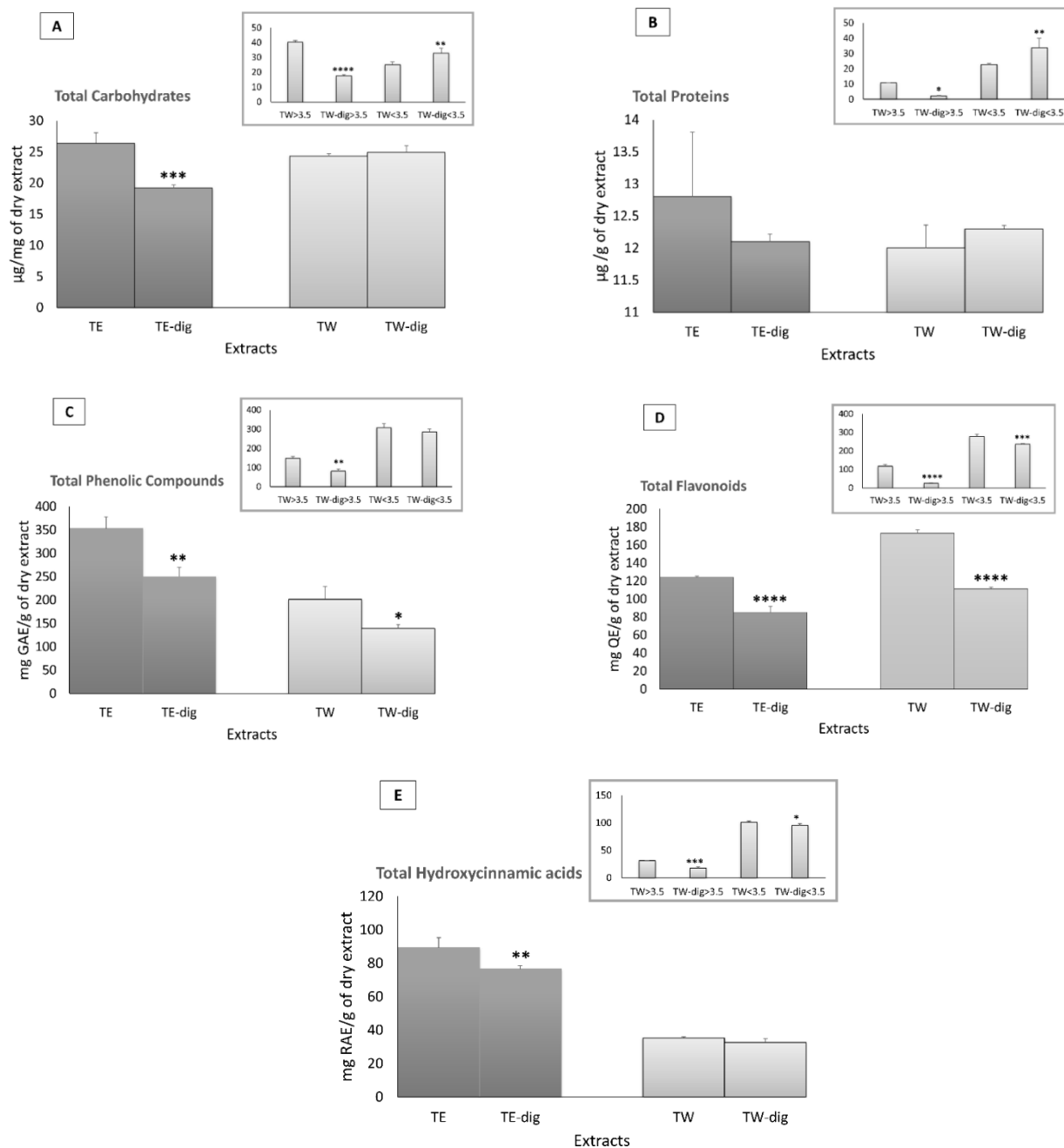
Figure 3.2 Quantification of total carbohydrate contents (TCC) (A), total protein content (TPrC) (B), total phenol content (TPC) (C), total flavonoid content (TFC) (D), and total hydroxycinnamic acid content (THAC) (E) of TW and TE, and dialyzed fractions before and after simulated in vitro digestion. All the contents were quantified spectrophotometrically and expressed as µg/mg of the dry extract, µg/g of dry extract, mg of gallic acid equivalent per g of dry powder extract (mg GAE/g dry extract), mg of quercetin equivalent per g of dry powder extract (mg QE/g dry extract), and mg of rosmarinic acid equivalents (RAE) per gram of dried weight extract (mg of RAE/g extract), respectively. Samples were measured in triplicate, and significant differences between digested and undigested extracts are denoted by symbols: * $p < 0.05$, ** $p < 0.01$, *** $p < 0.001$, and **** $p < 0.0001$.
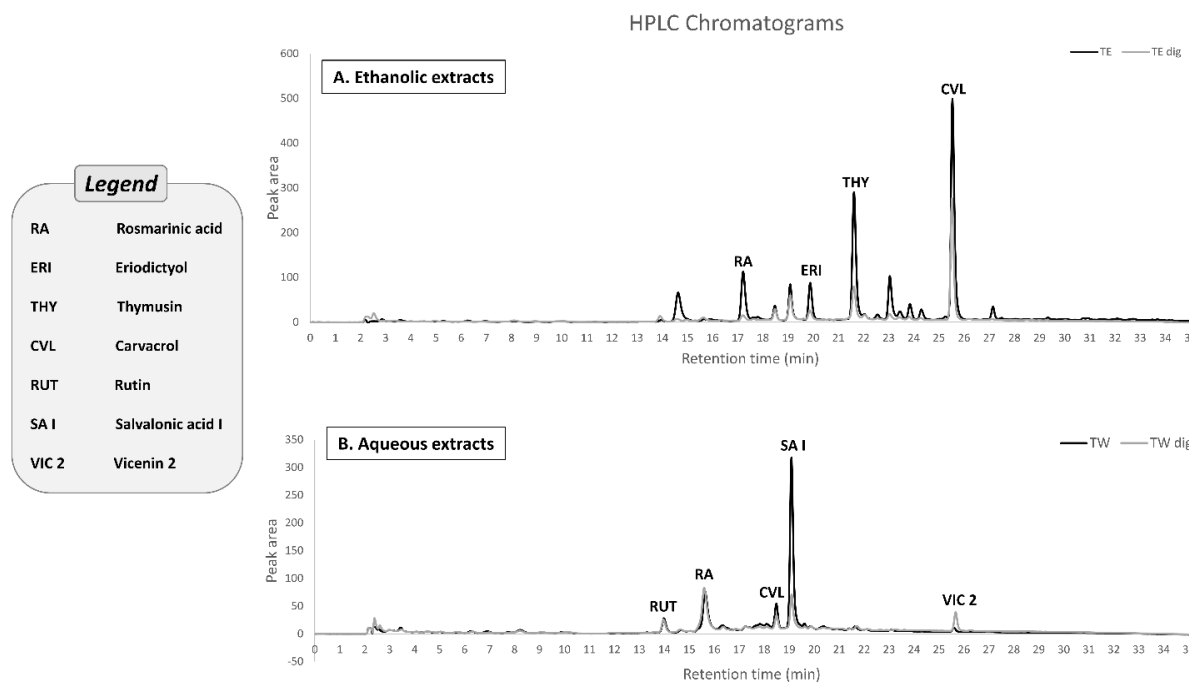
Figure 3.3 HPLC–UV chromatographic profiles for both ethanolic and aqueous extracts of Thymbra spicata before and after digestion wherein their pure polyphenols were recorded at 280 nm: (A) Chromatogram of the ethanolic extract (TE and TE-dig) showing the following peaks: 1: carvacrol; 2: thymusin; 3: rosmarinic acid; 4: eriodictyol. (B) Chromatogram of the aqueous extract (TW and TW-dig) showing the following peaks: 1: salvalonic acid I; 2: rosmarinic acid; 3: carvacrol; 4: vicenin; 5: rutin.

We characterized the aqueous and ethanolic extracts from T. spicata aerial parts before (TW and TE) and after (TW-dig and TE-dig) the simulated digestion. For TW, we also assessed the low (<3.5 kDa) and the high (>3.5 kDa) mw fractions obtained by dialysis.

The aqueous and ethanolic crude extracts exhibited a similar content of carbohydrates. The simulated digestion significantly reduced the TCC in the ethanolic extract (from 26.4 in TE to 19.2 µg/mg in TE-dig), without affecting the aqueous extract. However, upon simulated digestion, we observed a different distribution of carbohydrates between the two fractions: TCC was reduced in the high mw fraction (from 40.4 in TW to 17.6 µg/mg in TW-dig) and increased in the low mw fraction (from 25.2 in TW to 33 µg/mg in TW-dig) (Figure 3.2A). Moreover, the protein content was roughly similar in the crude extracts, and the simulated

digestion did not affect it considerably. However, the aqueous extract showed a redistribution of the protein content between the two mw fractions, leading to a TPrC reduction in the high mw fraction (from 10.8 in TW to 2.4 µg/g in TW-dig) and an increase in the low mw fraction (from 22.7 in TW to 33.9 µg/g in TW-dig) (Figure 3.2B).

As expected, the ethanolic extract was richer in phenolic compounds compared to the aqueous one (353 *vs* 201.4 mg GAE/g). After simulated digestion, the TPC significantly decreased in both the ethanolic (250 mg GAE/g) and the aqueous (138.9 mg GAE/g) extracts ((Figure 3.2C). For the aqueous extract, the simulated digestion reduced the TPC in the high mw fraction (from 148.7 to 81.6 mg GAE/g). By contrast, the aqueous extract was richer in flavonoids than the ethanolic extract (172.88 *vs* 123.84 mg QE/g).

After simulated digestion, the TFC significantly decreased in both the ethanolic (to 85.18 mg QE/g) and aqueous (to 111.26 mg QE/g) extracts, as well as in both the high (from 117.03 to 25.75 mg QE/g) and low mw fractions (from 278.13 to 236.24 mg QE/g) ((Figure 3.2D). The hydroxycinnamic acid content was higher in the ethanolic than in the aqueous extract (89.2 *vs* 35.4 mg RAE/g, respectively). The simulated digestion reduced the THAC in the crude ethanolic extract (76.5 mg RAE/g in TE-dig), while in the aqueous extract, the digestion redistributed the THAC between the two mw fractions (from 101.6 to 95.2 mg RAE/g for low mw fraction, and from 31.4 to 17.8 mg RAE/g in the high mw fraction) ((Figure 3.2E).

3.3.2.   HPLC–MS Characterization of the Phenolic Compounds

Both the extracts were characterized by HPLC–MS/MS analysis before and after digestion (Figure 3.3). In the ethanolic extract, we detected 14 PCs in both the undigested and digested preparations. The most abundant PCs were monoterpenoic phenols (carvacrol), polyphenolic acids (rosmarinic acid), flavonoids, and their derivatives (rutin, thymusin, and

Table 3.2 Phenolic compounds identified in TE (A) and TW (B) before and after digestion using HPLC–MS/MS in the negative ionization mode.

				(A): Ethanolic Extract (TE)				
a	RT (min)	Measured m/z	MS/MS fragments	Proposed Compound	TE Area (%)	TE-dig Area (%)	TE Peak Area	TE-dig Peak Area
1	14.1	593	575 503 473 383 353	Vicinin 2	0.34	2.89	46	137
2	14.5	303	285 177 125	Dihydroquercetin (taxifolin)	7.19	1.87	982	89
3	17.1	417	371 287 263	Eriodictyol derivative	8.69	2.84	1187	135
4	18.5	609	301	Rutin	2.04	4.04	278	192
5	19.1	359	223 197 179 161 133	Rosmarinic acid	5.73	10.53	782	500
6	19.7	287	269 151 135 107	Eriodictyol	6.09	4.07	831	193
7	21.5	329	314	Thymusin	21.20	14.64	2894	695
8	23	285	257 243 151	Apiginin	0.85	0.63	116	30
9	22.8	269	201 181 149	Luteolin	6.64	2.40	906	114
10	23.3	343	328 313 300 285	Unknown	0.97	0.93	132	44
11	24	165	149	P-cymene-2,3-diol	2.23	1.14	305	54
12	24.3	343	328 313	Cirsilineol	1.38	0.82	189	39
13	25.7	–	–	Carvacrol	34.81	52.94	4752	2513

14	27.3	329	314 299 286 271	3,4,3',4'-tetrahydroxy-5,5'-diisopropyl-2,2'-dimethylbiphenyl	1.85	0.25	253	12

(B): Aqueous Extract (TW)

1	8.1	305	225	Gallocatechin	2.35	1.16	114	33
2	12.2	387	369 225 207 163	Tuberonic acid glucoside	0.00	0.00	0	0
3	14	593	575 503 473 383 353	Vicenin 2	5.68	8.40	275	239
4	15	637	461 351 285	Luteolin-O-diglucuronide	0.00	0.00	0	0
5	15.4	537	493 339	Salvalonic acid I	19.51	42.27	945	1203
6	15.7	477	397 373 343 301	Quercetin-glucuronide	0.00	0.00	0	0
7	16.3	595	473 429 287	Eriodictyol-rutinoside	0.62	2.14	30	61
8	16.5	623	433 287	Luteolin-glucuronide-hexoside	0.23	0.88	11	25
9	17	717	537 519 475 365 339	Salvalonic acid E\B	1.94	3.34	94	95
10	17.4	461	285	Luteolin 7-O-glucuronide	0.00	0.00	0	0
11	17.6	593	285	Luteolin-O-rutioside	0.00	0.00	0	0

12	17.9	441	418 405 373 305 225 175	Unknown	0.00	0.00	0	0
13	18.1	521	359 179 161	Rosmarinic acid-glucoside	0.00	0.00	0	0
14	18.5	609	301	Rutin	7.80	7.48	378	213
15	19.1	359	223 197 179 161 133	Rosmarinic acid	57.41	18.80	2781	535
16	19.7	549	387	Tuberonic acid derivate	1.09	1.09	53	31
17	19.8	607	559 427 299 284	Methyl kaempferol O-rutinoside	1.03	1.65	50	47
18	21.6	491	443 311 267	Salvalonic acid C	1.09	2.57	53	73
19	25.7	–	–	Carvacrol	1.24	10.22	60	291

eriodictyol derivative, etc.). The aqueous extract contained less PCs; 19 PCs were detected in both the undigested and digested preparations, which can be classified into three main groups: phenolic acids, phenolic monoterpenoids, and flavonoids. Carvacrol is the most abundant PC in the ethanolic extract (34.8% in TE and 52.9% in TE-dig), rosmarinic acid in TW (57.4%), and salvalonic acid in TW-dig (42.3%).

To compare the chromatograms of the two extracts, we normalized them for their TPC. The analysis revealed some differences in the percentages of the major PCs (Table 3.2). The simulated digestion led to an enrichment in carvacrol abundance in the ethanolic extract (from 34.8 to 52.9%; $p \leq 0.01$) and to a reduction in rosmarinic acid abundance in the aqueous extract (from 57.4% to 18.8%; $p \leq 0.01$). In TW, the reduction in rosmarinic acid was almost balanced by the increase in salvalonic acid (from 19.5% to 42.3%; $p \leq 0.01$). Moreover, a redistribution

in phenols, flavonoids, and hydroxycinnamic acids was observed between the two mw fractions, with the low mw fraction being enriched in both TPC (from 1.53 to 2.06) and TFC (from 1.61 to 2.12), balanced by a reduction in the high mw fraction of TFC (from 0.68 to 0.23) and THAC (from 0.89 to 0.54) (Figure 3.4)

3.3.3. Effect of Simulated Digestion on Antioxidant Proprieties

The antioxidant potential of each extract before and after the simulated digestion was evaluated by three different spectrophotometric assays. A higher antioxidant activity was observed for the ethanolic extract compared to the aqueous one. Both extracts showed significant changes in the antioxidant potentials upon digestion, as well as between the mw fractions obtained by dialysis before and after digestion (Table 3.3A).
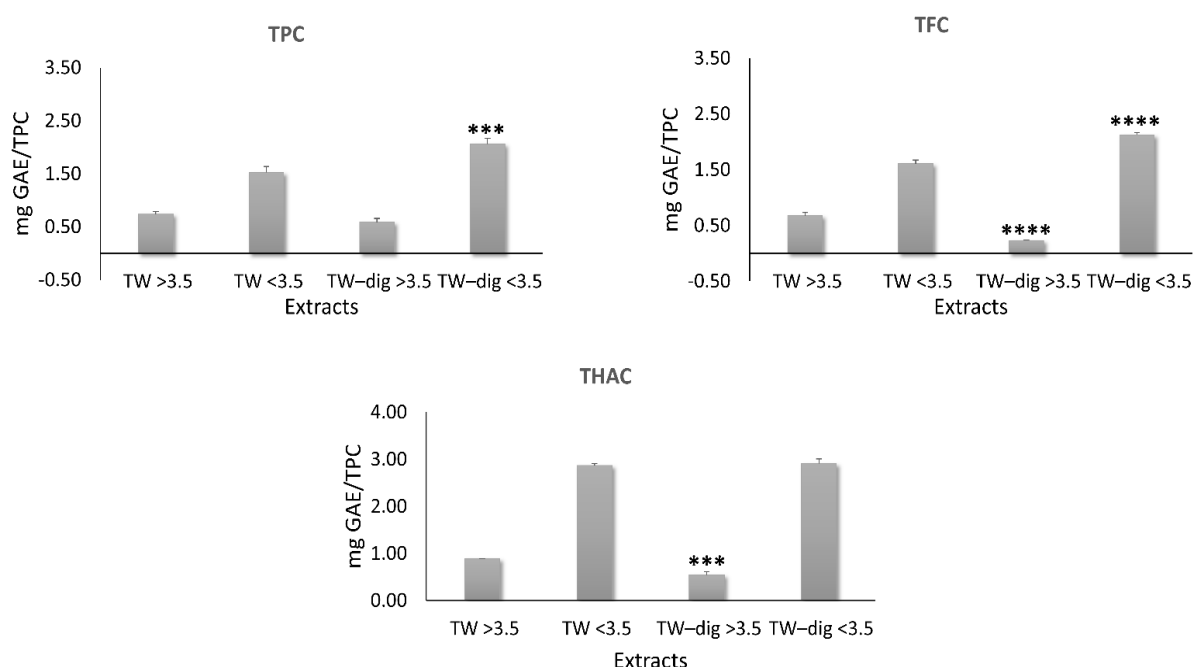
Figure 3.4 Normalized total phenol content (TPC), total flavonoid content (TFC), and total hydroxycinnamic acid content (THAC) of high and low mw fractions of the aqueous extract by the TPC of the corresponding extracts. Significant differences between digested and undigested extracts are denoted by symbols: ***$p < 0.001$ and ****$p < 0.0001$.

Influence of Simulated In Vitro Gastrointestinal Digestion on the Phenolic Profile, Antioxidant, and Biological Activity of Thymbra spicata L. Extracts

Table 3.3 (A) The radical scavenging activity of the T. spicata extracts before and after digestion. Values are reported as Trolox equivalent (µg TE/mg dry extract). (B) Pearson correlation (two-tailed) between TFC, THAC, TPC, and antioxidant parameters (DPPH, ABTS, and FRAP). All values are mean ± SD from at least three independent experiments. Samples were measured in triplicate for each experiment. Significance is denoted by symbols: $*p < 0.05$, $**p < 0.01$, and $***p < 0.001$.

(A)Radical Scavenging Assays													
Assays	**DPPH**				**ABTS**				**FRAP**				**TPC**
Samples	Trolox equivalent	Trolox equivalent/TPC	SD	SD/TPC	Trolox equivalent	Trolox equivalent/TPC	SD	SD/TPC	Trolox equivalent	Trolox equivalent/TPC	SD	SD/TPC	
TW (total)	90	0.446872	12.3	0.061072	210.6	1.0456802	32.4	0.1608739	73.5	0.364945	15.6	0.077458	201.4
TW<3.5kDa	90.8	0.295381	9.8	0.031880	234	0.7612232	25.9	0.0842550	146.1	0.475277	18.9	0.061483	307.4
TW>3.5kDa	80.3	0.540013	7.9	0.053127	250	1.6812374	32.4	0.2178884	78.5	0.527909	10.8	0.072629	148.7
TW dig	83.8	0.603312 *	9.5	0.068395	173.7	1.2505400	19.1	0.1375090	62.8	0.452124	9.2	0.066235	138.9
TW dig<3.5kDa	86.4	0.301781	11.1	0.038771	182.4	0.6370940 **	17.5	0.0611247	140.9	0.492141	16.1	0.056235	286.3
TW dig>3.5kDa	65.1	* 0.797794	7.9	0.096814	250	3.0637255	32.4	0.3970588	42.3	0.518382	7.6	0.093137	81.6
TE	89.5	0.253541 *	12.1	0.034278	250	0.7082153	32.4	0.0917847	92.2	0.26119 *	6.1	0.01728	353
TE dig	94	0.376000	12.4	0.049600	210.7	0.8428000	23.9	0.0956000	88.3	0.3532	7.9	0.0316	250

(B) Pearson Correlation (Two-Tailed)					
TFC	**THAC**	**TPC**	**ABTS**	**DPPH**	**FRAP**
TFC		0.6797	0.6274	0.3923	0.5646
THAC	0.6797		0.9375***	0.4215	0.6726
TPC	0.6274	0.9375***		0.5867	0.7612*

After normalizing the Trolox equivalent values for the TPC in each extract, we appreciated a higher antioxidant activity for the digested extracts than for the crude ones. Briefly, in the ethanolic extract, DPPH increased from 0.25 (TE) to 0.37 (TE-dig), and in the aqueous extract from 0.44 (TW) to 0.60 (TW-dig).

Regarding the FRAP assay, ethanolic extract showed an increase in the reducing capacity after digestion from 0.26 (TE) to 0.35 (TE-dig). Conversely, the ABTS assay of the aqueous extract showed a reduction in the high mw fraction from 3.06 (TW-dig > 3.5 kDa) to 1.68 (TW-dig > 3.5 kDa) (Table 3.3A).

Finally, the correlation analysis between the phytochemical contents (in terms of TPC, THAC, and TFC) and the three antioxidant activities (evaluated as DPPH, ABTS, and FRAP) for all the extracts showed a significant and strong correlation between DPPH and TPC (r2 = 0.7612). Moreover, a good correlation was calculated between FRAP and the phytochemical contents: FRAP and TFC (r2 = 0.8952), FRAP and THAC (r2 = 0.8913), and FRAP and TPC (r2 = 0.7755) (Table 3.3B). These results indicate that the phenolic compounds contained in the extracts are the major contributor for the antioxidant capacity.

Table 3.4 IC50 values (50% cell viability inhibitory concentration) determined for T. spicata ethanolic extracts (TE and TE dig) and Carvacrol (CVL) in the three cell lines over long-term (24h) under analysis.

Cell-lines	TE	TE-dig	CVL
MDA-MB 231	58.447	112.103	23.278
HCT116	110.238	**147.51**	59.625
A375	31.443	107.067	**19.912**
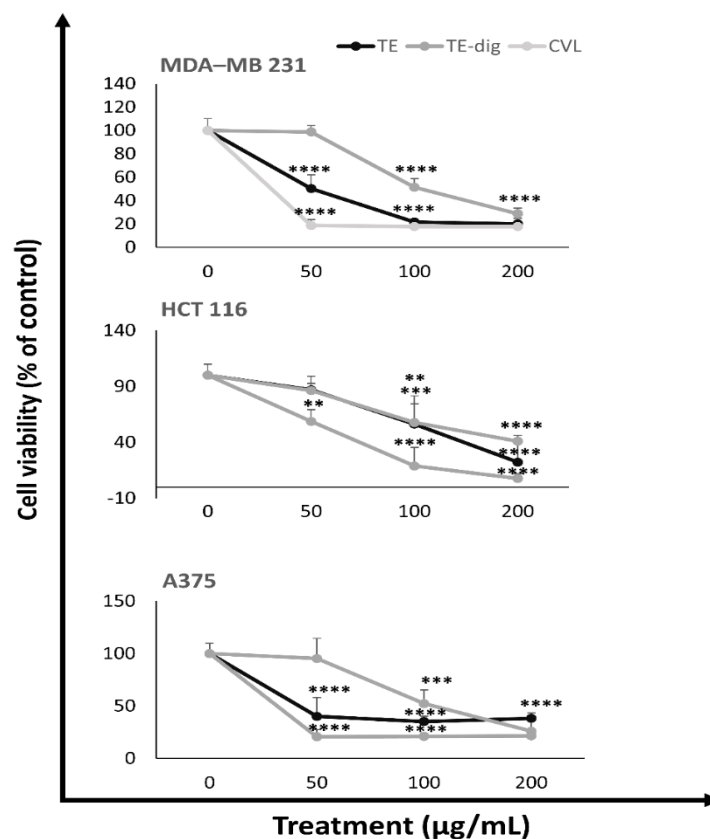
Figure 3.5 Antiproliferative activity of TE, TE-dig, and CVL on three representative human cancer cell lines: breast (MDA-MB 231), colon (HCT 116), and melanoma (A375) cells. The cell viability was expressed as a percentage (%) with respect to the control. Data represent the mean of at least five independent experiments. Statistical analysis for cell viability data was performed using two-way ANOVA followed by Tukey's post-test (* $p < 0.05$, ** $p < 0.01$, *** $p < 0.001$, **** $p < 0.0001$).

3.3.4. In Vivo Effects: Cytotoxic Activity and Oxidative Stress in Cancer Cells

The anti-proliferative effects of the different extracts before and after digestion were assessed using three human cancer cell lines representative of the most common human cancers, i.e., MDA-MB 231, HCT116, and A375 cells (Figure 3.5). No significant cytotoxic effects were observed for the aqueous extract (data not shown). By contrast, all the ethanolic

extracts, both undigested and digested, significantly reduced the cell viability of all cancer cell lines in a concentration-dependent manner. Carvacrol is the most abundant component of the ethanolic extract, and it was employed as a positive control. After 24 h of treatment at the highest concentration (200 µg/mL), both the extracts (TE and TE-dig) and carvacrol dramatically reduced the cell viability in MDA-MB 231 (to 20.1%, 28.8%, and 17.9%; respectively), in HCT116 cells (to 22.3%, 41.1%, and 7.8%, respectively), and in A375 cells (to 38.2%, 26%, and 21.6%, respectively). From the IC50 values listed in Table 3.4, we can deduce that carvacrol is the most cytotoxic agent for A375 cells at 24h (IC50 of about 19.912 µg/mL), as well as for MDA-MB 231 cells (IC50 about 23.278 µg/mL) and HCT 116 cells (IC50 about 59.625 µg/mL), and other intermediate inhibitory effects have been exhibited on the other cell lines.

In attempt to decipher the mechanisms sustaining the cytotoxic effects, we assessed the oxygen and nitrogen radical production. A dose-dependent increase in ROS production was detected in the breast cancer cell line MDA-MD 231 treated with either the crude or digested extracts. At the highest concentration (200 µg/mL), ROS production increased to +158.1% for TE-dig and +154.1% for TE, but carvacrol was more efficient in inducing ROS production (+238.8%). Similar results were recorded for the colon cancer cell line.

On HCT116, carvacrol stimulated ROS production (+253.8%) more than the crude and digested extracts (TE +151.9% and TE-dig +163.6%) at the highest concentration. Moreover, for the melanoma cancer cell A375, carvacrol stimulated ROS production (+293.4%) more than the crude and digested extracts (+191.7% for TE-dig and +142.7% for TE) at the highest concentration (Figure 3.6A).
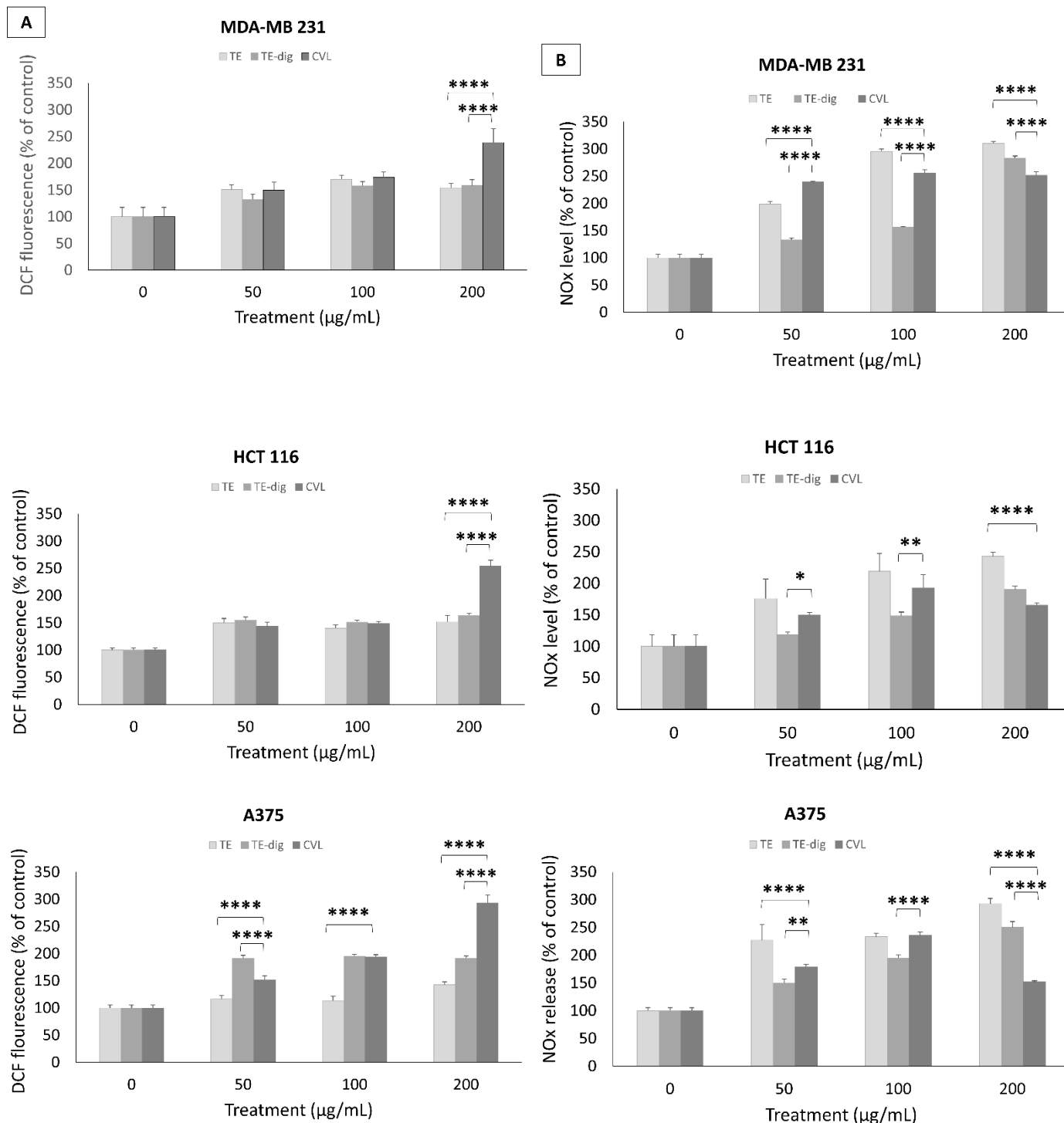
Figure 3.6 Pro-apoptotic effects of TE, TE-dig, and CVL on three cell lines: MDA-MB 231, HCT116, and A375, were assessed by measuring the ROS (A) and NO production (B) using spectrophotometric and fluorometric analyses, respectively. Values are expressed as % of control. Data represent the mean of five independent experiments. Statistical analysis for cell viability data was performed using two-way ANOVA followed by Tukey's post-test (* $p < 0.05$, ** $p < 0.01$, *** $p < 0.001$, **** $p < 0.001$).

An opposite trend was observed in terms of NO release. In this case, the extracts, at the highest concentration (200 µg/mL), were stronger than carvacrol in triggering the NO release in MDA-MB231 (+283.% for TE-dig, +310.4% for TE, and +251.6% for CVL), as well as in HCT116 and A375 cells, where the release was maximum for TE (+242.7% and +292.6%, respectively) followed by TE-dig (+190.4% and +250.4%, respectively) and by CVL (+165.3% and +151.7%, respectively) in the three cell lines (Figure 3.6B).

3.4. Discussion

Although many studies emphasized the uncountable positive effects on human health of the phenolic compounds contained in certain edible or medicinal plants, only a few reports have investigated the possible influence of the gastrointestinal digestion on their efficacy. The main finding of our study using a simulated in vitro GI digestion is that the digestion boosters the antioxidant activity of T. spicata extracts, while it reduces the antiproliferative potential. We may attribute these differences in the biological activity of the extracts to the modifications in the phenolic profile caused by the simulated digestion.

To our knowledge, no studies have previously documented the possible changes in bioactivity of T. spicata extracts or preparations after transit in the gastrointestinal tract. In this context, we assessed the content of the main macromolecules and the phenolome in ethanolic and aqueous extracts from T. spicata leaves, and for the aqueous extract, we also distinguished between the low and high mw fractions.

Regarding the ethanolic extract, the simulated digestion led to a significant decrease in almost all components, while in the aqueous extract, it led to a reduction of only phenols and flavonoids. Although the simulated digestion reduced the carvacrol content in the ethanolic extract in absolute terms, carvacrol became the most abundant PC in relative terms. On the other hand, in the aqueous extract, the simulated digestion significantly increased the content

of salvalonic acid, which became the most abundant PC in relative terms (Table 3.2). The increase in salvalonic acid content likely depends on the reduction in the RA upon digestion, taking into consideration the fact that salvalonic acid derives form condensation of two units of RAs, and this compound appears to be the precursor to many related salvianolic acid derivatives [123]. Therefore, we could hypothesize that the reduction in the rosmarinic acid (RA) upon digestion had been balanced by the increase in the SA.

We wish to emphasize as the biotransformation of parental phenolic compounds during the digestive process could mainly depend on the enzymes and the physiological environment of the GI tract (pH, temperature, and electrolytes) [124]. Indeed, Karas et al. [125] suggested that about 10% of the PCs remain undigested in the plant matrix, with only 90% of them being digested and released. However, the effects of digestion might vary according to the plant materials, and in the literature, we found two different outcomes: one stating the increase in phenolic compounds upon digestion [126], and the other one showing a reduction [127]. Indeed, our data are in accordance with reports showing a reduction such as those showing a reduced PC content in Brassica oleracea [128], as well as in Chilean white strawberry [129] upon digestion.

The idea is that the GI digestion may be unable to release all PCs, leaving a considerable amount of non-extractable polyphenols (NEPs) being trapped by dietary fibers, macromolecules (i.e., proteins), or polysaccharides through hydrophobic, hydrogen, and covalent bonds [130]. Therefore, NEPs reach the colon nearly intact [131]; however, only the phenolic components released from the matrix are absorbable from the GI barriers, and this could explain the enrichment in the secondary metabolites that we observed in the low mw fractions (mainly carbohydrates and proteins). NEPs may be released from the food matrix in the colon by the action of microbiota thus becoming bioavailable, absorbed, and bioactive

[132], and this point specifically will inform our upcoming investigations. In conclusion, our findings indicate that the effect of digestion was greater on the ethanolic extract, and this was likely to due to degrees of solubility of different phyto-constituents.

In a previous paper [10], we demonstrated the great antioxidative potential of the T. spicata ethanolic extract, being higher than the aqueous one. Interestingly, the antioxidant potential of both the ethanolic and aqueous extracts was boosted by the simulated digestion. This could be related to the noticeable enrichment of each extract in terms of bioactive compounds, namely, carvacrol in the digested ethanolic extract, and salvalonic acid in the aqueous digested extract according to previous scientific reports [133].

Although polyphenols are generally considered as antioxidant compounds, at very high concentrations, they are known to play a prooxidant effect that might promote apoptosis, especially in highly proliferative cells such as cancer cells [134], [135]. A previous study of our group reported remarkable antiproliferative and pro-apoptotic effects on tumor cell lines for the ethanolic extract from T. spicata when tested at a rather high concentration (100 mg/mL) [42]. In the present study, we verified that the in vitro cytotoxic activity of the ethanolic extract on cancer cell lines was maintained after the simulated digestion, but with lower efficacy compared with the crude extract. As widely reported, the antiproliferative activity of a plant is firmly correlated with the PCs [136]. Accordingly, we observed a decreased antiproliferative potency for the digested extract compared to the crude one, and this result parallels well with the reduced PC content upon digestion, in particular the reduction in carvacrol, which is the most potent antiproliferative agent in our study.

We evaluated the free radical production to clarify the mechanisms sustaining the anti-proliferative activity of the ethanolic extract before and after digestion. The results of the present study showed that the pro-oxidant property of the ethanolic extract was not only

maintained after the digestion, but it was even bigger in terms of ROS production when compared to TE-dig. On the other hand, the NO release was higher in the crude extract compared to the digested one.

Interestingly, we observed that both the crude and digested ethanolic extracts were less potent in ROS production compared to carvacrol, while in terms of NO release, the extracts were more potent than carvacrol. This can indicate that the antiproliferative potential of T. spicata is exerted by acting as ROS-mediating apoptosis and inducing the release of cytotoxic mediators. Nevertheless, further studies should be performed at this level to have a clear idea about the mechanistic mode of action.

3.5. Conclusions

In summary, although we observed a reduction in the PCs and modulation in the phenolome of both ethanolic and aqueous T. spicata extracts upon the simulated GI digestion, the antioxidant activity was significantly enhanced. However, the antiproliferative potential of the ethanolic extract was reduced. Accordingly, we can come to an assumption that the digestion process had an impact on the nutritional value of T. spicata, but it kept its biological effectiveness.

As a final word, we can confidently say that T. spicata can represent a good and considerable source of PCs with potent antioxidant and antiproliferative bioactivities. In particular, the detected panel of bioactive compounds in T. spicata makes this edible plant a potent candidate to be used as a dietary supplement for different therapeutic purposes.

Chapter 4   Supplementation with *Thymbra spicata* extract ameliorates lifespan, body-weight gain and Paraquat-induced oxidative stress in *Drosophila melanogaster*: an age- and sex-related study

4.1.   Introduction

Aging is a natural physiological process resulting from an imbalance between stressors and stress buffering mechanisms bringing on accumulation of unrepaired damages [137]. The oxidative stress is one of the factors involved in aging processes, and it is mainly derived from an excess of free radicals and oxidants such as the reactive oxygen species (ROS) leading to an imbalance of cell homeostasis [138]. Oxidative stress triggers inflammation processes through the activation of a variety of genes implicated in many pathways [139]. On the other hand, a ROS overproduction induces a network of defense responses including the expression of genes coding for antioxidant enzymes such as heme oxygenase (HO) and thioredoxin reductase (TrxR) [140], [141], pro- and anti-inflammatory cytokines such as tumor necrosis factor alpha (TNFα) and other interleukins [142]. An impair in the body weight control seems to be strictly associated to a reduction in lifespan also through triggering the risk of many metabolic disorders [36].

Food-based antioxidants are known to boost the antioxidant defense thus they might increase the longevity [143], [144]. Dietary polyphenols are plant-derived bioactive compounds that have emerged as promising anti-aging candidates. In this context, *Thymbra spicata* L., a medicinal plant member of *Lamiaceae* family, has gained popularity for its health-promoting properties that are held accountable for potentially affecting the longevity of the individual. *T. spicata* is traditionally used in flavoring a variety of food either as a single plant e.g. herbal tea and salad, or in a combination of a group of blended plants and spices making the most well-known Lebanese herbal mixture; Za'atar [20]. Evidences from cellular and

animal studies have highlighted that *T. spicata* possesses potent antioxidant and anti-inflammatory activities that have been described in models of endothelial dysfunction and fatty-liver disease [8]–[10]. In particular, a previous study of our group showed that the two polyphenol-enriched extracts from *T. spicata* (aqueous-TW and ethanolic-TE) were able to decrease both the lipid accumulation in steatotic hepatocytes, and the release of nitric oxide in dysfunctional endothelial cells [10]. Based on these reports, we could hypothesize that *T. spicata* might act also on mechanisms being associated with age-related cellular and molecular dysfunctions.

Drosophila melanogaster, commonly known as "fruit fly" has served as an excellent model for many diseases including obesity, diabetes, and aging [145], [146]. Indeed, the flies share with humans a panel of highly conserved genes and as a result a large number of key metabolic pathways [147]. Particularly, oxidative stress and antioxidant defense responses are rather conserved from *Drosophila* to mammals. Moreover, *Drosophila* model is quite relevant for the ability to be genetically manipulated, multiple life stages, and a short lifespan, knowing that lifespan analysis is a rate-limiting step [148]. The use of *Drosophila* as an *in vivo* model to study the potential health-promoting effects of food-derived polyphenols has been widely noticed [37], [149], [150].

In the present study, starting from previous *in vitro* studies, we translated the investigation to an *in vivo* model, using *Drosophila*, in an attempt to deepen our knowledge on the molecular pathways sustaining the beneficial effects of *T. spicata*. Therefore, both young (1-week old) and early-adult (3-weeks old) flies were fed with diet supplemented with either aqueous and ethanolic extracts from *T. spicata*. This fly model allowed us to investigate *in vivo* the properties of both extracts as anti-aging, antioxidative, and weight loss potential, taking the sex differences into account.

4.2. Materials and Methods

4.2.1. Chemicals

All chemicals, unless otherwise indicated, were supplied by Sigma-Aldrich Corp (Milan, Italy).

Table 4.1 Most abundant bioactive phenolic compounds in *T. spicata* extracts identified by HPLC-MS/MS as previously reported [10].

ETHANOLIC EXTRACT (TE)	
Bioactive Phenolic Compounds	*Percentage of abundance (%)*
Carvacrol	36.84
Thymusin	20.25
Eriodictyol derivative	9.45
Luteolin	7.95
Eriodictyol	6.8
AQUEOUS EXTRACT (TW)	
Bioactive Phenolic Compounds	*Percentage of abundance (%)*
Rosmarinic acid	38.6
Salvalonic acid I	10.17
Rutin	7.17
Salvalonic acid E/B	5.85
Luteolin-O-diglucuronide	4.81

4.2.2. Plant collection and extraction

The fresh Arieal parts of *Thymbra spicata* were collected from flowering plants growing wild in "*Maarakeh*"- South Lebanon, 280m above sea level (33° 16′35.59″N and 35° 19′02.89″).

After authentication for taxonomic identity by Dr. G. Tohme, President of the National Council for Scientific Research (CNRS) of Lebanon, a voucher specimen was deposited in the Herbarium of the Faculty of Sciences at the Lebanese University, Hadath-Beirut, Lebanon (voucher number L1.125/1).

The leaves were chopped, and shade dried at room temperature for 3 weeks and then grounded to coarse powder to ease the extraction. The plant materials were extracted with two different solvents following a well-standardized procedure [151]. Two different extracts were prepared using either ethanol (100%) or distilled water as solvent as previously described [10]. Both extracts were freeze-dried in Alpha 1–4 LD plus lyophilizer (CHRIST, Osterode am Harz, Germany) and stored at 4 °C until use. Table 4.1 resumes the major polyphenols identified in the two extracts. The total phenol content (TPC) was assessed previously for both extracts by spectrophotometric assays showing that the TPC of ethanolic extract is higher than to that of aqueous extract [10].

4.2.3. Fly strains, husbandry, and rearing

The *Drosophila melanogaster* Canton-S wild-type strain was kindly provided by Prof. Daniela Grifoni (University of L'Aquila, Italy). Fly eggs and larvae were maintained at constant temperature (25°C) and humidity (60%) under 12/12h light-dark on a standard Formula 4–24 ® media (Carolina Biological, Burlington, NC, USA). The composition of the diet, listed by the manufacturer is as follows: oat flour, soy flour, wheat flour, other starches, dibasic calcium phosphate, calcium carbonate, citric acid, niocinamide, riboflavin, sodium chloride, sodium

iron pyrophosphate, sucrose, thiamine, mononitrate, brewer's yeast, emulsifier preservatives, mold inhibitor, and food coloring. Yeast granules (*Saccharomyces cerevisiae*) were added to each vial after diet hydration. Newly eclosed males and females were collected every 24 hrs, anesthetized by FlyNap (Carolina Biological), and then separated under the stereomicroscope according to the sex. Adult flies were reared in control medium at a density of 30 individuals per vial until the start of the supplementation. At least 10 vials per each experimental group/sex were prepared to obtain the desired numbers of flies (n=250) in each experimental group.

A stock solution (6 mg/mL) of each extract was prepared in dimethyl sulfoxide (DMSO) or in water, for TE and TW respectively, and kept at 4°C. For supplementation, the stock solutions were diluted in water obtaining the "supplemented water" containing the final concentration of extract (15μg/mL) that was used to soak the medium. The extracts were tested on two distinct age cohorts: 1-week (representing the young flies), starting from the first day of 1 week old flies and 3-week (considered early-old flies) starting from the first day of 3 weeks old flies (each group of 250 flies/sex/group). The diet of control groups was lifelong soaked only with water. Figure 4.1 summarizes the experimental setup.

4.2.4. Longevity assay

A total of 1500 female and 1500 male fruit flies were randomly divided into 3 groups of study assuming: control diet (CTRL), TE-supplemented diet (TE), and TW-supplemented diet (TW), for each age category: 1- week (1W) and 3-weeks (3W). The flies were transferred into fresh medium twice a week and scored for deaths virtually on each day of transfer until all flies were dead.

4.2.5. Food intake evaluation

Food rates of consumption were measured using the capillary feeder method (CAFE) as previously described [149]. The assay was performed on flies never supplemented (7 days old male and female flies). On the day of the experiments, flies were separated into CAFE vials (three replicates of ten flies for vial: 30 flies sex/treatment), weighted, and starved for two hours. After the starvation, flies were fed for six hours with 2.5% sucrose (Ctrl) or 2.5% sucrose + TE extract (TE) or 2.5% sucrose + TW extract (TW), respectively. Then flies were transferred back on the regular food medium (Formula 4–24 ® media soaked with water) till the day after. The trial has been repeated three times on three consecutive days. To account for evaporation of the liquid food, three vials were set up with feeding capillaries but without flies. Fly's feeding consumption was evaluated measuring the amount of liquid consumed from the microcapillary tube (in mm) as described by Fiocca et al. [152] and data were reported as µL/mg of fly weight/hour.

4.2.6. Body weight measurement

Body weights of flies were measured once a week starting from the first day of treatment (T0). In details, the weight of a single fly was estimated by calculating the difference between the vial weight before and after flies' transfer, to be divided by the total number of the remaining alive flies.
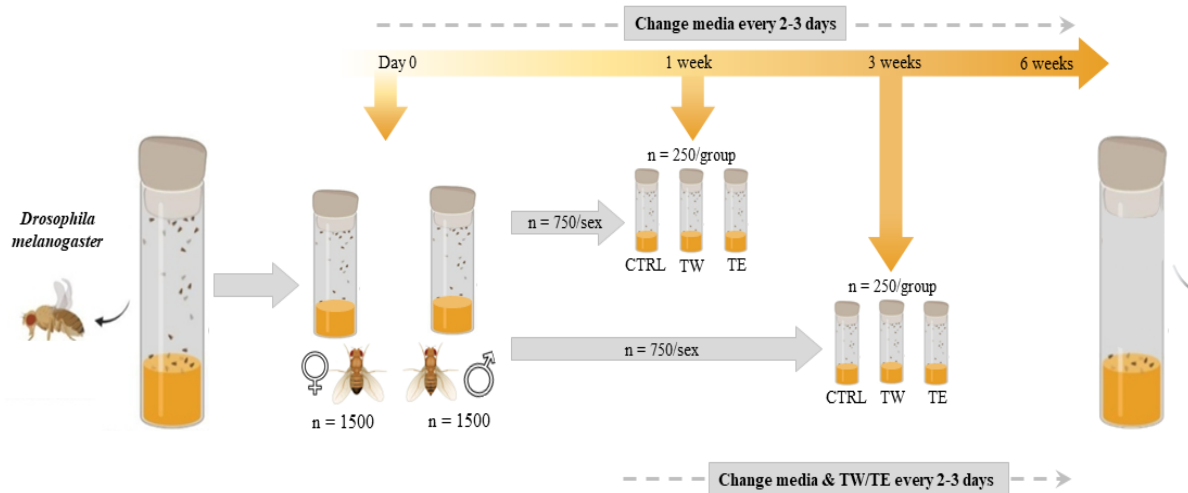
Figure 4.1: Experimental design. A representative scheme summarizing the experimental setup of our in vivo study with Drosophila melanogaster. The newly eclosed males and females were collected every 24hrs and then separated under the stereomicroscope according to the sex. A total of 1500 female and 1500 male fruit flies were randomly divided into 3 groups of study where at least 10 vials per each experimental group/sex were prepared with a density of 30 individuals per vial to obtain the desired numbers of flies (n=250) in each experimental group, assuming: control diet (CTRL), ethanolic extract-supplemented diet (TE), and aqueous extract-supplemented diet (TW), for each age category: young (1-week old) and early-old (3-weeks old). The flies were transferred into fresh medium twice a week and scored for deaths virtually on each day of transfer until all flies were dead.

4.2.7. Paraquat-induced oxidative stress

A stock solution of 2.5mM Paraquat (1,1'-Dimethyl-4,4'-bipyridinium dichloride), a herbicide triggering mitochondrial oxidative stress and decreasing motor ability [153], was prepared in 2.5% sucrose solution. For the experiments, two groups of young (1W) females (n=180) were fed with a diet supplemented with the T. spicata aqueous extract (TW) for 2 weeks, or without supplementation (CTRL). The early-old flies (3W) were then subdivided into a double series of new vials utilized for the capillary feeder method (CAFE) prepared as described previously [149]. Briefly, after 2hr of starvation, microcapillary tubes were inserted into the vials through a 200μL pipette tip in the foam plug. For both TW-supplemented or

control-diet flies, four microcapillary tubes were used per vial after filling with 2.5% sucrose in the presence (TW) or in the absence (CTRL) of the 2.5mM Paraquat solution. These flies had access to the two different solutions for 40 hr. The number of dead flies was recorded.

4.2.8. Climbing assay

After the oxidative stress assay, the surviving flies were transferred without anesthesia to 10 cm high tubes (10 flies for tube) for the Climbing assay [154]. Flies were allowed to recover for 5 min and then they were forced to the bottom of the tubes by tapping the tubes on a foam pad resting on a rigid surface. Flies' locomotion was observed for 10 seconds and the number of flies that reached or passed the five-centimetres line within this period as well as the total number of flies were recorded. The test was repeated ten times with a rest interval of one minute between one test and the next [154] and the percentages of flies able to reach or pass the five-centimetres line were calculated.

4.2.9. TBARS assay

Samples were prepared by homogenizing the full-body of each group of flies being collected and frozen during the study following a standard protocol [155]. In details, 0.1 M of potassium phosphate buffer pH 7.4 was added to the fly sample in a ratio of 1:5 (mg fly body: µL buffer). The homogenate was obtained using Teflon Potter-Elvehjem homogenizer. The lipid peroxidation end products were quantified using the thiobarbituric acid reactive substances (TBARS) assay, which is based on the reaction of malondialdehyde (MDA; 1,1,3,3-tetramethoxypropane) with thiobarbituric acid (TBA) [70]. Briefly, 1 vol. of sample homogenates were incubated at 95°C for 60 mins with 2 vol. of TBA solution (0.75% TBA, 10% trichloroacetic acid, 0.1 M HCl) for color development. After cooling, samples were

centrifuged (8000 x g for 10 mins) and the absorbance of the supernatant was measured at 532 nm. TBARS tissue levels were expressed as nmol MDA/mg protein.

4.2.10. Protein content quantification

The protein content was determined by the Bradford assay using serum bovine albumin (BSA) as a standard [67].

4.2.11. RNA extraction and quantitative real-time PCR

The total RNA was extracted from flies being collected and frozen at specific time conditions during the study: T0, T1 (2 weeks after supplementation), and T2 (4 weeks after supplementation). The frozen fly samples were mechanically homogenized and then, the mRNA was isolated using RNeasy Mini Kit (QIAGEN GmbH, Hilden, Germany). NanoVue Spectrophotometer (GE Healthcare, Milano, Italy) was used to measure the yield and purity of the RNA. Only samples with ratios A260/A280>1.8 were used.

For each sample, 1µg of total RNA was reverse transcribed to obtain cDNA using iScript cDNA Synthesis Kit (Bio-Rad Laboratories, Hercules, CA, USA) following the manufacturer's instructions. The subsequent polymerase chain reaction (PCR) was performed in a total volume of 10µL containing 2µL of dH2O RNAsi free, 2.5µL (12.5ng) of cDNA, 5µL SsoAdvanced Universal SYBR Green Supermix (Bio-Rad Laboratories), and 0.5µL (500nM) of each primer. The relative quantity of target mRNA was calculated using the comparative Cq (represents the cycle number at which the amount of amplified target reaches the fixed threshold) method and was normalized for the expression of ribosomal protein L32 (*rpl32*). The expression of the target genes was then calculated as relative quantity of mRNA (fold induction) with respect to controls (at T0). The used primer pairs are illustrated in Table 4.2.

Table 4.2 List of primers for real-time PCR.

Gene	Primer Name	Primer Sequence 5'-> 3'
HO	Fwd	ATGTCAGCGAGCGAAGAAACA
HO	Rev	TGGCTTTACGCAACTCCTTTG
TrxR1	Fwd	TGGATCTGCGCGACAAGAAAG
TrxR1	Rev	GAAGGTCTGGGCGGTGATTG
TotA	Fwd	AACTGCTCTTATGTGCTTTG
TotA	Rev	TCAGCAATTCTAAGGTTGTC
RPL32	Fwd	GCCCACCGGATTCAAGAAGT
RPL32	Rev	CTTGCGCTTCTTGGAGGAGA

4.2.12. Statistical analysis

All results were expressed as mean ±SD. GraphPad Prism 8.0.1 software was used for statistical evaluation. Comparisons between different conditions were performed using one-way ANOVA with Tukey's post-test. Difference between two different conditions was calculated by student's t-test. All statistical analysis were performed by GraphPad Software Prism 8.0.1, Inc. (San Diego, CA, USA). For lifespan assessment, Kaplan–Meier survival curves were generated by OASIS2 [156].

4.3. RESULTS

4.3.1. T. spicata supplementation ameliorates the D. melanogaster lifespan

The possible anti-aging effect of T. spicata extracts was tested on both young and early-old (1 week- and 3 week-old, respectively) male and female flies upon feeding a standard diet supplemented with either TE or TW (15µg/mL in total polyphenols). The flies that were reared on food containing only water were taken as control (Figure 4.2). The results reported different

effects on the lifespan depending on both the fly sex (male vs female) and the extraction solvent (water vs ethanol). In details, we observed an extended lifespan (+ 5.8%; $p < 0.05$) in young females feeding TW-supplemented diet with respect to control (Figure 4.2A), whereas no effects could be appreciated on the young males (Figure 4.2B). For the early-old flies, no effects could be appreciated for both female and male flies. On the other hand, the ethanolic extract TE did not exert any considerable effect on both young and early-old flies.

LONGEVITY
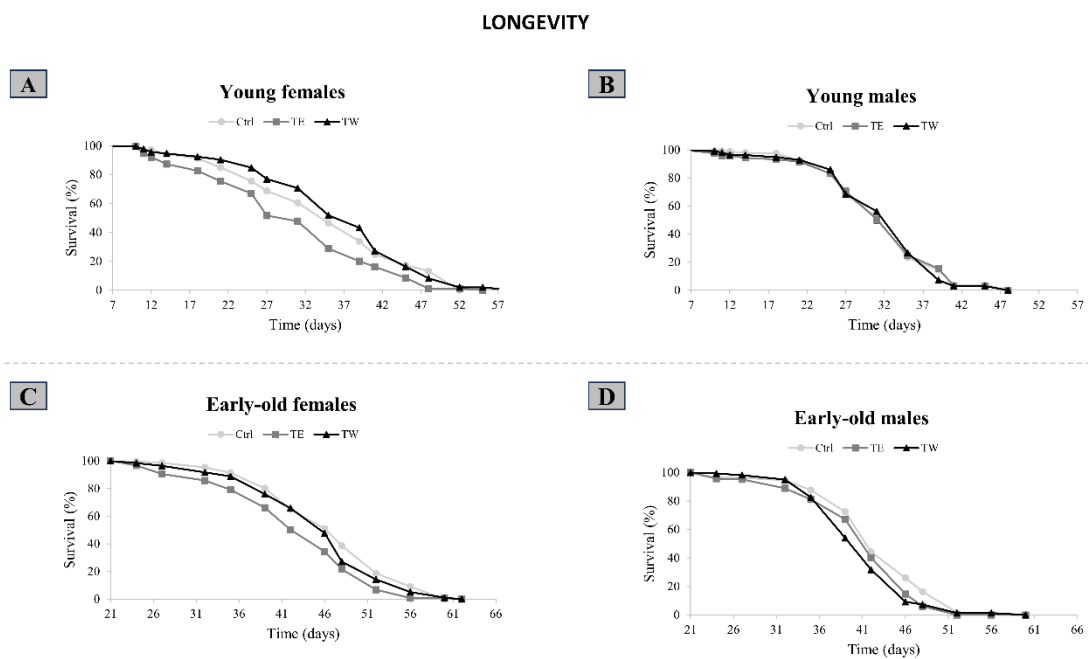
Figure 4.2: *Effects of T. spicata supplementation on the D. melanogaster lifespan*

Survival curves of young (A) and early-old (B) female and male *Drosophila* reared on different diets. The flies were supplemented with either 15µg/mL of ethanolic extract (TE) or aqueous extract (TW), or only standard diet. Data are represented as percentage of survival of flies (%) as a function of time (in days). The Kaplan–Meier test was used to detect the significant differences among the three groups of the flies (OASIS2). Lifespan improved significantly in young female flies supplemented with TW (A: $p < 0.05$).
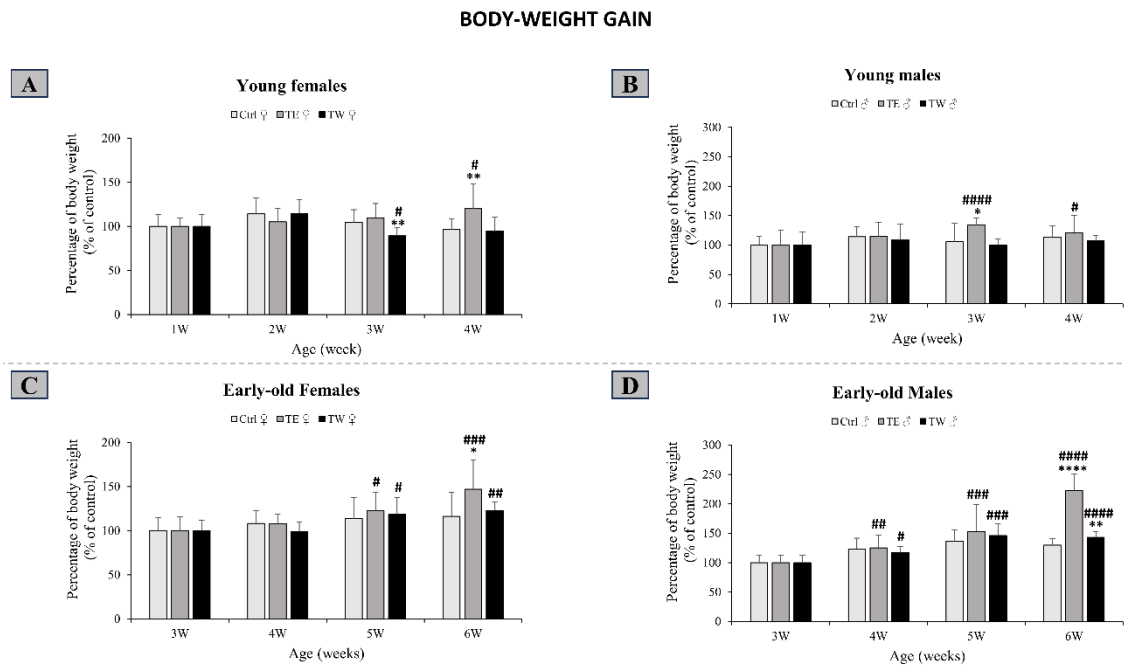
BODY-WEIGHT GAIN

Figure 4.3: Effects of T. spicata supplementation on the D. melanogaster body-weight gain

Effect of TE and TW on the body-weight gain of young (A) and early-old (B) female and male Drosophila. Data are reported as percentage of body weight (%), which was studied by calculating the percentage of the average of the recorded weights of each group of flies with respect to T0 (day of supplementation), as a function of time (in weeks). Significant differences are denoted by symbols: Ctrl-1W/Ctrl-3W vs different treatments # $p<0.05$, ## $p<0.01$, ### $p<0.001$, and #### $p<0.0001$, and inner Ctrl vs treatments * $p<0.05$ and ** $p<0.01$.

4.3.2. T. spicata supplementation reduces the D. melanogaster body-weight gain

Based on the lipid lowering activity previously described in vitro for the T. spicata extracts [10], here we tested in vivo their weight-loss potential on both young and early-old flies (Figure 4.3). We observed a slight but significant reduction in the body-weight gain of the TW-supplemented young females at the third week (-15% vs inner Ctrl, and -11% vs 1W; $p<0.01$ and $p<0.05$, respectively), whereas the TE supplementation led to a remarkable increase in the body-weight gain at the fourth week (+24% vs inner Ctrl and +20% vs 1W;

p<0.01 and p<0.05, respectively) (Figure 4.3A). An increase in the body-weight gain was observed also in the young males feeding TE-supplemented diet starting from the third week (+29% vs inner Ctrl and +34% vs 1W; p<0.05 and p<0.0001, respectively). (Figure 4.3B).

On the other hand, both TE- and TW-supplementation led to a general increase in the body-weight gain of the early-old females starting from the fifth week compared to the third week (+23% and +19% vs 3W; p<0.05, respectively) (Figure 4.3C) as well as in the early-old males where the body-weight gain started to increase from the fourth week (+25% and +17% vs 3W; p<0.01 and p<0.05, respectively) (Figure 4.3D).

Of note, the food consumption evaluated by the CAFE assay was not affected by the supplementation with the TW or TE extracts in both male and female flies (data not shown), thus excluding that the changes in the body-weight gain and in the lifespan of flies might depend on different food consumption [157].

CLIMBING,PARAQUAT, & TBARS ASSAYS
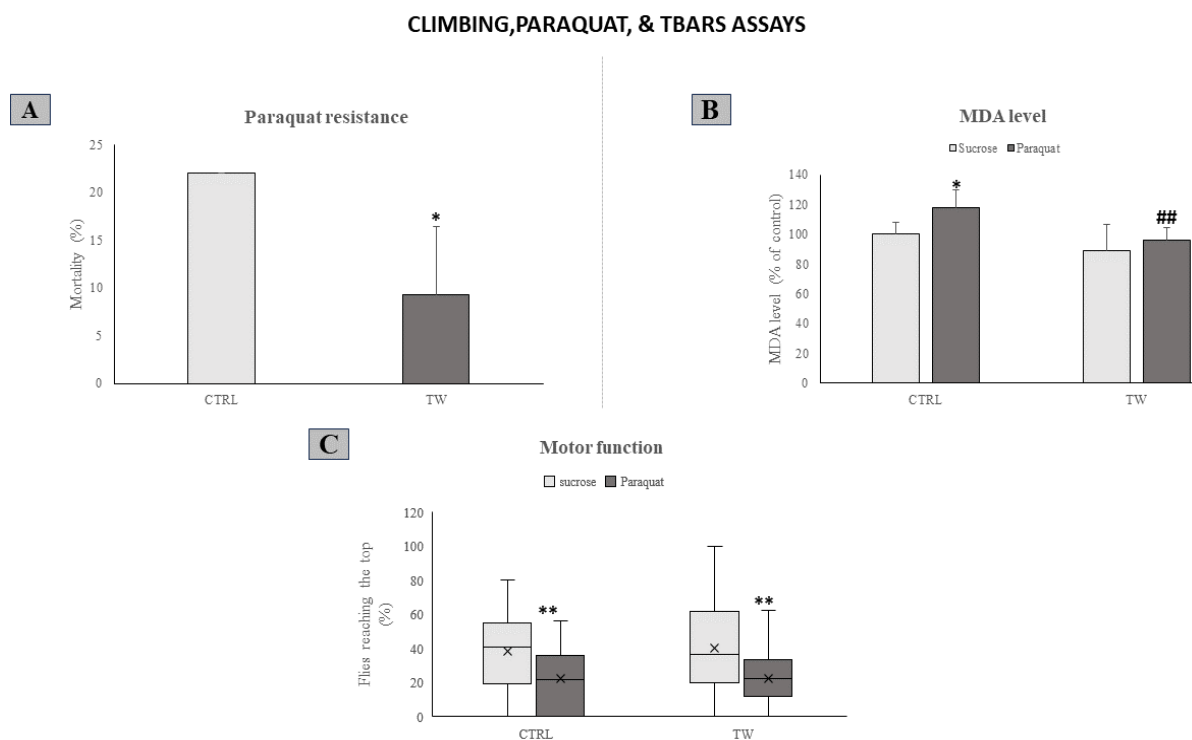
Figure 4.4: Effects of T. spicata supplementation on the oxidative stress

Young female flies fed a TW-supplemented (TW) or standard diet (CTRL) were subjected to Paraquat stress for 40 hrs. (A) The mortality was represented in (%) with respect to the CTRL and expressed as mean ± SD. The significant difference is denoted by symbol: CTRL vs TW *$p \leq 0.05$. (B) Lipid peroxidation in Paraquat-insulted flies was studied by measuring the MDA level using TBARS assay as nmol MDA/mg of sample protein. Values are reported as % of control and mean ± S.D from at least three independent experiments. Significant differences are denoted by symbols: CTRL-sucrose vs CTRL-Paraquat *$p \leq 0.05$, and CTRL - Paraquat vs TW-Paraquat ##$p \leq 0.01$. (C) The motor function in Paraquat-insulted flies was studied in terms of the climbing ability. Data are expressed as mean ± SD.

4.3.3. T. spicata supplementation protects the D. melanogaster against oxidative stress

Based on the observed beneficial effects of TW supplementation on both the lifespan and body weight gain of young females, we focused on this cohort of flies for the further investigations. We assessed the possible protective effects of TW on young females exposed to Paraquat, which is a strong inducer of oxidative stress *in vivo* [158], [159]. We observed that TW supplementation improved the fly mortality caused by Paraquat (9.3% *vs* 22% of mortality in TW-treated *vs* Ctrl flies, respectively; $p<0.05$) (Figure 4.4A).

In parallel, we measured the lipid peroxidation at the whole-body level of young females by TBARS assay (Figure 4.4B). Upon exposure to 2.5mM Paraquat for 40 hrs., the MDA level increased in Paraquat-insulted flies (+26% compared to Ctrl flies, $p<0.05$). When Paraquat-insulted flies were feeding by TW-supplemented diet, the MDA increase was significantly reduced (-30% with respect to Paraquat-insulted flies as control; $p<0.01$).

4.3.4. T. spicata supplementation modulates the expression of defense-related genes

Based on the above results, we tested the expression of genes potentially involved in the antioxidant defense (*Ho* and *Trxr1*), and stress tolerance (*TotA*) by RT-PCR (Fig. 5). The control young females showed an age-related up-regulation of *HO* expression reaching significance at T2 (4.10 fold induction *vs* T0; p<0.0001), while a dramatic decrease occurred in the TW-supplemented flies (0.38 fold induction at T2 *vs* T0; p<0.0001) (Figure 4.5A). Similarly, *Trxr1* gene in control females showed an age-related up-regulation with a maximum at T2 (3.75 fold induction *vs* T0; p<0.0001), and a down-regulation in the TW-supplemented flies (0.4 fold induction at T2 *vs* CTRL at T2; p< 0.0001) (Figure 4.5B).
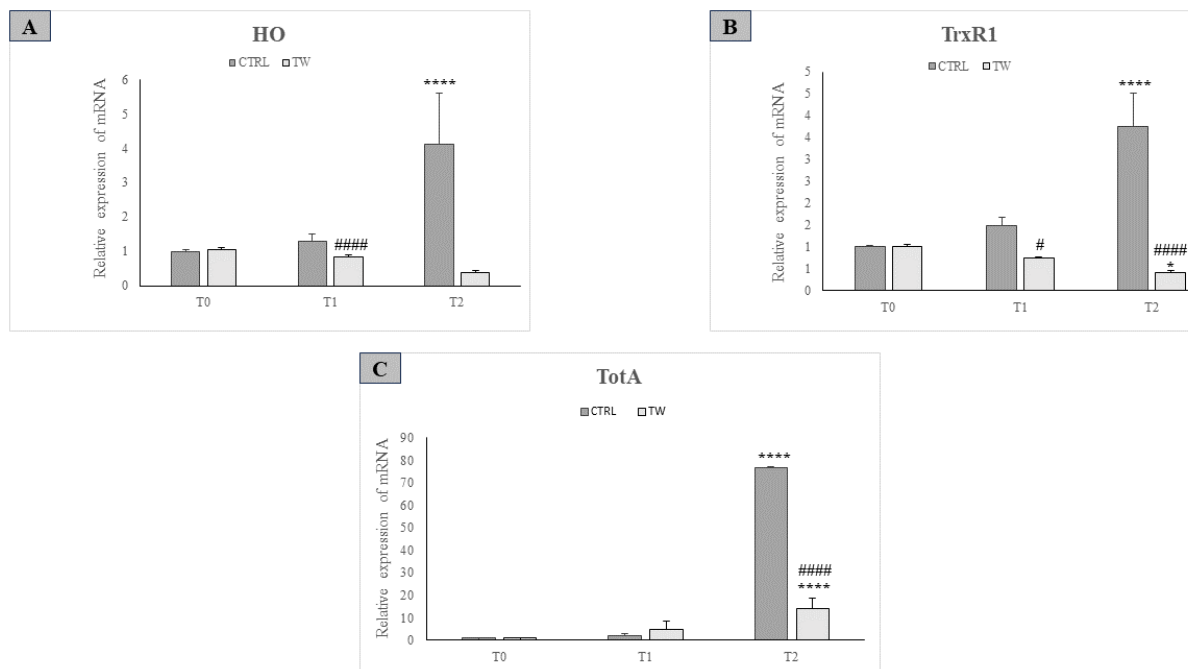
Figure 4.5: *T. spicata supplementation modulates the expression of defense-related genes*

Two antioxidant genes **(A)** HO and **(B)** TrxR1, and one stress tolerance-related gene **(C)** TotA were analyzed by real-time PCR. Three-time intervals were analyzed: T0 (day of supplementation), T1 (2 weeks after supplementation), and T2 (4 weeks after supplementation). The relative quantity of target mRNA was calculated by the comparative Cq method using ribosomal protein L32 (RPL32) as housekeeping gene and expressed as fold induction with respect to controls. Values are mean ± S.D. from at least three independent experiments. Statistical significance between groups is denoted by symbols: CTRL-T0 *vs* CTRL at different times *p≤0.05, **** p≤0.0001, CTRL-T1 *vs* TW-T1 #p≤0.05, and CTRL-T2 *vs* TW-T2 #### p≤0.0001.

Also the environmental stress-activated gene *TotA* showed an age-related up-regulation with a maximum at T2 in both control flies (76.70 fold induction *vs* CTRL at T0; $p<0.0001$), and in TW-fed flies (13.92 fold induction *vs* CTRL at T2; $p<0.0001$) although the up-regulation was markedly lower than in control (Figure 4.5C).

4.4. DISCUSSION

The present study employed the *D. melanogaster* fly as an *in vivo* model to investigate the anti-aging, body-weight control, and antioxidant potentials of two polyphenol-enriched extracts from *T. spicata* leaves. The main findings of this study, taking in consideration both the age (young *vs* early old) and the sex of the flies, demonstrated the potency of *T. spicata* leaves, in particular the water extract, to extend the lifespan of the young female flies, reduce their body-weight gain, and protect them against oxidative stress.

Aging is a complex biological process developed by the progressive deterioration of individual´s function and capacity to recover from different inner and external disturbances, leading to increased morbidity and mortality. Although aging cannot be prevented, slowing down the rate of aging is entirely possible to achieve. In this context, medicinal herbs are recognized by the "nourishing of life" and their role as anti-aging phytoterapics is gaining attention [160], [161].

T. spicata is a thyme-like plant extremely rich in phenolic compounds and, therefore, represents a promising candidate as phytotherapy and nutraceutical herb. Our previous study reported the phenolome characterization of both the aqueous and ethanolic extract (TW and TE) from *T. spicata* aerial parts [10]. These results indicated that the aqueous extract was more effective in reducing hepatic steatosis, and the ethanolic extract had higher antioxidant potential [10]. Therefore, based on our previous in vitro results, for the in vivo study that is rather

complex and of long duration we selected the extract concentration (15 µg/ml) which resulted the most effective on the cells [10], [20], [162].

The present study demonstrates, for the first time, the beneficial effects in vivo of a dietary supplementation with T. spicata. First, we found that exclusively the aqueous extract ameliorated the fly lifespan in a sex-dependent manner. Indeed, TW-supplementation significantly increased the mean lifespan of young females (1W-old) compared to the control group feeding a standard diet. As longevity seems to be related to the control of body-weight and lipid metabolism homeostasis, we assessed in parallel the body-weight gain. Indeed, a recent paper [163] reported that the lysosomal lipase-deficient mice showed premature death, while nematodes overexpressing it were lean, long-lived individuals, furthermore, flies lacking the triacylglycerol lipase were obese and short-lived. We found also for the body-weight control a sex-dependent effect. The aqueous extract was effective in young females but not in males. By contrast, the ethanolic extract enhanced the body-weight gain in all the cohorts of flies of both sexes and ages, and so did also the TW extract in early-old female and male flies.

Of note, we observed a sex- and age-dependent effect of the T. spicata supplementation according to many studies on functional food in flies that described differences with sex. Indeed, the anatomical and physiological characteristics of each sex may influence the response to diet, also depending on the energy demand making the two sexes differentially sensitive to specific nutrients [164]. Moreover, also the marital-status of the flies plays a role: i.e. virgin females live significantly longer than mated females due to egg production and mating costs [165].

The different biological activity of the two extracts can be explained by the different phenolome profile characterizing them. In detail, the aqueous extract is rich in hydrophilic compounds, especially the rosmarinic acid, a phenolic acid deriving from the caffeic acid.

Conversely, the ethanolic extract is extremely rich in volatile organic compounds, especially carvacrol (2-methyl-5-(1-methylethyl)-phenol), a phenolic monoterpenoid with one hydroxyl group (-OH). We can hypothesize that both the chemical structure of the different polyphenolic compounds, and, most importantly, their different bioavailability can influence their efficacy *in vivo* on the *Drosophila* lifespan. In fact, a published study on quercetin and its derivatives revealed that the quercetin 3-*O*-β-d-glucopyranoside-(4→1)-β-d-glucopyranoside was the most potent quercetin derivative in terms of lifespan extension on the *Caenorhabditis elegans* model probably due to its highest hydrophilicity [166]. We wish to mention that the weight-loss potential of TW could be sustained also by salvianolic acid (SA) which is the most abundant polyphenol detected when TW had been subjected to a simulated *in vitro* digestion [162]. In fact, a large body of *in vitro* and *in vivo* evidences showed that SA reduces obesity and obesity-related disorders by suppressing adipogenesis and decreasing body-weight in high-fat diet animal model [167], and hepatoprotective effects against lipotoxicity [168]–[170]. The anti-obesity effects of SA could be assigned to its ability in improving lipid and glucose metabolisms [171].

A crucial factor sustaining the aging is the over-accumulation of ROS and oxidant species. The idea that ROS might act on the aging process due to the accumulation of ROS-induced damages has been postulated many years ago [33]. This theory has been confirmed in many animal models showing reduced oxidative damage and/or increased resistance to oxidative stress in the longer-lived animals [172]. In order to better understand the mechanisms through which the aqueous extract improves the mean half-life, we tested its protective effects against Paraquat, which is a strong oxidative stress inducer [173], [174]. We observed that Paraquat increased mortality of the young female flies, and supplementation with TW was protective by decreasing their mortality rate. The mortality could depend on the Paraquat-

induced oxidative stress. Indeed, in control young females, the exposure to Paraquat triggered oxidative stress that we verified in terms of increased lipid peroxidation, and the TW supplementation reduced the Paraquat-induced lipid peroxidation. However, when we checked the motor function of young female flies we observed an impair after Paraquat insult, but TW did not rescue the climbing ability. Taken together, our results demonstrated that the protective role of dietary intake of TW occurs mainly by reducing the fly mortality rather than by improving the motor function impair. These findings are in line with a recent report [175] demonstrating that xanthohumol, a flavonoid abundant in Humulus lupulus, improved the resistance against oxidative stress being induced by both hydrogen peroxide and Paraquat. Another study on Drosophila reported that an enhanced resistance against oxidative stress reduced the fly mortality upon ethanol consumption [176].

In an attempt to better characterize the molecular pathways sustaining the beneficial effects of the extract on lifespan and body-weight control, we investigated the expression of genes directly implicated in antioxidant (*HO* and *TrxR1*), and stress tolerance (*TotA*) processes.

Regarding the antioxidant defense, we tested two genes: heme oxygenase and thioredoxin. *Ho* is known to protect against oxidative stress [177] by acting on apoptotic and autophagic processes in *Drosophila* [178]. Also *Trxr1* in *Drosophila* protects against oxidative stress, being the thioredoxin system a major player in glutathione metabolism [179]. We observed an age-related down-regulation in both the *Ho* and *Trxr1* expression in TW-supplemented flies. However, some studies on fruit fly cohorts reported that lack of glutathione reductase stimulates antioxidant defense [180], and that the consumption of chili-supplemented food extends lifespan, although the activity of glutathione-S-transferase (GST) was decreased [181], suggesting that the extension is not mediated by a strengthening of antioxidant defenses. Therefore, we could suggest that the downregulation of *Ho* and *Trxr1* genes upon TW

supplementation can be a consequence of the lower level of oxidative stress caused by the extract activity.

Regarding the stress tolerance, we tested the Turandot A (TotA) gene belonging to a family of stress-induced genes [182], which are stimulated by severe stresses [183]. Therefore, we observed an age-related up-regulation of TotA expression in control flies, while this up-regulation was lower in TW-supplemented flies. This result could be attributed to the antioxidant protection of TW which in turn will keep the flies in a consistent "not severe" stress condition.

In conclusion, our data demonstrate, for the first time, that dietary intake of T. spicata, in particular the aqueous extract, is able to extend the lifespan and reduce the body-weight gain of fruit flies in age-related and sex-dependent manners. Our hypothesis is that the extension of lifespan might be mediated by two key processes: (i) decreasing the body-weight gain, and (ii) boosting the antioxidant defense. The different health-promoting efficacy observed for the two extracts should be attributed to their differences in the panel concentration, bioavailability, and properties of the polyphenols, with the aqueous extracts exhibiting the best nutraceutics potential. Nevertheless, further studies should be carried out to investigate if and how the efficacy of T. spicata might affect other parameters including the fertility of the flies.

Chapter 5   Conclusion

The primary research interest of my PhD activity was focused on investigating the potential of both extracts from medicinal plants, such as *Thymbra spicata* L., and some bioactive compounds as beneficial agents for the treatment and/or prevention of overweight, obesity and obesity-related disorders, especially the hepatic steatosis and endothelium dysfunction.

Firstly, starting from the previous results published by our group demonstrating the antisteatotic and antioxidant activities of extracts from leaves of *T. spicata* using *in vitro* models of non-alcoholic fatty liver disease (NAFLD), we assessed *in vitro* the lipid-lowering and protective effects of carvacrol, the most abundant polyphenol contained in the ethanolic extract from *T. spicata* [10]. For this research, we employed two cellular models of hepatic steatosis and endothelial dysfunction. To deepen our understanding on the mechanism of action of carvacrol, we investigated if and how the binding of carvacrol to albumin, which is the physiological transporter of many compounds in the blood, might be altered by the presence of high levels of fatty acids, which are characteristic of plasma of patients. Our findings demonstrated that carvacrol counteracts lipid accumulation and oxidative stress in hepatocytes and protect endothelial cells from oxidative stress and dysfunction. Moreover, the binding of carvacrol to albumin is influenced by high levels of circulating fatty acids that might compete with carvacrol for binding to albumin influencing its transport and bio-distribution. These results suggest a good potential of the *T. spicata* ethanolic extract in ameliorating dysfunction of hepatic and endothelial cells *in vitro*, probably depending on the action of its main polyphenol [184].

As *T. spicata* is an edible plant, it was still unclear whether and how the pattern of phenolic compounds (PCs) found in this plant, as well as their bioactivity, could be modified

during the gastrointestinal transit. For that reason, we investigated the possible loss of phytochemicals that occur throughout the sequential steps of a simulated *in vitro* gastrointestinal (GI) digestion of aqueous and ethanolic extracts of aerial parts of *T. spicata*. Crude, digested, and dialyzed extracts were characterized in terms of their phenolic profile and biological activities. Total contents of carbohydrates, proteins, PCs, flavonoids, and hydroxycinnamic acids were quantified. The changes in the PC profile and in bioactive compounds upon the simulated GI digestion were monitored by HPLC–MS/MS analysis. The antioxidant activity was measured by different spectrophotometric assays, and the antiproliferative potential was assessed using three representative human cancer cell lines. We observed that the simulated GI digestion reduced the phytochemical contents in both aqueous and ethanolic extracts from *T. spicata* and modified the phenolic profile. Interestingly, both *T. spicata* extracts improved their antioxidant activity after digestion, while a partial reduction in the antiproliferative activity was observed for the ethanolic extract. Therefore, our results could provide a scientific basis for the employment of *T. spicata* extract as valuable nutraceutical [162].

The promising *in vitro* outcomes suggested us to pass to *in vivo* models in the attempt to investigate the molecular pathways sustaining the beneficial effects of *T. spicata*. We employed *Drosophila melanogaster* as a typical model for many diseases including aging. Accordingly, we studied *in vivo* the effects of supplementation with either aqueous (TW) or ethanolic (TE) extract from *T. spicata* focusing on the lifespan, body-weight gain, and antioxidant responses of *D. melanogaster* in age- and sex-dependent manner. The water extract was able to extend the lifespan of young female flies, while no effect was observed for the ethanolic extract. In young females, the pro-longevity potential of TW-supplementation was associated with significant effects in reducing the body-weight gain. Furthermore, the TW-supplementation stimulated the antioxidant defense upon exposure to Paraquat, a strong

oxidative stress inducer. Indeed, the TW-supplementation rescued both the Paraquat-induced mortality and counteracted the Paraquat-induced lipid peroxidation, without effects on the locomotor impairment. The expression of a panel of antioxidant defense-related genes was checked showing, for most of them, a down-regulation in TW-supplemented flies with respect to control flies. This study provides insight on the efficacy of dietary supplementation with T. *spicata* in delaying the aging in *D. melanogaster*, possibly by strengthening the antioxidant defenses and the body-weight control. Therefore, the water extract from *T. spicata* could be a promising nutraceutics for aging prevention, and further clinical investigation are required to clarify this aspect [185].

In conclusion, the previously mentioned findings demonstrate a good potential of carvacrol as lipid-lowering agent in steatotic hepatocytes, and as antioxidant and cytoprotective compounds in dysfunctional endotheliocytes *in vitro*. In fact, although the gastrointestinal digestion modified the phenolic profile, but the detected panel of bioactive compounds in *T. spicata* makes this edible plant a potent candidate to be used as a dietary supplement for different therapeutic purposes as the digestion process had an impact on the nutritional value of *T. spicata*, but it kept its biological effectiveness. Additionally, these health-promoting effects were translated into *in vivo* model using *D. melanogaster* showing remarkable anti-aging characteristics possibly through strengthening the antioxidant defenses and improving the body-weight control, but further clinical research will be necessary to clarify the beneficial effects of *T. spicata*.

Bibliography

[1]   M. Khoury, D. Stien, V. Eparvier, N. Ouaini, and M. El Beyrouthy, "Report on the Medicinal Use of Eleven Lamiaceae Species in Lebanon and Rationalization of Their Antimicrobial Potential by Examination of the Chemical Composition and Antimicrobial Activity of Their Essential Oils," *Evidence-Based Complement. Altern. Med.*, vol. 2016, pp. 1–17, 2016, doi: 10.1155/2016/2547169.

[2]   E. Napoli, L. Siracusa, and G. Ruberto, "New Tricks for Old Guys: Recent Developments in the Chemistry, Biochemistry, Applications and Exploitation of Selected Species from the Lamiaceae Family," *Chem. Biodivers.*, vol. 17, no. 3, Mar. 2020, doi: 10.1002/cbdv.201900677.

[3]   K. Carović-Stanko *et al.*, "Medicinal plants of the family Lamiaceae as functional foods – a review," *Czech J. Food Sci.*, vol. 34, no. No. 5, pp. 377–390, Nov. 2016, doi: 10.17221/504/2015-CJFS.

[4]   M. Bekut, S. Brkić, N. Kladar, G. Dragović, N. Gavarić, and B. Božin, "Potential of selected Lamiaceae plants in anti(retro)viral therapy.," *Pharmacol. Res.*, vol. 133, pp. 301–314, Jul. 2018, doi: 10.1016/j.phrs.2017.12.016.

[5]   N. Vukovic, S. Sukdolak, S. Solujic, and N. Niciforovic, "Antimicrobial Activity of the Essential Oil Obtained from Roots and Chemical Composition of the Volatile Constituents from the Roots, Stems, and Leaves of Ballota nigra from Serbia," *J. Med. Food*, vol. 12, no. 2, pp. 435–441, Apr. 2009, doi: 10.1089/jmf.2008.0164.

[6]   M. Ünlü, G. Vardar-Ünlü, N. Vural, E. Dönmez, and Z. Y. Özbaş, "Chemical composition, antibacterial and antifungal activity of the essential oil of Thymbra spicata L. from Turkey," *Nat. Prod. Res.*, vol. 23, no. 6, pp. 572–579, Apr. 2009, doi: 10.1080/14786410802312316.

[7]   S. (Sonsuzer) Hancı, S. Sahin, and L. Yılmaz, "Isolation of volatile oil from thyme (Thymbra spicata) by steam distillation," *Nahrung/Food*, vol. 47, no. 4, pp. 252–255, Aug. 2003, doi: 10.1002/food.200390059.

[8]   E. K. Akkol *et al.*, "Cholesterol-reducer, antioxidant and liver protective effects of Thymbra spicata L. var. spicata," *J. Ethnopharmacol.*, vol. 126, no. 2, pp. 314–319, Nov. 2009, doi: 10.1016/j.jep.2009.08.020.

[9]   G. Avcı, E. Kupeli, A. Eryavuz, E. Yesilada, and I. Kucukkurt, "Antihypercholesterolaemic and antioxidant activity assessment of some plants used as remedy in Turkish folk medicine," *J. Ethnopharmacol.*, vol. 107, no. 3, pp. 418–423, Oct. 2006, doi: 10.1016/j.jep.2006.03.032.

[10]   M. Khalil *et al.*, "Antisteatotic and antioxidant activities of Thymbra spicata L. extracts in hepatic and endothelial cells as in vitro models of non-alcoholic fatty liver disease," *J. Ethnopharmacol.*, vol. 239, p. 111919, Jul. 2019, doi: 10.1016/j.jep.2019.111919.

[11]   I. L.-B. Amor *et al.*, "Phytochemistry and biological activities of Phlomis species," *J. Ethnopharmacol.*, vol. 125, no. 2, pp. 183–202, Sep. 2009, doi: 10.1016/j.jep.2009.06.022.

[12]   F. Diab, H. Zbeeb, F. Baldini, P. Portincasa, M. Khalil, and L. Vergani, "The Potential of Lamiaceae Herbs for Mitigation of Overweight, Obesity, and Fatty Liver: Studies and Perspectives," *Molecules*, vol. 27, no. 15, p. 5043, Aug. 2022, doi: 10.3390/molecules27155043.

[13]   P. G. Kopelman, "Obesity as a medical problem," *Nature*, vol. 404, no. 6778, pp. 635–643, Apr. 2000, doi: 10.1038/35007508.

[14]   L. Vergani, "Fatty Acids and Effects on In Vitro and In Vivo Models of Liver Steatosis," *Curr. Med. Chem.*, vol. 26, no. 19, pp. 3439–3456, Sep. 2019, doi:

10.2174/0929867324666170518101334.

[15]   E. M. Brunt *et al.*, "Nonalcoholic fatty liver disease," *Nat. Rev. Dis. Prim.*, vol. 1, no. 1, p. 15080, Dec. 2015, doi: 10.1038/nrdp.2015.80.

[16]   M. S. Siddiqui *et al.*, "Case definitions for inclusion and analysis of endpoints in clinical trials for nonalcoholic steatohepatitis through the lens of regulatory science," *Hepatology*, vol. 67, no. 5, pp. 2001–2012, May 2018, doi: 10.1002/hep.29607.

[17]   V. Zámbó, L. Simon-Szabó, P. Szelényi, É. Kereszturi, G. Bánhegyi, and M. Csala, "Lipotoxicity in the liver," *World J. Hepatol.*, vol. 5, no. 10, p. 550, Oct. 2013, doi: 10.4254/wjh.v5.i10.550.

[18]   E. Buzzetti, M. Pinzani, and E. A. Tsochatzis, "The multiple-hit pathogenesis of non-alcoholic fatty liver disease (NAFLD)," *Metabolism*, vol. 65, no. 8, pp. 1038–1048, Aug. 2016, doi: 10.1016/j.metabol.2015.12.012.

[19]   Y. Y. Huang, A. M. Gusdon, and S. Qu, "Nonalcoholic fatty liver disease: molecular pathways and therapeutic strategies," *Lipids Health Dis.*, vol. 12, no. 1, p. 171, Dec. 2013, doi: 10.1186/1476-511X-12-171.

[20]   M. Khalil *et al.*, "Unraveling the beneficial effects of herbal Lebanese mixture 'Za'atar'. History, studies, and properties of a potential healthy food ingredient," *J. Funct. Foods*, vol. 90, p. 104993, Mar. 2022, doi: 10.1016/j.jff.2022.104993.

[21]   J. D. Tune, A. G. Goodwill, D. J. Sassoon, and K. J. Mather, "Cardiovascular consequences of metabolic syndrome," *Transl. Res.*, vol. 183, pp. 57–70, May 2017, doi: 10.1016/j.trsl.2017.01.001.

[22]   J.-P. Montani, J. F. Carroll, T. M. Dwyer, V. Antic, Z. Yang, and A. G. Dulloo, "Ectopic fat storage in heart, blood vessels and kidneys in the pathogenesis of cardiovascular diseases," *Int. J. Obes.*, vol. 28, no. S4, pp. S58–S65, Dec. 2004, doi: 10.1038/sj.ijo.0802858.

[23] A. Deprince, J. T. Haas, and B. Staels, "Dysregulated lipid metabolism links NAFLD to cardiovascular disease," *Mol. Metab.*, vol. 42, p. 101092, Dec. 2020, doi: 10.1016/j.molmet.2020.101092.

[24] M. Nakamura and J. Sadoshima, "Cardiomyopathy in obesity, insulin resistance and diabetes," *J. Physiol.*, vol. 598, no. 14, pp. 2977–2993, Jul. 2020, doi: 10.1113/JP276747.

[25] D. F. Clayton, M. Weiss, and J. E. Darnell, "Liver-Specific RNA Metabolism in Hepatoma Cells: Variations in Transcription Rates and mRNA Levels," *Mol. Cell. Biol.*, vol. 5, no. 10, pp. 2633–2641, Oct. 1985, doi: 10.1128/mcb.5.10.2633-2641.1985.

[26] G. Vecchione *et al.*, "The Nutraceutic Silybin Counteracts Excess Lipid Accumulation and Ongoing Oxidative Stress in an In Vitro Model of Non-Alcoholic Fatty Liver Disease Progression," *Front. Nutr.*, vol. 4, Sep. 2017, doi: 10.3389/fnut.2017.00042.

[27] G. Marchesini *et al.*, "Association of nonalcoholic fatty liver disease with insulin resistance," *Am. J. Med.*, vol. 107, no. 5, pp. 450–455, Nov. 1999, doi: 10.1016/S0002-9343(99)00271-5.

[28] N. Villanova *et al.*, "Endothelial dysfunction and cardiovascular risk profile in nonalcoholic fatty liver disease," *Hepatology*, vol. 42, no. 2, pp. 473–480, Aug. 2005, doi: 10.1002/hep.20781.

[29] D. P. Faxon *et al.*, "Atherosclerotic Vascular Disease Conference," *Circulation*, vol. 109, no. 21, pp. 2617–2625, Jun. 2004, doi: 10.1161/01.CIR.0000128520.37674.EF.

[30] P. Libby, P. M. Ridker, and G. K. Hansson, "Progress and challenges in translating the biology of atherosclerosis," *Nature*, vol. 473, no. 7347, pp. 317–325, May 2011, doi: 10.1038/nature10146.

[31] M. Yáñez-Mó *et al.*, "Biological properties of extracellular vesicles and their

physiological functions," *J. Extracell. Vesicles*, vol. 4, no. 1, pp. 1–60, Jan. 2015, doi: 10.3402/jev.v4.27066.

[32]   A. Baragetti *et al.*, "Subclinical atherosclerosis is associated with Epicardial Fat Thickness and hepatic steatosis in the general population," *Nutr. Metab. Cardiovasc. Dis.*, vol. 26, no. 2, pp. 141–153, Feb. 2016, doi: 10.1016/j.numecd.2015.10.013.

[33]   D. Harman, "Aging: A Theory Based on Free Radical and Radiation Chemistry," *J. Gerontol.*, vol. 11, no. 3, pp. 298–300, Jul. 1956, doi: 10.1093/geronj/11.3.298.

[34]   L. C. D. Pomatto and K. J. A. Davies, "Adaptive homeostasis and the free radical theory of ageing," *Free Radic. Biol. Med.*, vol. 124, pp. 420–430, Aug. 2018, doi: 10.1016/j.freeradbiomed.2018.06.016.

[35]   C. Franceschi *et al.*, "Inflamm-aging. An evolutionary perspective on immunosenescence.," *Ann. N. Y. Acad. Sci.*, vol. 908, no. 1, pp. 244–54, Jun. 2000, doi: 10.1111/j.1749-6632.2000.tb06651.x.

[36]   V. Salvestrini, C. Sell, and A. Lorenzini, "Obesity May Accelerate the Aging Process," *Front. Endocrinol. (Lausanne).*, vol. 10, no. MAY, May 2019, doi: 10.3389/fendo.2019.00266.

[37]   C. Peng, H. Y. E. Chan, Y. Huang, H. Yu, and Z.-Y. Chen, "Apple Polyphenols Extend the Mean Lifespan of Drosophila melanogaster," *J. Agric. Food Chem.*, vol. 59, no. 5, pp. 2097–2106, Mar. 2011, doi: 10.1021/jf1046267.

[38]   T. E. Lopez *et al.*, "Green tea polyphenols require the mitochondrial iron transporter, mitoferrin , for lifespan extension in Drosophila melanogaster," *Arch. Insect Biochem. Physiol.*, vol. 93, no. 4, pp. 210–221, Dec. 2016, doi: 10.1002/arch.21353.

[39]   M. A. Wilson, B. Shukitt-Hale, W. Kalt, D. K. Ingram, J. A. Joseph, and C. A. Wolkow, "Blueberry polyphenols increase lifespan and thermotolerance in Caenorhabditis elegans," *Aging Cell*, vol. 5, no. 1, pp. 59–68, Feb. 2006, doi:

10.1111/j.1474-9726.2006.00192.x.

[40]   H. Sajed, A. Sahebkar, and M. Iranshahi, "Zataria multiflora Boiss. (Shirazi thyme) -
       An ancient condiment with modern pharmaceutical uses," *Journal of
       Ethnopharmacology*, vol. 145, no. 3. J Ethnopharmacol, pp. 686–698, Feb. 13, 2013.
       doi: 10.1016/j.jep.2012.12.018.

[41]   J. M. Lorenzo *et al.*, "Understanding the potential benefits of thyme and its derived
       products for food industry and consumer health: From extraction of value-added
       compounds to the evaluation of bioaccessibility, bioavailability, anti-inflammatory,
       and antimicrobial activities," *Critical Reviews in Food Science and Nutrition*, vol. 59,
       no. 18. Taylor and Francis Inc., pp. 2879–2895, Oct. 11, 2019. doi:
       10.1080/10408398.2018.1477730.

[42]   M. Khalil *et al.*, "Antitumor Activity of Ethanolic Extract from Thymbra Spicata L.
       aerial Parts: Effects on Cell Viability and Proliferation, Apoptosis Induction, STAT3,
       and NF-kB Signaling," *Nutr. Cancer*, vol. 73, no. 7, pp. 1193–1206, Aug. 2021, doi:
       10.1080/01635581.2020.1792517.

[43]   M. Al Hafi, M. El Beyrouthy, N. Ouaini, D. Stien, D. Rutledge, and S. Chaillou,
       "Chemical Composition and Antimicrobial Activity of Satureja, Thymus, and
       Thymbra Species Grown in Lebanon," *Chem. Biodivers.*, vol. 14, no. 5, May 2017,
       doi: 10.1002/cbdv.201600236.

[44]   A. Marchese *et al.*, "The natural plant compound carvacrol as an antimicrobial and
       anti-biofilm agent: mechanisms, synergies and bio-inspired anti-infective materials,"
       Biofouling, vol. 34, no. 6, pp. 630–656, Jul. 2018, doi:
       10.1080/08927014.2018.1480756.

[45]   G. C. Farrell and C. Z. Larter, "Nonalcoholic fatty liver disease: From steatosis to
       cirrhosis," *Hepatology*, vol. 43, no. S1, pp. S99–S112, Feb. 2006, doi:

10.1002/hep.20973.

[46] C. D. Byrne and G. Targher, "NAFLD: A multisystem disease," *Journal of Hepatology*, vol. 62, no. S1. Elsevier, pp. S47–S64, 2015. doi: 10.1016/j.jhep.2014.12.012.

[47] S. L. Friedman, B. A. Neuschwander-Tetri, M. Rinella, and A. J. Sanyal, *Mechanisms of NAFLD development and therapeutic strategies*, vol. 24, no. 7. 2018. doi: 10.1038/s41591-018-0104-9.

[48] R. Loomba and A. J. Sanyal, "The global NAFLD epidemic," *Nature Reviews Gastroenterology and Hepatology*, vol. 10, no. 11. Nat Rev Gastroenterol Hepatol, pp. 686–690, Nov. 2013. doi: 10.1038/nrgastro.2013.171.

[49] L. Bhatia, E. Scorletti, N. Curzen, G. F. Clough, P. C. Calder, and C. D. Byrne, "Improvement in non-alcoholic fatty liver disease severity is associated with a reduction in carotid intima-media thickness progression," *Atherosclerosis*, vol. 246, pp. 13–20, Mar. 2016, doi: 10.1016/j.atherosclerosis.2015.12.028.

[50] B. S. P. Bentham Science Publisher, "Current Pharmacological Treatment of Nonalcoholic Fatty Liver," *Curr. Med. Chem.*, vol. 13, no. 24, pp. 2889–2900, Sep. 2006, doi: 10.2174/092986706778521878.

[51] J. C. P. Silva and J. G. Jones, "Improving Metabolic Control Through Functional Foods," *Curr. Med. Chem.*, vol. 26, no. 19, pp. 3424–3438, May 2017, doi: 10.2174/0929867324666170523130123.

[52] S. Pisonero-Vaquero, J. Gonzalez-Gallego, S. Sanchez-Campos, and M. Garcia-Mediavilla, "Flavonoids and Related Compounds in Non-Alcoholic Fatty Liver Disease Therapy," *Curr. Med. Chem.*, vol. 22, no. 25, pp. 2991–3012, Sep. 2015, doi: 10.2174/0929867322666150805094940.

[53] L. Leboffe, A. di Masi, F. Polticelli, V. Trezza, and P. Ascenzi, "Structural Basis of

Drug Recognition by Human Serum Albumin," *Curr. Med. Chem.*, vol. 27, no. 30, pp. 4907–4931, Mar. 2019, doi: 10.2174/0929867326666190320105316.

[54]   F. Yang, Y. Zhang, and H. Liang, "Interactive association of drugs binding to human serum albumin," *International Journal of Molecular Sciences*, vol. 15, no. 3. Molecular Diversity Preservation International, pp. 3580–3595, Feb. 27, 2014. doi: 10.3390/ijms15033580.

[55]   Z. Zhivkova, "Studies on Drug – Human Serum Albumin Binding: The Current State of the Matter," *Curr. Pharm. Des.*, vol. 21, no. 14, pp. 1817–1830, Apr. 2015, doi: 10.2174/1381612821666150302113710.

[56]   R. Kaissi, F. Abdallah, S. Haidar, S. Fourmentin, and H. Greige-Gerges, "Binding of Monoterpenes to Human Serum Albumin: Investigation of the Effect of Hydrophobicity and Structure," *J. Colloid Sci. Biotechnol.*, vol. 4, no. 1, pp. 71–78, Mar. 2015, doi: 10.1166/jcsb.2015.1113.

[57]   O. Herrera-Calderon *et al.*, "Carvacrol: An in silico approach of a candidate drug on HER2, PI3Kα, mTOR, HER-α, PR, and EGFR receptors in the breast cancer," *Evidence-based Complement. Altern. Med.*, vol. 2020, 2020, doi: 10.1155/2020/8830665.

[58]   K. Yamasaki *et al.*, "Long chain fatty acids alter the interactive binding of ligands to the two principal drug binding sites of human serum albumin," *PLoS One*, vol. 12, no. 6, p. e0180404, Jun. 2017, doi: 10.1371/journal.pone.0180404.

[59]   Y. Ni *et al.*, "Circulating Unsaturated Fatty Acids Delineate the Metabolic Status of Obese Individuals," *EBioMedicine*, vol. 2, no. 10, pp. 1513–1522, Oct. 2015, doi: 10.1016/j.ebiom.2015.09.004.

[60]   R. Feng *et al.*, "Free fatty acids profile among lean, overweight and obese non-alcoholic fatty liver disease patients: A case - Control study," *Lipids Health Dis.*, vol.

16, no. 1, Sep. 2017, doi: 10.1186/s12944-017-0551-1.

[61]　"Unbound free fatty acid levels in human serum - PubMed."
https://pubmed.ncbi.nlm.nih.gov/7751810/ (accessed Apr. 26, 2021).

[62]　E. Grasselli *et al.*, "Non-receptor-mediated actions are responsible for the lipid-lowering effects of iodothyronines in FaO rat hepatoma cells," *J. Endocrinol.*, vol. 210, no. 1, pp. 59–69, Jul. 2011, doi: 10.1530/JOE-11-0074.

[63]　M. Khalil *et al.*, "Protective effects of extracts from Ephedra foeminea Forssk fruits against oxidative injury in human endothelial cells," *J. Ethnopharmacol.*, vol. 260, p. 112976, Oct. 2020, doi: 10.1016/j.jep.2020.112976.

[64]　Z. Wang, Y. Wang, Y. Chen, and J. Lv, "The IL-24 gene protects human umbilical vein endothelial cells against H2O2-induced injury and may be useful as a treatment for cardiovascular disease," *Int. J. Mol. Med.*, vol. 37, no. 3, pp. 581–592, Mar. 2016, doi: 10.3892/ijmm.2016.2466.

[65]　"PubChem." https://pubchem.ncbi.nlm.nih.gov/ (accessed Dec. 05, 2023).

[66]　L. C. Li, Z. W. Wang, X. P. Hu, Z. Y. Wu, Z. P. Hu, and Y. Le Ruan, "MDG-1 inhibits H2O2-induced apoptosis and inflammation in human umbilical vein endothelial cells," *Mol. Med. Rep.*, vol. 16, no. 3, pp. 3673–3679, Sep. 2017, doi: 10.3892/mmr.2017.6957.

[67]　M. M. Bradford, "A rapid and sensitive method for the quantitation of microgram quantities of protein utilizing the principle of protein-dye binding," *Anal. Biochem.*, vol. 72, no. 1–2, pp. 248–254, May 1976, doi: 10.1016/0003-2697(76)90527-3.

[68]　M. Grandl and G. Schmitz, "Fluorescent high-content imaging allows the discrimination and quantitation of E-LDL-induced lipid droplets and Ox-LDL-generated phospholipidosis in human macrophages," *Cytom. Part A*, vol. 77, no. 3, pp. 231–242, Mar. 2010, doi: 10.1002/cyto.a.20828.

[69]   B. Halliwell and M. Whiteman, "Measuring reactive species and oxidative damage in vivo and in cell culture: how should you do it and what do the results mean?," *Br. J. Pharmacol.*, vol. 142, no. 2, pp. 231–255, May 2004, doi: 10.1038/sj.bjp.0705776.

[70]   H. Iguchi, S. Kojo, and M. Ikeda, "Lipid peroxidation and disintegration of the cell membrane structure in cultures of rat lung fibroblasts treated with asbestos," *J. Appl. Toxicol.*, vol. 13, no. 4, pp. 269–275, Jul. 1993, doi: 10.1002/jat.2550130409.

[71]   L. C. Green, D. A. Wagner, J. Glogowski, P. L. Skipper, J. S. Wishnok, and S. R. Tannenbaum, "Analysis of nitrate, nitrite, and [15N]nitrate in biological fluids," *Anal. Biochem.*, vol. 126, no. 1, pp. 131–138, Oct. 1982, doi: 10.1016/0003-2697(82)90118-X.

[72]   L. G. Rodriguez, X. Wu, and J. L. Guan, "Wound-healing assay.," *Methods Mol. Biol.*, vol. 294, pp. 23–29, 2005, doi: 10.1385/1-59259-860-9:023.

[73]   F. Mohammadi, A. K. Bordbar, A. Divsalar, K. Mohammadi, and A. A. Saboury, "Analysis of binding interaction of curcumin and diacetylcurcumin with human and bovine serum albumin using fluorescence and circular dichroism spectroscopy," *Protein J.*, vol. 28, no. 3–4, pp. 189–196, May 2009, doi: 10.1007/s10930-009-9184-1.

[74]   G. J. van der Vusse, "Albumin as fatty acid transporter," in *Drug Metabolism and Pharmacokinetics*, Japanese Society for the Study of Xenobiotics, 2009, pp. 300–307. doi: 10.2133/dmpk.24.300.

[75]   J. R. Lakowicz, *Principles of fluorescence spectroscopy*. Springer, 2006. doi: 10.1007/978-0-387-46312-4.

[76]   A. H. Hegde, S. N. Prashanth, and J. Seetharamappa, "Interaction of antioxidant flavonoids with calf thymus DNA analyzed by spectroscopic and electrochemical methods," *J. Pharm. Biomed. Anal.*, vol. 63, pp. 40–46, Apr. 2012, doi: 10.1016/j.jpba.2012.01.034.

[77]   Z. E. Suntres, J. Coccimiglio, and M. Alipour, "The Bioactivity and Toxicological Actions of Carvacrol," *Crit. Rev. Food Sci. Nutr.*, vol. 55, no. 3, pp. 304–318, Feb. 2015, doi: 10.1080/10408398.2011.653458.

[78]   E. Kim, Y. Choi, J. Jang, and T. Park, "Carvacrol Protects against Hepatic Steatosis in Mice Fed a High-Fat Diet by Enhancing SIRT1-AMPK Signaling," *Evidence-Based Complement. Altern. Med.*, vol. 2013, pp. 1–10, 2013, doi: 10.1155/2013/290104.

[79]   I. Khan *et al.*, "Carvacrol inhibits cytochrome P450 and protects against binge alcohol-induced liver toxicity," *Food Chem. Toxicol.*, vol. 131, Sep. 2019, doi: 10.1016/j.fct.2019.110582.

[80]   S. S. Palabiyik *et al.*, "The protective effects of carvacrol and thymol against paracetamol-induced toxicity on human hepatocellular carcinoma cell lines (HepG2)," *Hum. Exp. Toxicol.*, vol. 35, no. 12, pp. 1252–1263, Dec. 2016, doi: 10.1177/0960327115627688.

[81]   B. Aristatile, K. S. Ai-Numair, C. Veeramani, and K. V. Pugalendi, "Antihyperlipidemic effect of carvacrol on d-galactosamine-induced hepatotoxic rats," *J. Basic Clin. Physiol. Pharmacol.*, vol. 20, no. 1, pp. 15–28, 2009, doi: 10.1515/JBCPP.2009.20.1.15.

[82]   W. Zhao, C. Deng, Q. Han, H. Xu, and Y. Chen, "Carvacrol may alleviate vascular inflammation in diabetic db/db mice," *Int. J. Mol. Med.*, vol. 46, no. 3, pp. 977–988, Sep. 2020, doi: 10.3892/ijmm.2020.4654.

[83]   Z. Hakimi *et al.*, "Protective Effects of Carvacrol on Brain Tissue Inflammation and Oxidative Stress as well as Learning and Memory in Lipopolysaccharide-Challenged Rats," *Neurotox. Res.*, vol. 37, no. 4, pp. 965–976, Apr. 2020, doi: 10.1007/s12640-019-00144-5.

[84]   D. Q. H. Wang, P. Portincasa, and B. A. Neuschwander-Tetri, "Steatosis in the Liver,"

in *Comprehensive Physiology*, Wiley, 2013, pp. 1493–1532. doi: 10.1002/cphy.c130001.

[85]   L. Vergani, F. Baldini, M. Khalil, A. Voci, P. Putignano, and N. Miraglia, "New Perspectives of S-Adenosylmethionine (SAMe) Applications to Attenuate Fatty Acid-Induced Steatosis and Oxidative Stress in Hepatic and Endothelial Cells," *Molecules*, vol. 25, no. 18, p. 4237, Sep. 2020, doi: 10.3390/molecules25184237.

[86]   S. Spahis, E. Delvin, J. M. Borys, and E. Levy, "Oxidative Stress as a Critical Factor in Nonalcoholic Fatty Liver Disease Pathogenesis," *Antioxidants and Redox Signaling*, vol. 26, no. 10. Mary Ann Liebert Inc., pp. 519–541, Apr. 01, 2017. doi: 10.1089/ars.2016.6776.

[87]   X. Pi, L. Xie, and C. Patterson, "Emerging roles of vascular endothelium in metabolic homeostasis," *Circulation Research*, vol. 123, no. 4. Lippincott Williams and Wilkins, pp. 477–494, 2018. doi: 10.1161/CIRCRESAHA.118.313237.

[88]   J. Davignon and P. Ganz, "Role of endothelial dysfunction in atherosclerosis," *Circulation*, vol. 109, no. 23 SUPPL. Circulation, Jun. 15, 2004. doi: 10.1161/01.cir.0000131515.03336.f8.

[89]   S. Gao *et al.*, "Protective effects of salvianolic acid B against hydrogen peroxide-induced apoptosis of human umbilical vein endothelial cells and underlying mechanisms," *Int. J. Mol. Med.*, vol. 44, no. 2, pp. 457–468, 2019, doi: 10.3892/ijmm.2019.4227.

[90]   K. Zhou, Y. Ma, and M. S. Brogan, "Chronic and non-healing wounds: The story of vascular endothelial growth factor," *Med. Hypotheses*, vol. 85, no. 4, pp. 399–404, Oct. 2015, doi: 10.1016/j.mehy.2015.06.017.

[91]   M. Rezaeinasab, A. Benvidi, S. Gharaghani, and H. R. Zare, "Chemometrics approaches based on electrochemical methods for the investigation of interaction

between bovine serum albumin and carvacrol with the aim of its application to protein sensing," *J. Electroanal. Chem.*, vol. 845, pp. 48–56, Jul. 2019, doi: 10.1016/j.jelechem.2019.05.040.

[92] J. R. Simard, P. A. Zunszain, J. A. Hamilton, and S. Curry, "Location of High and Low Affinity Fatty Acid Binding Sites on Human Serum Albumin Revealed by NMR Drug-competition Analysis," *J. Mol. Biol.*, vol. 361, no. 2, pp. 336–351, Aug. 2006, doi: 10.1016/j.jmb.2006.06.028.

[93] J. R. Simard *et al.*, "Locating high-affinity fatty acid-binding sites on albumin by x-ray crystallography and NMR spectroscopy," *Proc. Natl. Acad. Sci. U. S. A.*, vol. 102, no. 50, pp. 17958–17963, Dec. 2005, doi: 10.1073/pnas.0506440102.

[94] L. Zhu, F. Yang, L. Chen, E. J. Meehan, and M. Huang, "A new drug binding subsite on human serum albumin and drug–drug interaction studied by X-ray crystallography," *J. Struct. Biol.*, vol. 162, no. 1, pp. 40–49, Apr. 2008, doi: 10.1016/j.jsb.2007.12.004.

[95] P. Novotná and M. Urbanová, "Bilirubin, model membranes and serum albumin interaction: The influence of fatty acids," *Biochim. Biophys. Acta - Biomembr.*, vol. 1848, no. 6, pp. 1331–1340, Jun. 2015, doi: 10.1016/j.bbamem.2015.02.026.

[96] S. Khalili *et al.*, "Kekik aktif maddeler ile insan serum albüminleri arasındaki etkileşimlerin yapısal analizleri," *Turkish J. Biochem.*, vol. 42, no. 4, pp. 459–467, 2017, doi: 10.1515/tjb-2017-0008.

[97] A. Kri{ko, M. Kveder, S. Pe~ar, and G. Pifat, "A Study of Caffeine Binding to Human Serum Albumin."

[98] "Guyton & Hall Textbook of Medical Physiology - 1st Edition." https://www.elsevier.com/books/guyton-and-hall-textbook-of-medical-physiology/vaz/978-81-312-3019-0 (accessed Apr. 07, 2021).

[99]   B. Rizzuti, R. Bartucci, L. Sportelli, and R. Guzzi, "Fatty acid binding into the highest affinity site of human serum albumin observed in molecular dynamics simulation," *Arch. Biochem. Biophys.*, vol. 579, no. 1, pp. 18–25, 2015, doi: 10.1016/j.abb.2015.05.018.

[100]   C. J. Dillard and J. B. German, "Phytochemicals: nutraceuticals and human health," *J. Sci. Food Agric.*, vol. 80, no. 12, pp. 1744–1756, Sep. 2000, doi: 10.1002/1097-0010(20000915)80:12<1744::AID-JSFA725>3.0.CO;2-W.

[101]   M. Bagherniya, V. Nobili, C. N. Blesso, and A. Sahebkar, "Medicinal plants and bioactive natural compounds in the treatment of non-alcoholic fatty liver disease: A clinical review," *Pharmacol. Res.*, vol. 130, pp. 213–240, Apr. 2018, doi: 10.1016/j.phrs.2017.12.020.

[102]   A. Medina-Remón *et al.*, "Effects of total dietary polyphenols on plasma nitric oxide and blood pressure in a high cardiovascular risk cohort. The PREDIMED randomized trial," *Nutr. Metab. Cardiovasc. Dis.*, vol. 25, no. 1, pp. 60–67, Jan. 2015, doi: 10.1016/j.numecd.2014.09.001.

[103]   J. Wang, Y. Song, M. Gao, X. Bai, and Z. Chen, "Neuroprotective Effect of Several Phytochemicals and Its Potential Application in the Prevention of Neurodegenerative Diseases," *Geriatrics*, vol. 1, no. 4, p. 29, Nov. 2016, doi: 10.3390/geriatrics1040029.

[104]   R. H. Liu, "Potential Synergy of Phytochemicals in Cancer Prevention: Mechanism of Action," *J. Nutr.*, vol. 134, no. 12, pp. 3479S-3485S, Dec. 2004, doi: 10.1093/jn/134.12.3479S.

[105]   K. E. Heim, A. R. Tagliaferro, and D. J. Bobilya, "Flavonoid antioxidants: chemistry, metabolism and structure-activity relationships," *J. Nutr. Biochem.*, vol. 13, no. 10, pp. 572–584, Oct. 2002, doi: 10.1016/S0955-2863(02)00208-5.

[106]   D. Lin *et al.*, "An Overview of Plant Phenolic Compounds and Their Importance in

Human Nutrition and Management of Type 2 Diabetes," *Molecules*, vol. 21, no. 10, p. 1374, Oct. 2016, doi: 10.3390/molecules21101374.

[107] D. Dupont *et al.*, "Can dynamic in vitro digestion systems mimic the physiological reality?," *Crit. Rev. Food Sci. Nutr.*, vol. 59, no. 10, pp. 1546–1562, May 2019, doi: 10.1080/10408398.2017.1421900.

[108] J. Grgić, G. Šelo, M. Planinić, M. Tišma, and A. Bucić-Kojić, "Role of the Encapsulation in Bioavailability of Phenolic Compounds," *Antioxidants*, vol. 9, no. 10, p. 923, Sep. 2020, doi: 10.3390/antiox9100923.

[109] J. M. Carbonell-Capella, M. Buniowska, F. J. Barba, M. J. Esteve, and A. Frígola, "Analytical Methods for Determining Bioavailability and Bioaccessibility of Bioactive Compounds from Fruits and Vegetables: A Review," *Compr. Rev. Food Sci. Food Saf.*, vol. 13, no. 2, pp. 155–171, Mar. 2014, doi: 10.1111/1541-4337.12049.

[110] N. Stanisavljević *et al.*, "Antioxidant and antiproliferative activity of chokeberry juice phenolics during in vitro simulated digestion in the presence of food matrix," *Food Chem.*, vol. 175, pp. 516–522, May 2015, doi: 10.1016/j.foodchem.2014.12.009.

[111] H. Ge, Y. Chen, J. Chen, J. Tian, X. Liang, and L. Chen, "Evaluation of antioxidant activities of ethanol extract from Ligusticum subjected to in-vitro gastrointestinal digestion," *Food Chem. Toxicol.*, vol. 119, no. December 2017, pp. 417–424, Sep. 2018, doi: 10.1016/j.fct.2017.12.035.

[112] M. E. Cam *et al.*, "The methanolic extract of Thymus praecox subsp. skorpilii var. skorpilii restores glucose homeostasis, ameliorates insulin resistance and improves pancreatic β-cell function on streptozotocin/nicotinamide-induced type 2 diabetic rats," *J. Ethnopharmacol.*, vol. 231, pp. 29–38, Mar. 2019, doi: 10.1016/j.jep.2018.10.028.

[113] H. J. D. Dorman, O. Bachmayer, M. Kosar, and R. Hiltunen, "Antioxidant Properties of Aqueous Extracts from Selected Lamiaceae Species Grown in Turkey," *J. Agric.*

Food Chem., vol. 52, no. 4, pp. 762–770, Feb. 2004, doi: 10.1021/jf034908v.

[114] M. Minekus *et al.*, "A standardised static in vitro digestion method suitable for food –
an international consensus," *Food Funct.*, vol. 5, no. 6, pp. 1113–1124, 2014, doi:
10.1039/C3FO60702J.

[115] B. Larsen, D. M. S. A. Salem, M. A. E. Sallam, M. M. Mishrikey, and A. I. Beltagy,
"Characterization of the alginates from algae harvested at the Egyptian Red Sea coast,"
Carbohydr. Res., vol. 338, no. 22, pp. 2325–2336, Oct. 2003, doi: 10.1016/S0008-
6215(03)00378-1.

[116] D. B. Silva, I. C. C. Turatti, D. R. Gouveia, M. Ernst, S. P. Teixeira, and N. P. Lopes,
"Mass Spectrometry of Flavonoid Vicenin-2, Based Sunlight Barriers in Lychnophora
species," *Sci. Rep.*, vol. 4, no. 1, p. 4309, May 2015, doi: 10.1038/srep04309.

[117] A. Arvouet-Grand, B. Vennat, A. Pourrat, and P. Legret, "Standardization of propolis
extract and identification of principal constituents.," *J. Pharm. Belg.*, vol. 49, no. 6, pp.
462–8, 1994, Accessed: Apr. 26, 2022. [Online]. Available:
http://www.ncbi.nlm.nih.gov/pubmed/7884635

[118] L. Custódio *et al.*, "Methanol extracts from Cystoseira tamariscifolia and Cystoseira
nodicaulis are able to inhibit cholinesterases and protect a human dopaminergic cell
line from hydrogen peroxide-induced cytotoxicity," *Pharm. Biol.*, vol. 54, no. 9, pp.
1687–1696, Sep. 2016, doi: 10.3109/13880209.2015.1123278.

[119] R. Srinivasan, M. J. N. Chandrasekar, M. J. Nanjan, and B. Suresh, "Antioxidant
activity of Caesalpinia digyna root," *J. Ethnopharmacol.*, vol. 113, no. 2, pp. 284–291,
Sep. 2007, doi: 10.1016/j.jep.2007.06.006.

[120] R. Re, N. Pellegrini, A. Proteggente, A. Pannala, M. Yang, and C. Rice-Evans,
"Antioxidant activity applying an improved ABTS radical cation decolorization
assay," *Free Radic. Biol. Med.*, vol. 26, no. 9–10, pp. 1231–1237, May 1999, doi:

10.1016/S0891-5849(98)00315-3.

[121] O. Firuzi, A. Lacanna, R. Petrucci, G. Marrosu, and L. Saso, "Evaluation of the antioxidant activity of flavonoids by 'ferric reducing antioxidant power' assay and cyclic voltammetry," *Biochim. Biophys. Acta - Gen. Subj.*, vol. 1721, no. 1–3, pp. 174–184, Jan. 2005, doi: 10.1016/j.bbagen.2004.11.001.

[122] R. F. Hussain, A. M. E. Nouri, and R. T. D. Oliver, "A new approach for measurement of cytotoxicity using colorimetric assay," *J. Immunol. Methods*, vol. 160, no. 1, pp. 89–96, Jan. 1993, doi: 10.1016/0022-1759(93)90012-V.

[123] S. Habtemariam, "Molecular Pharmacology of Rosmarinic and Salvianolic Acids: Potential Seeds for Alzheimer's and Vascular Dementia Drugs," *Int. J. Mol. Sci.*, vol. 19, no. 2, p. 458, Feb. 2018, doi: 10.3390/ijms19020458.

[124] R. Guo *et al.*, "Phenolic compounds, antioxidant activity, antiproliferative activity and bioaccessibility of Sea buckthorn (Hippophaë rhamnoides L.) berries as affected by in vitro digestion," *Food Funct.*, vol. 8, no. 11, pp. 4229–4240, Nov. 2017, doi: 10.1039/C7FO00917H.

[125] M. Karaś, A. Jakubczyk, U. Szymanowska, U. Złotek, and E. Zielińska, "Digestion and bioavailability of bioactive phytochemicals," *Int. J. Food Sci. Technol.*, vol. 52, no. 2, pp. 291–305, Feb. 2017, doi: 10.1111/ijfs.13323.

[126] E. Celep, Y. İnan, S. Akyüz, and E. Yesilada, "The bioaccessible phenolic profile and antioxidant potential of Hypericum perfoliatum L. after simulated human digestion," *Ind. Crops Prod.*, vol. 109, pp. 717–723, Dec. 2017, doi: 10.1016/j.indcrop.2017.09.032.

[127] Y. İnan, I. Kurt-Celep, S. Akyüz, T. H. Barak, E. Celep, and E. Yesilada, "An investigation on the enzyme inhibitory activities, phenolic profile and antioxidant potentials of Salvia virgata Jacq," *South African J. Bot.*, vol. 143, pp. 350–358, Dec.

2021, doi: 10.1016/j.sajb.2020.12.007.

[128] T. Scrob, A. Hosu, and C. Cimpoiu, "The Influence of in Vitro Gastrointestinal Digestion of Brassica oleracea Florets on the Antioxidant Activity and Chlorophyll, Carotenoid and Phenolic Content," *Antioxidants*, vol. 8, no. 7, p. 212, Jul. 2019, doi: 10.3390/antiox8070212.

[129] S. Thomas-Valdés, C. Theoduloz, F. Jiménez-Aspee, A. Burgos-Edwards, and G. Schmeda-Hirschmann, "Changes in polyphenol composition and bioactivity of the native Chilean white strawberry (Fragaria chiloensis spp. chiloensis f. chiloensis) after in vitro gastrointestinal digestion," *Food Res. Int.*, vol. 105, pp. 10–18, Mar. 2018, doi: 10.1016/j.foodres.2017.10.074.

[130] J. Pérez-Jiménez, M. E. Díaz-Rubio, and F. Saura-Calixto, "Non-extractable polyphenols, a major dietary antioxidant: occurrence, metabolic fate and health effects," *Nutr. Res. Rev.*, vol. 26, no. 2, pp. 118–129, Dec. 2013, doi: 10.1017/S0954422413000097.

[131] F. Saura-Calixto, J. Serrano, and I. Goñi, "Intake and bioaccessibility of total polyphenols in a whole diet," *Food Chem.*, vol. 101, no. 2, pp. 492–501, Jan. 2007, doi: 10.1016/j.foodchem.2006.02.006.

[132] S. Ketnawa, F. C. Reginio, S. Thuengtung, and Y. Ogawa, "Changes in bioactive compounds and antioxidant activity of plant-based foods by gastrointestinal digestion: a review," *Crit. Rev. Food Sci. Nutr.*, pp. 1–22, Jan. 2021, doi: 10.1080/10408398.2021.1878100.

[133] Z. Xiao *et al.*, "Pharmacological Effects of Salvianolic Acid B Against Oxidative Damage," *Front. Pharmacol.*, vol. 11, Nov. 2020, doi: 10.3389/fphar.2020.572373.

[134] L. Wen *et al.*, "Identification of a flavonoid C -glycoside as potent antioxidant," *Free Radic. Biol. Med.*, vol. 110, pp. 92–101, Sep. 2017, doi:

10.1016/j.freeradbiomed.2017.05.027.

[135] T. Bacchetti, C. Morresi, L. Bellachioma, and G. Ferretti, "Antioxidant and Pro-Oxidant Properties of Carthamus Tinctorius, Hydroxy Safflor Yellow A, and Safflor Yellow A," *Antioxidants*, vol. 9, no. 2, p. 119, Jan. 2020, doi: 10.3390/antiox9020119.

[136] W. Xia *et al.*, "Wild pink bayberry fruit: the effect of in vitro gastrointestinal digestion on phytochemical profiles, and antioxidant and antiproliferative activities," *Food Funct.*, vol. 12, no. 5, pp. 2126–2136, Mar. 2021, doi: 10.1039/d0fo02370a.

[137] A. Bektas, S. H. Schurman, R. Sen, and L. Ferrucci, "Aging, inflammation and the environment," *Exp. Gerontol.*, vol. 105, pp. 10–18, May 2018, doi: 10.1016/j.exger.2017.12.015.

[138] T. Finkel and N. J. Holbrook, "Oxidants, Oxidative Stress and Biology of Ageing," *Insight Rev. Artic.*, vol. 408, no. November, pp. 239–247, 2000, [Online]. Available: www.nature.com

[139] T. Hussain, B. Tan, Y. Yin, F. Blachier, M. C. B. Tossou, and N. Rahu, "Oxidative Stress and Inflammation: What Polyphenols Can Do for Us?," *Oxid. Med. Cell. Longev.*, vol. 2016, pp. 1–9, 2016, doi: 10.1155/2016/7432797.

[140] R. Stocker, "Induction of Haem Oxygenase as a Defence Against Oxidative Stress," *Free Radic. Res. Commun.*, vol. 9, no. 2, pp. 101–112, Jan. 1990, doi: 10.3109/10715769009148577.

[141] A. P. Fernandes and A. Holmgren, "Glutaredoxins: Glutathione-Dependent Redox Enzymes with Functions Far Beyond a Simple Thioredoxin Backup System," *Antioxid. Redox Signal.*, vol. 6, no. 1, pp. 63–74, Feb. 2004, doi: 10.1089/152308604771978354.

[142] I. Eleftherianos and J. C. Castillo, "Molecular Mechanisms of Aging and Immune System Regulation in Drosophila," *Int. J. Mol. Sci.*, vol. 13, no. 8, pp. 9826–9844, Aug. 2012, doi: 10.3390/ijms13089826.

[143] É. Le Bourg, "Oxidative stress, aging and longevity in Drosophila melanogaster," *FEBS Lett.*, vol. 498, no. 2–3, pp. 183–186, Jun. 2001, doi: 10.1016/S0014-5793(01)02457-7.

[144] J. Luo, H. Si, Z. Jia, and D. Liu, "Dietary Anti-Aging Polyphenols and Potential Mechanisms," *Antioxidants*, vol. 10, no. 2, p. 283, Feb. 2021, doi: 10.3390/antiox10020283.

[145] Y. He and H. Jasper, "Studying aging in Drosophila," *Methods*, vol. 68, no. 1, pp. 129–133, Jun. 2014, doi: 10.1016/j.ymeth.2014.04.008.

[146] M. Gáliková and P. Klepsatel, "Obesity and Aging in the Drosophila Model.," *Int. J. Mol. Sci.*, vol. 19, no. 7, p. 1896, Jun. 2018, doi: 10.3390/ijms19071896.

[147] M. Jafari, "Drosophila melanogaster as a model system for the evaluation of anti-aging compounds," *Fly (Austin).*, vol. 4, no. 3, pp. 253–257, Jul. 2010, doi: 10.4161/fly.4.3.11997.

[148] Y. Yi, W. Xu, Y. Fan, and H.-X. Wang, "Drosophila as an emerging model organism for studies of food-derived antioxidants," *Food Res. Int.*, vol. 143, no. 68, p. 110307, May 2021, doi: 10.1016/j.foodres.2021.110307.

[149] D. Beghelli *et al.*, "Pterostilbene Promotes Mean Lifespan in Both Male and Female Drosophila Melanogaster Modulating Different Proteins in the Two Sexes," *Oxid. Med. Cell. Longev.*, vol. 2022, pp. 1–21, Feb. 2022, doi: 10.1155/2022/1744408.

[150] S.-H. Lee and K.-J. Min, "Drosophila melanogaster as a model system in the study of pharmacological interventions in aging," *Transl. Med. Aging*, vol. 3, pp. 98–103, Jan. 2019, doi: 10.1016/j.tma.2019.09.004.

[151] G. Lupidi *et al.*, "Antiproliferative activities of Artemisia herba-alba ethanolic extract in human colon cancer cell line (HCT116)," *Altern. Med. Stud.*, vol. 1, no. 1, p. 14, Nov. 2011, doi: 10.4081/ams.2011.e14.

[152] K. Fiocca *et al.*, "Mannitol ingestion causes concentration-dependent, sex-biased mortality in adults of the fruit fly (Drosophila melanogaster)," *PLoS One*, vol. 14, no. 5, p. e0213760, May 2019, doi: 10.1371/journal.pone.0213760.

[153] S. T. Madabattula *et al.*, "Quantitative Analysis of Climbing Defects in a Drosophila Model of Neurodegenerative Disorders," *J. Vis. Exp.*, vol. 2015, no. 100, Jun. 2015, doi: 10.3791/52741.

[154] O. Gevedon *et al.*, "In Vivo Forward Genetic Screen to Identify Novel Neuroprotective Genes in Drosophila melanogaster," *J. Vis. Exp.*, vol. 2019, no. 149, Jul. 2019, doi: 10.3791/59720.

[155] I. A. Adedara, C. V. Klimaczewski, N. B. V. Barbosa, E. O. Farombi, D. O. Souza, and J. B. T. Rocha, "Influence of diphenyl diselenide on chlorpyrifos-induced toxicity in Drosophila melanogaster," *J. Trace Elem. Med. Biol.*, vol. 32, pp. 52–59, Oct. 2015, doi: 10.1016/j.jtemb.2015.05.003.

[156] S. K. Han *et al.*, "OASIS 2: online application for survival analysis 2 with features for the analysis of maximal lifespan and healthspan in aging research," *Oncotarget*, vol. 7, no. 35, pp. 56147–56152, Aug. 2016, doi: 10.18632/oncotarget.11269.

[157] S. E. Schriner *et al.*, "Extension of Drosophila Lifespan by Rhodiola rosea through a Mechanism Independent from Dietary Restriction," *PLoS One*, vol. 8, no. 5, p. e63886, May 2013, doi: 10.1371/journal.pone.0063886.

[158] D. Kojić *et al.*, "Effect of fullerenol nanoparticles on oxidative stress induced by paraquat in honey bees.," *Environ. Sci. Pollut. Res. Int.*, vol. 27, no. 6, pp. 6603–6612, Feb. 2020, doi: 10.1007/s11356-019-07385-z.

[159] G. O. Noriega, S. Gonzales, M. L. Tomaro, and A. M. del C. Batlle, "Paraquat-generated Oxidative Stress in Rat Liver Induces Heme Oxygenase-1 and Aminolevulinic Acid Synthase," *Free Radic. Res.*, vol. 36, no. 6, pp. 633–639, Jan.

2002, doi: 10.1080/10715760290029065.

[160] L.-R. Shen *et al.*, "Curcumin-supplemented diets increase superoxide dismutase activity and mean lifespan in Drosophila," *Age (Omaha).*, vol. 35, no. 4, pp. 1133–1142, Aug. 2013, doi: 10.1007/s11357-012-9438-2.

[161] D. R. Valenzano, E. Terzibasi, T. Genade, A. Cattaneo, L. Domenici, and A. Cellerino, "Resveratrol Prolongs Lifespan and Retards the Onset of Age-Related Markers in a Short-Lived Vertebrate," *Curr. Biol.*, vol. 16, no. 3, pp. 296–300, Feb. 2006, doi: 10.1016/j.cub.2005.12.038.

[162] F. Diab *et al.*, "Influence of Simulated In Vitro Gastrointestinal Digestion on the Phenolic Profile, Antioxidant, and Biological Activity of Thymbra spicata L. Extracts," *Antioxidants*, vol. 11, no. 9, p. 1778, Sep. 2022, doi: 10.3390/antiox11091778.

[163] A. A. Johnson, "Lipid Hydrolase Enzymes: Pragmatic Prolongevity Targets for Improved Human Healthspan?," *Rejuvenation Res.*, vol. 23, no. 2, pp. 107–121, Apr. 2020, doi: 10.1089/rej.2019.2211.

[164] S. Davies, R. Kattel, B. Bhatia, A. Petherwick, and T. Chapman, "The effect of diet, sex and mating status on longevity in Mediterranean fruit flies (Ceratitis capitata), Diptera: Tephritidae.," *Exp. Gerontol.*, vol. 40, no. 10, pp. 784–92, Oct. 2005, doi: 10.1016/j.exger.2005.07.009.

[165] T. Chapman, M. Takahisa, H. K. Smith, and L. Partridge, "Interactions of mating, egg production and death rates in females of the Mediterranean fruitfly, Ceratitis capitata," *Proc. R. Soc. London. Ser. B Biol. Sci.*, vol. 265, no. 1408, pp. 1879–1894, Oct. 1998, doi: 10.1098/rspb.1998.0516.

[166] Y.-L. Xue *et al.*, "Isolation and Caenorhabditis elegans Lifespan Assay of Flavonoids from Onion," *J. Agric. Food Chem.*, vol. 59, no. 11, pp. 5927–5934, Jun. 2011, doi:

10.1021/jf104798n.

[167] P. Wang *et al.*, "Salvianolic Acid B Inhibited PPARγ Expression and Attenuated Weight Gain in Mice with High-Fat Diet-Induced Obesity," *Cell. Physiol. Biochem.*, vol. 34, no. 2, pp. 288–298, 2014, doi: 10.1159/000362999.

[168] L.-C. Meng *et al.*, "Salvianolic acid B ameliorates non-alcoholic fatty liver disease by inhibiting hepatic lipid accumulation and NLRP3 inflammasome in ob/ob mice," *Int. Immunopharmacol.*, vol. 111, p. 109099, Oct. 2022, doi: 10.1016/j.intimp.2022.109099.

[169] C. Ding *et al.*, "New insights into salvianolic acid A action: Regulation of the TXNIP/NLRP3 and TXNIP/ChREBP pathways ameliorates HFD-induced NAFLD in rats," *Sci. Rep.*, vol. 6, no. 1, p. 28734, Jun. 2016, doi: 10.1038/srep28734.

[170] S. Li *et al.*, "Activation of the AMPK-SIRT1 pathway contributes to protective effects of Salvianolic acid A against lipotoxicity in hepatocytes and NAFLD in mice," *Front. Pharmacol.*, vol. 11, no. November, pp. 1–15, Nov. 2020, doi: 10.3389/fphar.2020.560905.

[171] X. Wang *et al.*, "Effects of salvianolic acid A on intestinal microbiota and lipid metabolism disorders in Zucker diabetic fatty rats," *Diabetol. Metab. Syndr.*, vol. 14, no. 1, Dec. 2022, doi: 10.1186/S13098-022-00868-Z.

[172] V. I. Pérez *et al.*, "Is the oxidative stress theory of aging dead?," *Biochim. Biophys. Acta - Gen. Subj.*, vol. 1790, no. 10, pp. 1005–1014, Oct. 2009, doi: 10.1016/j.bbagen.2009.06.003.

[173] G. Pezzoli and E. Cereda, "Exposure to pesticides or solvents and risk of Parkinson disease," *Neurology*, vol. 80, no. 22, pp. 2035–2041, May 2013, doi: 10.1212/WNL.0b013e318294b3c8.

[174] C. M. Tanner *et al.*, "Rotenone, Paraquat, and Parkinson's Disease," *Environ. Health*

Perspect., vol. 119, no. 6, pp. 866–872, Jun. 2011, doi: 10.1289/ehp.1002839.

[175] N. Wongchum and A. Dechakhamphu, "Xanthohumol prolongs lifespan and decreases stress-induced mortality in Drosophila melanogaster," *Comp. Biochem. Physiol. Part C Toxicol. Pharmacol.*, vol. 244, p. 108994, Jun. 2021, doi: 10.1016/j.cbpc.2021.108994.

[176] S. Deepashree, S. Niveditha, T. Shivanandappa, and S. R. Ramesh, "Oxidative stress resistance as a factor in aging: evidence from an extended longevity phenotype of Drosophila melanogaster," *Biogerontology*, vol. 20, no. 4, pp. 497–513, Aug. 2019, doi: 10.1007/s10522-019-09812-7.

[177] A. Loboda *et al.*, "Heme Oxygenase-1 and the Vascular Bed: From Molecular Mechanisms to Therapeutic Opportunities," *Antioxid. Redox Signal.*, vol. 10, no. 10, pp. 1767–1812, Oct. 2008, doi: 10.1089/ars.2008.2043.

[178] T. Al L. Abaquita, M. Damulewicz, D. Bhattacharya, and E. Pyza, "Regulation of Heme Oxygenase and Its Cross-Talks with Apoptosis and Autophagy under Different Conditions in Drosophila," *Antioxidants*, vol. 10, no. 11, p. 1716, Oct. 2021, doi: 10.3390/antiox10111716.

[179] M. J. Svensson and J. Larsson, "Thioredoxin-2 affects lifespan and oxidative stress in Drosophila," *Hereditas*, vol. 144, no. 1, pp. 25–32, Feb. 2007, doi: 10.1111/j.2007.0018-0661.01990.x.

[180] S. M. Kanzok *et al.*, "Substitution of the Thioredoxin System for Glutathione Reductase in Drosophila melanogaster," *Science (80-.).*, vol. 291, no. 5504, pp. 643–646, Jan. 2001, doi: 10.1126/science.291.5504.643.

[181] U. V. Semaniuk *et al.*, "Chili-supplemented food decreases glutathione- S -transferase activity in Drosophila melanogaster females without a change in other parameters of antioxidant system," *Redox Rep.*, vol. 27, no. 1, pp. 221–229, Dec. 2022, doi:

10.1080/13510002.2022.2123884.

[182] S. Ekengren, Y. Tryselius, M. S. Dushay, G. Liu, H. Steiner, and D. Hultmark, "A humoral stress response in Drosophila," *Curr. Biol.*, vol. 11, no. 9, pp. 714–718, May 2001, doi: 10.1016/S0960-9822(01)00203-2.

[183] S. Ekengren and D. Hultmark, "A Family of Turandot-Related Genes in the Humoral Stress Response of Drosophila," *Biochem. Biophys. Res. Commun.*, vol. 284, no. 4, pp. 998–1003, Jun. 2001, doi: 10.1006/bbrc.2001.5067.

[184] M. Khalil *et al.*, "Beneficial Effects of Carvacrol on In Vitro Models of Metabolically-Associated Liver Steatosis and Endothelial Dysfunction: A Role for Fatty Acids in Interfering with Carvacrol Binding to Serum Albumin," *Curr. Med. Chem.*, vol. 29, no. 30, pp. 5113–5129, Sep. 2022, doi: 10.2174/0929867329666220401103643.

[185] D. Farah *et al.*, "The protective effects of Thymbra spicata L. extracts on lifespan, body-weight control, and oxidative stress defence in Drosophila melanogaster: an age- and sex-related study," *J. Funct. Foods*, 2023, doi: [Submitted-2023].